MICROSCOPIC FUEL CONSUMPTION AND EMISSION MODELING

by

Kyoungho Ahn

Thesis submitted to the Faculty of the
Virginia Polytechnic Institute and State University
In partial fulfillment of the requirements for the degree of

Master of Science
in
Civil and Environmental Engineering

Michael W. Van Aerde, Chair
Antonio A. Trani, Co-Chair
Wei H. Lin
Hesham Rakha

December 5, 1998
Blacksburg, Virginia

Key Words: Fuel consumption and emission modeling, Transportation, ITS evaluation, Microscopic modeling

Microscopic Fuel Consumption and Emission Modeling

by

Kyoungho Ahn

ABSTRACT

Mathematical models to predict vehicle fuel consumption and emission metrics are presented in this thesis. Vehicle fuel consumption and emissions are complex functions to be approximated in practice due to numerous variables affecting their outcome. Vehicle energy and emissions are particularly sensitive to changes in vehicle state variables such as speed and acceleration, ambient conditions such as temperature, and driver control inputs such as acceleration pedal position and gear shift speeds, among others.

Recent empirical studies have produced large amounts of data concerning vehicle fuel consumption and emissions rates and offer a wealth of information to transportation planners. Unfortunately, unless simple relationships are found between fuel consumption and vehicle emission metrics, their application in microscopic traffic and macroscopic planning models becomes prohibitive computationally. This thesis describes the development of microscopic energy and emission models using nonlinear multiple regression and neural network techniques to approximate vehicle fuel consumption and emissions field data. The energy and emission models described in this thesis utilized data collected by the Oak Ridge National Laboratory. The data include microscopic fuel consumption and emission measurements (CO, HC, and NO_x) for eight light duty vehicles as a function of vehicle speed and acceleration. The thesis describes modeling processes and the tradeoffs between model accuracy and computational efficiency. Model verification results are included for two vehicle driving cycles. The models presented estimate vehicle fuel consumption within 2.5% of their actual measured values. Vehicle emissions errors fall in the range of 3-33% with correlation coefficients ranging between

0.94 and 0.99.

Future transportation planning studies could also make use of the modeling approaches presented in the thesis. The models developed in this study have been incorporated into a microscopic traffic simulation tool called INTEGRATION to further demonstrate their application and relevance to traffic engineering studies. Two sample Intelligent Transportation Systems (ITS) application results are included. In the case studies, it was found that vehicle fuel consumption and emissions are more sensitive to the level of vehicle acceleration than to the vehicle speed. Also, the study shows signalization techniques can reduce fuel consumption and emissions significantly, while incident management techniques do not affect the energy and emissions rates notably.

ACKNOWLEDGMENTS

I would like to express appreciation to my advisor, Dr. Michel Van Aerde whom I respect and admire greatly. He offered generosity, professional guidance and financial support. I also wish to express special thanks to Dr. Antonio Trani, my co-advisor. He gave me kindness, helpful guidance and discussions. Thanks are extended to Dr. Hesham Rakha, colleague and my committee member. He always gave me the chance to discuss research and other issues. Also, I appreciate Dr. Wei Lin, who offered advice and helpful discussions.

I greatly appreciate my parents, my bother and mother-in-law, in Korea, for their endless sacrifice in bringing me up and offering me an opportunity to be here. I am thankful to Youn-soo Kang, Hojong Baik, Heung-Gweon Sin and other colleagues at Virginia Tech.

Finally this work is dedicated to my sincere love, my wife, Junghwa, who gave me love, encouragement, patience, and confidence.

TABLE OF CONTENTS

LIST OF FIGURES

LIST OF TABLES

Chapter 1. Introduction

Vehicle fuel consumption and engine emissions are two critical aspects that are considered in the transportation planning process of highway facilities. Transportation is one of the major contributors to man-made polluting emissions. Recent studies indicate that as much as 45% of the pollutants released in the U.S. are a direct consequence of vehicle emissions [NRC 1995]. Highway vehicles, which contribute more than one-third of the total nationwide emissions, are the largest source of transportation-related emissions [Nizich et al. 1994]. Motor vehicles are the source of more than 75 percent of the national CO emissions, and about 35 percent of emissions of HC and NOx [Nizich et al. 1994].

The introduction of Intelligent Transportation Systems (ITS) makes a compelling case to compare alternative ITS and non-ITS investments with emphasis on energy and emission measures of effectiveness. However, until now, the benefits derived from ITS technology in terms of energy and emissions are not clear.

1.1 Objective of Thesis

The primary objective of this thesis is to develop mathematical models to predict vehicle fuel consumption and emissions under various traffic conditions. Current state-of-the-art models estimate fuel consumption and emission measures of effectiveness based on typical driving cycles. Most of these models offer simplified mathematical expressions to compute fuel and emissions based on average link speeds without much regard to the transient effects on speed and acceleration as the vehicle travels on a highway network. Moreover, most models use an aggregate modeling approach where a 'characteristic' vehicle is used to represent dissimilar vehicle populations. While this approach has been accepted by transportation planners and Federal Agencies to estimate highway impacts on the environment, it can be argued that modeling individual vehicle fuel consumption and emissions coupled with the modeling of vehicle kinematics on a highway network could result in more reliable predictions of actual vehicle fuel consumption and emissions. This thesis addresses this issue, presenting two mathematical models to predict fuel consumption and emissions for individual vehicles using instantaneous speed and acceleration as explanatory variables. The availability of relatively powerful computers on the average desktop today makes this approach feasible even for large highway networks.

The ultimate use of these models would be their integration into traffic network simulators to better understand the impacts of traffic policies, including introduction of ITS technology, on the environment.

1.2 Thesis Structure

This thesis is organized into five chapters. The second chapter provides a review of the relevant literature. The literature discusses the contribution of motor vehicle transportation to air pollution and energy consumption including air quality standards and requirements, those factors affecting fuel consumption and emissions. Various fuel consumption and emissions models are also described.

The third chapter shows some of the data sources used in the modeling approach presented. This describes two mathematical approaches proposed for modeling highway vehicle energy and emissions, and some of the validation results using field data.

In Chapter 4, the thesis provides an opportunity to apply the model in current ITS applications. The first example explores impacts of various traffic control systems. Secondly, the impacts of incident management techniques were analyzed to illustrate the benefits in terms of energy and emissions

Finally, Chapter 5 comprises a summary of the findings and future recommendations for continued research.

Chapter 2. Literature Review

2.1 Introduction

Chapter 2 discusses two fundamental issues related to motor vehicle fuel consumption and emission modeling. The first section describes the contributions of motor vehicle transportation to air pollution and energy consumption. Government legislation has evolved over recent years in order to reduce vehicle emissions. Initially, air quality standards and requirements are outlined and the significance of each pollutant is summarized. Also, the literature indicates the factors which affect fuel consumption and emissions. The second section reviews the current fuel consumption and emission models and its current research efforts. Finally, the capabilities of current traffic simulation models in terms of estimating fuel consumption and emissions are examined.

2.2 Contribution of Motor Vehicle Transportation to Air Pollution and Energy Consumption

Emissions from individual cars are generally regarded as low if looked at in isolation. However, since the number of motor vehicles in this country is large, the combined emissions and fuel consumption cannot be disregarded. In fact, personal automobiles are the single largest polluter in the United States.

2.2.1 Air Quality Standards and Requirements

Contributions of motor vehicles to air pollution were first studied in the early 1950s by a California researcher [EPA 1994b]. In this study, it was determined that traffic was to blame for the smoggy skies over Los Angeles. The first significant legislation to recognize the harmful effects of air pollution on pubic health was the Clean Air Act (CAA) in 1970. The CAA established the U.S. Environmental Protection Agency (EPA) and mandated that the EPA set health-based national ambient air quality standards (NAAQS) for six pollutants: carbon monoxide (CO), lead (pb), nitrogen dioxide (NO_2), ozone (O_3), particulate matter (PM-10) and sulfur dioxide (SO_2). This 1970 Amendment imposed some goals to achieve clean air by reducing 0.41 gram per mile HC standard and the 3.4 grams per mile CO standard by 1975 [EPA 1994a]. However, these standards were not achieved and the government delayed the HC standard until 1980 and the CO standard until 1981 as specified by the Clean Air Act of 1977. In the amendment, the NOx standard was relaxed to 1 gram per mile and the deadline was extended until 1981.

In 1990, the New Clean Air Act placed a heavy burden on the transportation community. This legislation was amended by Congress to require further reductions in HC, CO, NOx, and particulate emissions. It also introduced a comprehensive set of programs aimed at reducing pollution from vehicles. These included additional technological advances, such as lower tailpipe standards; enhanced vehicle inspection and maintenance (I/M) programs; more stringent emission testing procedures; new vehicle technologies and the use clean fuels; transportation management provisions; and possible regulation of emissions from nonroad vehicles [EPA 1994b].

The act defined deadlines to attain the goal based on the severity of air quality conditions. According to severity, urban areas were classified as marginal, moderate, serious, severe, and extreme. Forty areas ranked as marginal for ozone had 3 years from the baseline year, 1990, to attain the EPA standard. Twenty nine areas classified as moderate for ozone, and thirty seven for CO that were given classified as moderate and had 6 years to achieve the goal. There were twelve serious areas for ozone and one for CO with 9 years to establish compliance. There were nine severe cases for ozone and fifteen cases for CO with 17 years to achieve compliance. Only Los Angeles was classified as extreme for ozone and had 20 years to comply with the new standards [NRC 1995].

The requirements were also different from one another according to the rank of air quality severity. Areas of moderate or worse ozone classifications must submit revisions to State Implementation Plans (SIPs) showing that, during the period, ozone will be reduced by at least 15 percent. These areas must reduce ozone emissions by 3 percent per year until attainment is achieved. Moreover, areas classified as severe or extreme had to adopt transportation control measures (TCMs). TCMs are activities intended to decrease motor travel or otherwise reduce vehicle emissions. Areas with carbon monoxide specifications had to forecast vehicle miles traveled (VMT) annually, and if the actual VMT exceeds the expected VMT, they had to adopt TCMs. Furthermore, areas designated as serious for CO emissions were required to adopt TCMs [NRC 1995].

The amendment of 1990 defined sanctions for noncompliance. For failure to submit an SIP, EPA disapproval of an SIP, failure to make a required submission, or failure to implement any SIP requirement, highway projects assisted by the federal government could be withheld. Additionally, if sanctions were commanded, the department of transportation (DOT) could only approve highway projects that would not increase single-vehicle trips [NRC 1995].

2.2.2 Transportation and Pollutants

Transportation is one of the major contributors to man-made polluting emissions. Generally, emission sources are categorized by four main sources: transportation (highway vehicles), stationary fuel combustion (electrical utilities), industrial processes (chemical refining) and solid waste disposal [Horowitz 1982]. According to current estimates, transportation sources are responsible for about 45 percent of nationwide emissions of the EPA defined pollutants [NRC 1995]. Highway vehicles, which contribute more than one-third of the total nationwide emissions of the six criteria pollutants, are the largest source of transportation-related emissions [Nizich et al. 1994]. Motor vehicles are the source of more than 75 percent of the national CO emissions, and about 35 percent of emissions of HC and NOx [Nizich et al. 1994].

Most of emissions are generated in the combustion process and from evaporation of the fuel itself. Gasoline and diesel fuels are comprised of hydrocarbons and compounds of hydrogen and carbon atoms. In a perfect combustion, all the hydrogen in the fuel is converted to water and the carbon is changed to carbon dioxide. Unfortunately, the perfect combustion process is impossible to achieve in the real word, and many pollutants result as by-products of this combustion process and from evaporation of the fuel [EPA 1994a].

The principal pollutants emitted from typical motor engines are carbon monoxide, hydrocarbon, and oxides of nitrogen. Carbon monoxide (CO), a product of incomplete combustion, is a colorless, odorless and poisonous gas. CO reduces the flow of oxygen in the bloodstream and is harmful to every living organism. In some urban areas, the motor vehicle contribution to carbon monoxide emissions can exceed 90 percent [EPA 1993a].

Hydrocarbon (HC) emissions result from fuel that does not burn completely in the engine. It reacts with nitrogen oxides and sunlight to form ozone, which is a major component of smog. Ozone is one of the EPA's defined pollutants known to cause irritations of the eyes, damage the lung tissue and affect the well-being of the human respiratory system. Furthermore, hydrocarbons emitted by vehicle exhaust systems are also toxic and are known to cause cancer in the long term [EPA 1994a].

While CO and HC are the products of the incomplete combustion of motor fuels, oxides of nitrogen (NOx) are formed differently. NOx is formed by the reaction of nitrogen and oxygen atoms during high pressure and temperature, the chemical processes that occur during the combustion. NOx also leads to the formation of ozone and contributes to the formation of acid rain [EPA 1994a].

The air/fuel (A/F) ratio is one of the most important variables affecting the efficiency of catalytic converters and the level of exhaust emissions (Johnson 1988). The highest CO and HC levels are produced under fuel-rich conditions, and the highest NOx level is emitted under fuel-lean conditions. Generally, fuel-rich operations occur during cold-start conditions, or under heavy engine loads such as during rapid accelerations at high speeds and on steep grades. Therefore, high levels of CO and HC are generated on congested highways and in other high traffic density areas.

2.2.3 Factors Affecting Emission Rates

Emissions deriving from transportation sources are the functions of several variables. These variables have been categorized as follows [NRC 1995]:

- travel-related factors,
- highway network characteristics,
- vehicle characteristics.

The following paragraphs describe in detail these factors.

Travel-related factors

Pollutants emitted from motor vehicles are dependent on the number of trips and the distance traveled. Emissions relating to trip factors vary according to the percentages of different vehicle operation modes, such as exhaust emissions and evaporative emissions. The former includes start-up emissions, which are classified as cold-start or hot-start depending on how long the vehicle has been turned off, and running emissions, which are emitted during a hot stabilized mode. The latter comprise running losses and hot soak emissions produced from fuel evaporation when an engine is still hot at the end of a trip, and diurnal emissions, which result from the gasoline tank regardless of whether the vehicle is operated or not [NRC 1995].

Speed, acceleration and engine load of the vehicle are also significant factors contributing to emission rates. According to current model estimates such as MOBILE5a developed by the EPA and EMFAC7F developed by the California Air Resources Board (CARB), emissions are generally high under low speed, congested driving conditions. Emissions fall at intermediate speeds, low density traffic conditions. On the other hand, NOx has a different attribute, showing the highest point at high speed [NRC 1995]. However, these estimates have some problems. For example, sharp acceleration, which contributes high emission rates, is not explained in existing traffic models. Acceleration, which causes a vehicle to operate in a fuel-rich mode, must be used as an input factor to estimate accurate emission rates in these models.

Highway-Related Factors

Emission rates of motor vehicles also depend on the geometric design of the highway. Highways with facilities such as signalized intersections, freeway lamps, toll booths and weaving sections may increase the emission levels due to the engine enrichment from accelerations. Grade on highways is one of the large contributors affecting emission rates. On a steep grade, vehicles require more engine power, causing a high A/F ratio (high enrichment statues) in order to maintain the same speeds. Road conditions are also considered in estimating emissions.

Vehicle-Related and Other Factors

Vehicle characteristics such as engine sizes, horsepower and weight are also factors influencing emission rates on highways. Generally, vehicles with large engine sizes emit more pollutants than vehicles with small engine sizes, and large engine sizes are commonly accompanied by high maximum horsepower and heavy weights of vehicles.

Emission rates also vary with vehicle age. Older vehicles produce higher emission rates than newer fuel-injected vehicles during normal operation and vehicle starts (Enns et al. 1993). Furthermore, older vehicles are not held to the same restrictive vehicle standards as newer vehicles. According to known data, 1975-model vehicles emit more than three times the amount of CO and HC than the rates of 1990-model vehicles [DOT and EPA 1993].

Ambient temperature is an important parameter affecting both exhaust and evaporative emissions. The engine and emission control systems take longer to warm up at cold temperature increasing cold-start emissions. Moreover, as the temperature increases, evaporative emissions increase with higher emission rates.

2.2.4 Transportation and Energy Consumption

The primary energy source for the transportation sector is petroleum. The transportation sector consumes nearly two-thirds of the petroleum used in the United States. Highway traffic is responsible for nearly three-fourths of the total transportation energy use, with about 80 percent from automobiles, light trucks, and motorcycles, and about 20 percent from heavy trucks and buses [Davis 1994].

The principal factors affecting fuel consumption are closely related to those affecting emissions. Therefore, primary emission factors such as travel-related factors, highway conditions, and other vehicle factors are also considered as fuel economy factors.

Travel-Related Factors

Fuel consumption is highly dependent on many different traffic characteristics. Speed and acceleration are significant factors affecting fuel consumption rates. Generally, fuel consumption rates increase as speed and acceleration increases. Also, fuel economy is somewhat poor at lower average trip speeds due to frequent accelerations and stops. Also, fuel consumption rates are reduced by engine friction, tires and accessories such as power steering and air conditioning at low speeds and are dominated by the effect of aerodynamic drag on fuel efficiency at high speeds [An and Ross 1993a].

The modal operation of the vehicle also affects fuel consumption. Engines typically take several minutes to reach their normal operation. The cold-start fuel consumption experienced during the initial stages of the trip result in lower fuel efficiency than when the engines are fully warmed up [Baker 1994].

Highway-Related Factors

The highway related factors such as steep upgrades and poor road surface conditions also reduce fuel efficiency. On steep upgrades, vehicles require a heavy power output from their engines, consuming more fuel than under normal conditions. Also, rough roads can lead to significant incremental increases in fuel consumption by influencing the rolling resistance and aerodynamic drag generated. At typical highway speeds, a vehicle tested on a rough road increased its fuel consumption by five percent over a vehicle tested on a normal quality road [Baker 1994].

Vehicle-Related and Other Factors

Vehicle characteristics such as weights, engine sizes, and technologies are the primary factors affecting fuel economy. Generally, larger and heavier vehicles, vehicles with automatic transmissions, and vehicles with more power accessories (e.g., power seats and windows, power brakes and steering, and air conditioning) require more fuel than vehicles lacking these systems [Murrell 1980].

Without proper vehicle maintenance, fuel consumption can increase by as much as 40 percent [Baker 1994]. According to research, improper engine tuning can increase average fuel consumption by about 10 percent and wheel misalignment as small as 2 mm can cause an increase of fuel consumption by about 3 percent due to tire rolling resistance [Baker 1994].

Finally, the influence of weather conditions contributes to fuel economy. Fuel consumption rates worsen at low temperatures and with high winds, which result in aerodynamic losses [Murrell 1980]. For example, in Europe, fuel consumption in winter is worse than in summer by about 15 to 20 percent [Baker 1994].

2.3 Fuel Consumption and Emissions Models

Various models are available to estimate the contribution of motor vehicle transportation to air quality and energy use. However, many of the models are not well suited for estimating the effects of highway improvement projects such as ITS alternatives.

ITS implementations can affect energy consumption and emission rates in the corridor in which the improvement is located. Furthermore, those improvements can also improve the variability of travel such as destination, departure time, and trip mode. Finally, these results affect the fuel economy and emission levels in urban areas. In order to estimate these consequences of new projects, land use and travel demand models and emissions and fuel consumption models are required. The former is used to generate trips according to changes of highway traffic conditions and the later is used to estimate the impact of changes in travel activity on emission rates and energy consumption. Furthermore, atmospheric dispersion models are also used to estimate concentrations of pollutants produced by particular facilities, such as intersections.

2.3.1 Emission Models

Two main emission models commonly used in the United States are the Environmental Protection Agency's (EPA's) MOBILE model and the California Air Resources Board's (CARB's) EMFAC model. In both models, emission rates according to the models are a function of vehicle type and age, vehicle average speed, ambient temperature, and vehicle operating mode. Both models produce specific emission rates. These emission rates are multiplied by vehicle activities such as vehicle miles-traveled, number of trips, and vehicle-hours traveled in order to estimate total emission levels [NRC 1995].

Current estimates of emission rates of the MOBILE model and the EMFAC model are expressed as functions of average speeds and are based on vehicle testing on a limited number of driving cycles. The baseline emission rates are derived from the Federal Test Procedure (FTP), which is the vehicle test procedure commonly used for light duty vehicle testing and is composed of three different phases: a cold-start phase, a stabilized phase and a hot-start phase. In the MOBILE model, the emissions from vehicles operating in all three phases are used to estimate baseline emissions. The baseline emission rates for a vehicle class is the average result from the three phases of the FTP cycle at an average speed of 31.6 kph (19.6 mph), which is the average test speed of the entire FTP cycle. In the EMFAC model, the baseline emission rate is derived from only the stabilized phase of the FTP cycle with an average operating speed of 25.6 kph (16 mph) [Guensler et al. 1993].

Emission rates at other average speeds are multiplied by the appropriate speed correction factor (SCF) associated with a vehicle class and the operating speed. SCFs are derived from emissions data from testing vehicles on eleven other driving cycles and heavy-duty trucks on four drive cycles; each cycle has a different overall average speed. The SCFs are estimated from the average cycle speed on the average emission rate for the cycle. Therefore, speed-corrected emission rates used in emission models are highly dependant on the average cycle speed [NRC 1995].

The following paragraphs describe some of the limitations found in current models.

A limited set of driving cycles, which insufficiently represent specific traffic flow conditions, are used to estimate emission rates in current models. Many of the driving cycles are out of data (the FTP is more than 20 years old), and they do not represent current, real world driving conditions. Analyses of three cycles, which include the FTP cycle and two recently developed cycles (Freeway 6 and Arterial 1) with the same average speed, found that the FTP cycle underestimated driving conditions at higher speeds and acceleration, both of which are known to be sources of high emissions [NRC 1995].

Another problem with emission estimations is that current emission models predict emission rates solely on the basis of changes in average speed among traffic flow characteristics. Average trip speeds are not equivalent to link-specific speeds for portions of vehicle trips. This method of using average speeds cannot represent the distribution of speeds and accelerations of a trip, which vary by type of facility and level of congestion. For example, existing emission models cannot compare a highly congested freeway and a normal density arterial with the same average speed, though each has quite different distribution for speeds and accelerations causing distinct emission levels [NRC 1995].

2.3.2 Fuel Consumption Models

Fuel consumption models are mathematical relationships using contributions of fuel consumption such as the number of trips, the vehicle miles traveled, the number of stops, the vehicle's average speed, etc. Many models have been developed, and automotive fuel use is believed to be well approximated in current models.

Instantaneous Fuel Consumption Models

Instantaneous fuel consumption models are derived from a relationship between the fuel consumption rates and the instantaneous vehicle power. Second-by-second vehicle characteristics, traffic conditions and road conditions are required in order to estimate the expected fuel consumption. Due to the disaggregate characteristic of fuel consumption data, these models are usually implemented to evaluate individual transportation projects such as single intersections, toll plazas, sections of highway, etc.

From Newton's second law, it can be demonstrated that the net force on a vehicle in the direction of motion is proportional to its acceleration and the net force is required to overcome the aerodynamic, rolling resistance and grade resistance. Using these ideas, fuel consumption rates can be estimated as a function of the vehicle mass, drag coefficient, rolling resistance, frontal area, acceleration, speed, transmission efficiency, grade, and etc.

The original power-based model, proposed by Post et al. (1984), provides aggregate fuel consumption estimates for on-road driving within 2 percent of the actual fuel usage. Akcelik and Biggs (1989) contributed to improving the power-based model increasing accuracy. This model was embedded into a computer package which is based on vehicle speed and road geometry data with varying levels of detail. Another power-based approach, developed by An and Ross (1993b), established a simple analytic relationship between fuel economy, vehicle parameters, and driving cycle characteristics.

Modal Fuel Consumption Models

A modal fuel consumption model considers the different types of operating conditions a vehicle would experience on a typical trip. This type of model assumes that the driving mode elements are independent of each other and the sum of the component consumption equals the total amount of fuel consumed. The advantage of this model is its simplicity, generality, and conceptual clarity, as well as the direct relationship to existing traffic modeling techniques [Richardson et al. 1981]. This model is applicable to individual transportation projects similar to the instantaneous fuel consumption models.

The first drive mode is the duration of travel at constant speed. The second mode is the phase of either a full or partial stop-and-go from the constant speed (acceleration and deceleration duration). Finally, the stopped time or time spent idling is also counted to estimate an accurate fuel consumption. However, if these speeds are not available, they may be reasonably estimated from time or distance observations, or substituted for by the number of complete stops [Baker 1994].

The greatest shortcoming of the modal fuel consumption model is that it is difficult to introduce any differences in driver's behavior such as the acceleration and deceleration maneuvers of different drivers, or behaviors of the same driver under different situations. Baker (1994) tried to overcome this weakness employing driver's aggressiveness, such as aggressive, normal, and passive behavior modes. Nevertheless, each stop-and-go maneuver for every driver was considered the same.

Average Speed Models

Average speed models can be implemented as macroscopic fuel consumption models rather than the microscopic models such as instantaneous models and modal models. In these models, fuel consumption rates are functions of trip times, trip distance and average speed. These models are suitable for assessing the impacts on fuel consumption of various macroscopic transport management schemes. Average travel speed models should only be used for average speeds of less than 50 km/h, since these models do not adequately reflect an increase in aerodynamic drag resistance at high speeds [Akcelik 1985].

2.3.3 Status of Current Research, Modeling Methodologies, and Modeling Efforts

One of the main trends in the current research directed toward the design of better fuel consumption and emission models has focused on the effects of driving patterns on emissions as sharp accelerations and high speeds take place. Both of these conditions are not well represented by current driving cycles, and they are suspected of being major reasons for typical underestimation of emission levels [LeBlanc et al. 1994]. After surveys of driving behavior in selected cities, the EPA has confirmed that sharp acceleration and high speeds are not well represented in the baseline of the FTP drive cycle. The current maximum acceleration and speed of the FTP cycle, 5.3 kph/s and 90.7 kph (3.3 mph/s and 56.7 mph), are frequently exceeded in real-world driving conditions [EPA 1993b].

Recently, several modal-emission models have been used by many researchers. St. Denis and Winer have created both a speed-acceleration and a speed-load modal emissions model using data from a single Ford vehicle. Further, researchers at Sierra Research have extended the VEHSIM model, originally developed at GM to compute engine speed and load, to create a VEHSIME model that predicts emission rates for specified driving cycles. The model computes the second-by-second engine speed and load required to drive the cycle, then, using an emissions map (with interpolation), second-by-second emissions are approximated. The EPA has similarly extended the VEHSIM model to create a modal emission model called VEMISS. Researchers from the University of California, Riverside, have developed a power demand-based modal emission model that predicts second-by-second emissions given a specified vehicle operation [Barth et al. 1996]. Researchers at the University of Michigan have developed a physical model that predicts fuel economy given any driving cycle or trip characteristics, and they have recently extended the model to predict CO emissions. A new approach to modal-emission modeling is proposed by Barth (1996). This model, which is deterministic and based on analytical functions, describes the physical phenomena associated with vehicle operation and emissions productions [Barth et al. 1996, Barth et al. 1998]. Recently, the Georgia Tech Research Partnership has been developing a vehicle emissions model within a geographic information system (GIS) framework. This model, named the Mobile Emission Assessment System for Urban and Regional Evaluation (MEASURE), predicts emissions as a function of the vehicle operating mode (including cruise, acceleration, deceleration, idle, and power demand conditions that lead to fuel enrichment, or high A/F ratios) employing specific vehicle characteristics and speed/acceleration profiles [Guensler et al. 1998].

For a modal fuel consumption and emissions model, a conventional method for characterizing vehicle operating modes of idle, cruise, and different levels of acceleration/deceleration is to set up a speed/acceleration mode matrix. The matrix measures emissions associated with each mode. The result is the total amount of emissions produced for the specified vehicle activity with the associated emission matrix. The problem with such an approach is that it does not properly handle other variables that can affect emissions, such as road grade or use of accessories. In order to overcome this shortcoming, correction factors can be used, but this can be also problematic since their effect will typically be based on secondary testing not associated with the core model [Barth et al. 1996].

Another modal modeling method is an emissions map based on engine power and speed. Second-by-second emission tests are performed at numerous engine operating points, taking an average of steady state measurements. This model can estimate emission rates based on engine power and speed, the effects of acceleration, grade, and use of accessories. The problem associated with this approach is a deficiency in the relationship of the emission rate to vehicle speed and acceleration rates, or engine speed and engine load. Without knowing the underlying mathematical relationships, this methodology assumes a simple two-dimensional linear relationship among them. Due to measurement difficulties, most speed acceleration matrices or emission maps have only a very limited number of cells, resulting in the repetitive use of the above procedure in real applications. The error associated with a single cell or engine operational point could be accumulated into major computing errors in the final results [Barth et al. 1996].

2.3.4 Traffic Simulation Models with Fuel Consumption and Emissions Estimation Procedures

Traffic simulation models are generally used to estimate traffic flow changes on affected facility links as the result of highway capacity expansions and to provide a tool for evaluating the operation of a traffic system in terms of its individual components. Simulation models provide individual behaviors and interrelationships of road vehicles to predict the performance of the system. Fuel consumption and emissions are important outcomes of new highway facilities or ITS deployments and can be predicted using traffic simulation models.

NETSIM, a computer simulation model developed by the Federal Highway Administration (FHWA), is a microscopic model that performs a detailed simulation of traffic flow on urban streets. The original model has been improved, resulting in a new model called TRAF-NETSIM. TRAF-NETSIM provides traffic operation information by vehicle type (automobile, bus, and truck: each type has 16 potential sub-types with different operating and performance characteristics) and by the driver behavior characteristics (passive, normal, and aggressive). The vehicle performance, individual driver, and other characteristics such as turning movements, free speed, and headways are assigned stochastically. Every second, the trajectory of the vehicle is computed according to car following logic while responding to traffic control devices, pedestrian activity, transit operations, the performance of other neighboring vehicles, and a number of other conditions which influence driver behavior. Fuel consumption and emission rates are calculated based on a look-up table at each time step according to the speed and acceleration of the vehicle [Baker 1994, West et al. 1997].

FREQ (May, 1990) is a macroscopic, analytic, deterministic, freeway simulation and optimization program developed at the University of California at Berkeley. FREQ is designed to evaluate freeway operations in a single direction of travel and is widely used to evaluate the impacts of temporary freeway lane blockages, various freeway lane and ramp configurations, and high-occupancy vehicle (HOV) treatments. This model estimates the absolute volume of fuel consumption and vehicle emissions based on the total vehicle miles traveled and average speeds.

INTEGRATION (Van Aerde, 1998) is a microscopic traffic simulation and traffic assignment model developed in the mid 1980s. Unique characteristics of the INTEGRATION model is its approach to representing both freeway and signalized links using the same logic. Both the simulation and traffic assignment components are microscopic, integrated, and dynamic [Van Aerde 1998]. In this model, each individual vehicle follows pre-specified macroscopic traffic flow relationships, and due to this concept, which uses individual vehicles and macroscopic flow theory, this model is sometimes considered a mesoscopic model. Currently, the INTEGRATION model provides estimates of fuel consumption and vehicle emissions. Fuel consumption and emission rates are computed every second on the basis of the individual vehicle's current instantaneous speed. This computation also includes modal-based estimations considering accelerations and cold-start modules. Current default coefficients used to estimate fuel consumption and emission rates are derived from the Oldsmobile Toronado (1992) [Van Aerde 1998].

2.4 Summary of Chapter 2

The above review of the literature has shown the complex nature of the factors which affect the vehicle fuel consumption and emissions. Fuel consumption and emissions deriving from transportation sources are the functions of several variables such as travel-related factors, highway network characteristics, and vehicle characteristics. Especially, the factors such as vehicle speed and acceleration, start-up emissions, engine loads (air/fuel ratio) and the ambient temperature of the surrounding environment were identified as significant factors.

The next chapter describes several models that predict the fuel consumption and emission rates based on individual vehicle speed and acceleration profiles, which is one of the most significant factors. These models can be utilized to predict the fuel consumption on a second-by-second basis for individual vehicles and, therefore, are suitable for implementation in microscopic traffic simulation models.

Chapter 3. Model Development

3.1 Introduction

This chapter discusses the Oak Ridge National Laboratory data were utilized to develop the fuel consumption and emission models and several mathematical models that predict the MOEs based on individual vehicle speed and acceleration profiles.

The first section describes some of data sources that were utilized in the modeling approach. The second section describes several mathematical approaches to estimate vehicle fuel consumption and emissions. Finally, the chapter provides some of the validation results against some urban driving cycles.

3.2 Data Description

The data used for fuel consumption and emissions modeling was provided by the Oak Ridge National Laboratory (1997). These data are in the form of look-up tables for fuel consumption and emission rates as functions of vehicle speed and acceleration. Emissions data comprises hydrocarbon (HC), oxides of nitrogen (NOx) and carbon monoxide (CO). A total of eight vehicles of various weights and engine sizes were available for modeling [West et al. 1997]. These eight vehicles are representative of current internal combustion (IC) engine technology. The average engine size for all vehicles is 3.3 liters; the average number of cylinders is 5.8, and the average curb weight is 1497 kg (3300 lbs) [West et al. 1997]. Industry reports show that the average sales-weighted domestic engine size for 1995 was 3.5 liters, with an average of 5.8 cylinders [Ward's Automotive Yearbook 1996, Ward's Automotive Reports 1995]. Detailed specifications of test vehicles are provided in Appendix A of this document.

The raw data collected at the Oak Ridge National Lab (ORNL) contain 1300-1600 individual vehicle data points, each collected every second during various driving cycles. Typically, vehicle acceleration values range from –5 to 12 ft/s^2 (at intervals of 1 ft/s^2), and velocities vary from 0 to 110 ft/s. A sample data set for a popular minivan vehicle is shown in Figures 3-1 through 3-4. Note the large nonlinear behaviors observed for some of the energy and emission metrics as a function of speed and acceleration. Also note various ‘peaks’ and ‘valleys’ for fuel consumption, CO, HC and NOx as a result of gear shifts under various driving conditions. It is interesting to note that the ORNL data represent particular speed-acceleration conditions defining a unique vehicle performance envelope. For example, high power-to-weight ratio vehicles have better acceleration characteristics at high speeds than their low power-to-weight ratio counterparts. This inherent performance boundary is extremely important when these models are used in conjunction with microscopic traffic flow models, as they represent a physical kinematic constraint in the car-following equations of motion. A typical speed-acceleration performance boundary is shown in Figure 3-5 for a hypothetical composite vehicle. The composite vehicle data have been derived be taking average fuel consumption and emissions rates for all eight vehicles at various speeds and accelerations.

A graphical representation of the sample data (Villager) available from Oak Ridge National Lab is shown in Figures 3-1 through 3-4. Surface plots of the fuel consumption, CO, HC and NOx emission rates are shown in these Figures.

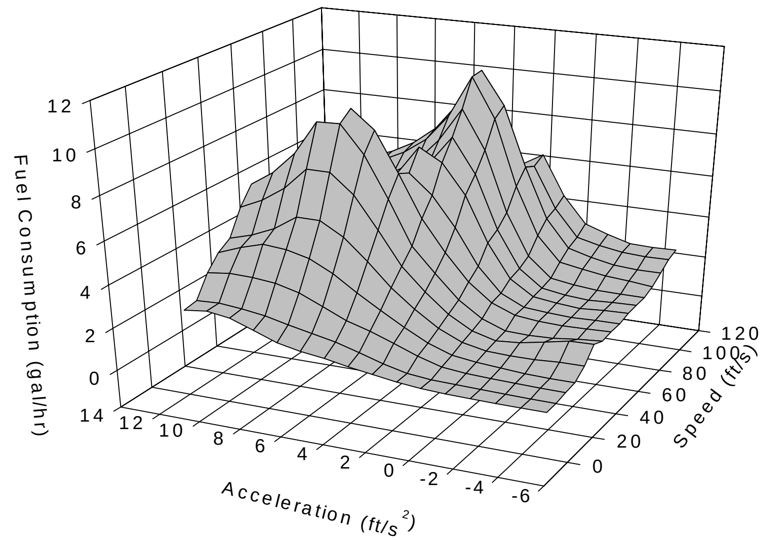

Figure 3-1 Fuel Consumption Data (Villager).

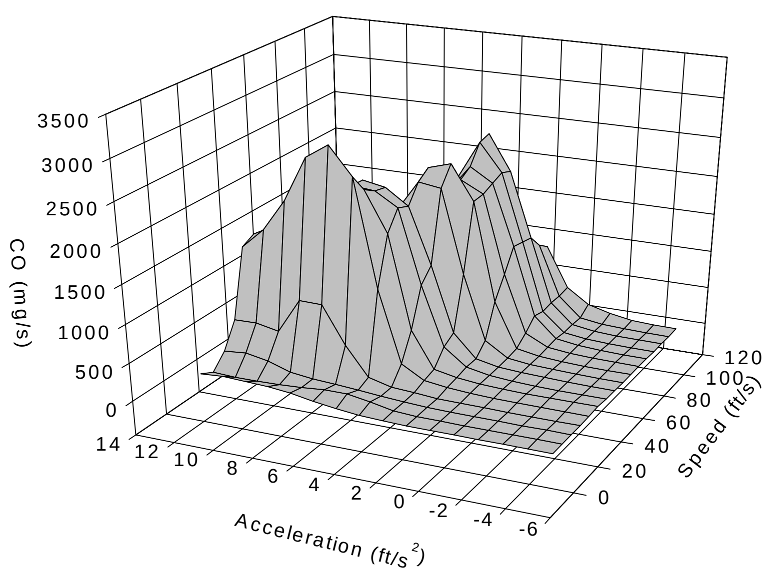

Figure 3-2 CO Emission Rate Data (Villager).

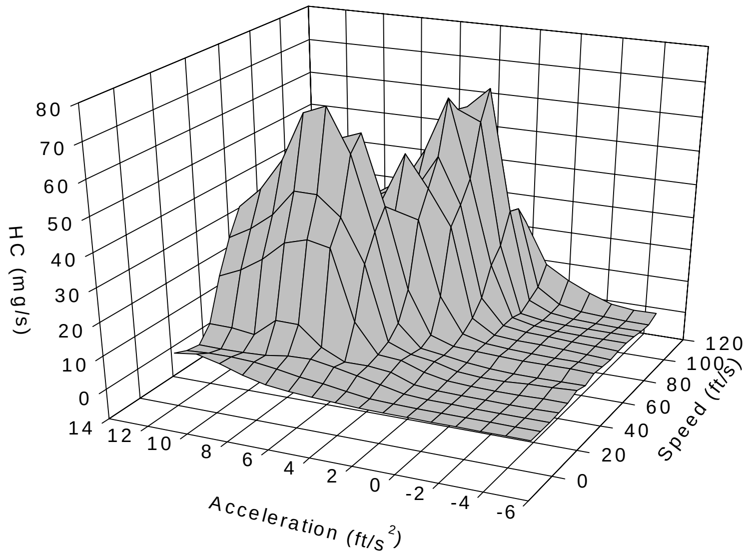

Figure 3-3 HC Emission Rate Data (Villager).

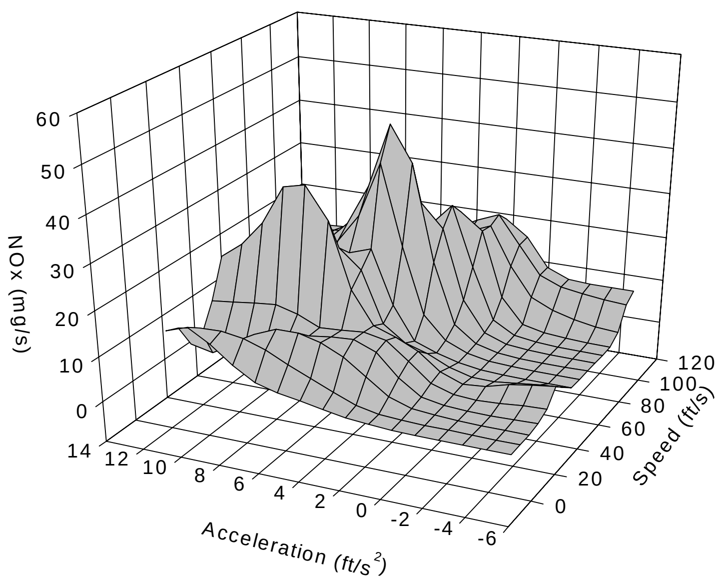

Figure 3-4 NOx Emission Rate Data (Villager).

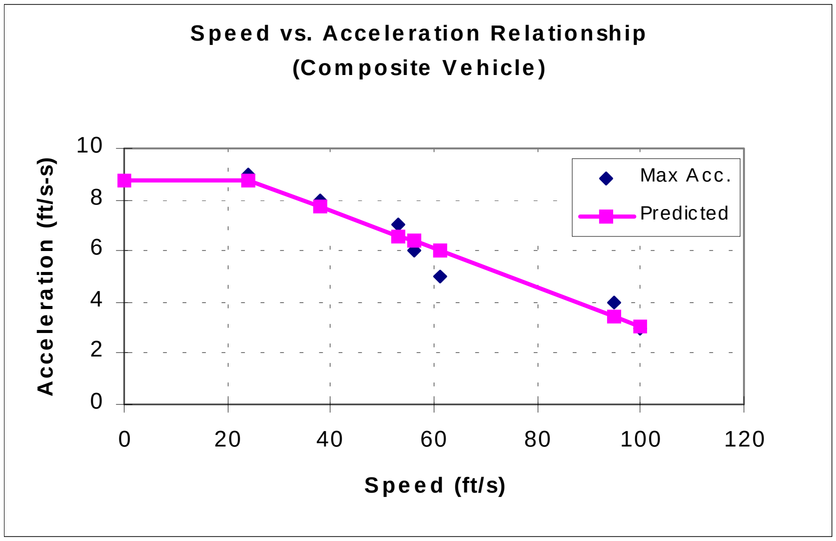

Figure 3-5 Speed and Maximum Acceleration Envelope for Composite Vehicle.

3.3 Model Description

This section describes several models for predicting the fuel consumption and emissions rates for any trip based on individual vehicle speed and acceleration profiles. These models can be utilized to predict the fuel consumption and emissions on a second-by-second basis for individual vehicles, and therefore are suitable for implementation in microscopic analysis. This approach can be more accurate for predicting the fuel consumption and emission rates than current models based on vehicle average speed or modal events (i.e., cruise, acceleration, deceleration, and idle). The models developed in this research document use speed and acceleration profiles as input data, and in a typical application, fuel consumption or the emission rates are model outputs. Second-by-second results are accumulated to predict the total fuel consumed or the total emissions released during a prescribed FTP cycle. Two types of mathematical models have been studied as part of this research effort:

- Nonlinear regression models, and
- Neural network models

The following paragraphs describe in detail the models studied.

3.3.1 Regression Model I

A first regression model was developed to predict the expected fuel consumption and emission rates using a combination of quadratic and cubic speed-acceleration terms. In this model, a regression coefficient technique was adopted. The raw data collected by the Oak Ridge National Lab have approximately 1300 to 1600 data points, with vehicle deceleration values ranging from -5 ft/s^2 to 12 ft/s^2 (at intervals of 1ft/s^2) and velocities spanning from 0 ft/s to 110 ft/s. Each speed has 18 data points, which correspond to 18 values of their acceleration.

A quadratic regression model (Model A) to predict fuel consumption or emission rates can be expressed in the following form,

$$\boldsymbol{F_A = a_s + b_s Acc + c_s Acc^2} \qquad \textbf{(3-1)}$$

where

F_A : fuel consumption or emission rates (gal/hr or milligram/s) for every speed sampled (111speeds)

a_s : intercept

b_s,c_s : coefficients of the regression equation

Acc : acceleration (ft/s^2)

In addition, Equation 3-1b represents a cubic regression model (Model B).

$$\boldsymbol{F_B = a_s + b_s Acc + c_s Acc^2 + d_s Acc^3} \qquad \textbf{(3-1b)}$$

These models were fitted for every speed (i.e. 0 ft/s to 110 ft/s). From these models, 111 intercepts and coefficients were extracted accordingly. Inspection of these results found that the intercepts and coefficients change according to certain patterns. To simplify these 111 regression models, another regression model was fitted using the intercepts and coefficients as data. In this model, the intercept and coefficients are independent variables, and speed is the dependent variable. This integrated model (Model C) can be expressed in quadratic form, as shown in Equation 3-2a.

$$\boldsymbol{F_C = (a_1+b_1S + c_1S^2) + (a_2+b_2S+c_2S^2)Acc + (a_3+b_3S+c_3S^2)Acc^2} \qquad \textbf{(3-2a)}$$

where

$a_s = a_1+b_1S + c_1S^2$

$b_s = a_2+b_2S+c_2S^2$

$c_s = a_3+b_3S+c_3S^2$

Using the same approach, combinations of quadratic and cubic models are presented in Equations 3-2b through 3-2d.

(Model D)

$$F_D = (a_1+b_1S+c_1S^2) + (a_2+b_2S+c_2S^2)Acc + (a_3+b_3S+c_3S^2)Acc^2 + (a_4+b_4S+c_4S^2)Acc^3 \quad \textbf{(3-2b)}$$

(Model E)

$$F_E = (a_1+b_1S+c_1S^2+d_1S^3) + (a_2+b_2S+c_2S^2+d_2S^3)Acc + (a_3+b_3S+c_3S^2+d_3S^3)Acc^2 \quad \textbf{(3-2c)}$$

(Model F)

$$F_F = (a_1+b_1S+c_1S^2+d_1S^3) + (a_2+b_2S+c_2S^2+d_2S^3)Acc + (a_3+b_3S+c_3S^2+d_3S^3)Acc^2 + (a_4+b_4S+c_4S^2+d_4S^3)Acc^3 \quad \textbf{(3-2d)}$$

In a similar manner as described for Models A and B, a speed-based model was fitted to the data using speed as the dependent variable. This new model (Model G) is presented in Equation 3-3a.

(Model G)

$$F_G = a_a + b_aS + c_aS^2 \quad \textbf{(3-3a)}$$

where

F_G : fuel consumption or emission rates (gal/hr or millgram/s) for a certain speed per one second

a_a : intercept

b_a, c_a : coefficients of equation

S : speed (ft/s)

A simple cubic model using speed as the only dependent variable is,

(Model H)

$$F_H = a_a + b_a S + c_a S^2 + d_a S^3 \qquad \textbf{(3-3b)}$$

Furthermore, integrated models incorporating combinations of quadratic and cubic terms are described as follows:

(Model I)

$$F_I = (a_1+b_1Acc+c_1Acc^2) + (a_2+b_2Acc+c_2Acc^2)S + (a_3+b_3Acc+c_3Acc^2)S^2 \qquad \textbf{(3-4a)}$$

where

$a_a = a_1+b_1Acc+c_1Acc^2$

$b_a = a_2+b_2Acc+c_2Acc^2$

$c_a = a_3+b_3Acc+c_3Acc^2$

(Model J)

$$F_J = (a_1+b_1Acc+c_1Acc^2) + (a_2+b_2Acc+c_2Acc^2)S + (a_3+b_3Acc+c_3Acc^2)S^2 + (a_4+b_4Acc+c_4Acc^2)S^3 \qquad \textbf{(3-4b)}$$

(Model K)

$$F_K = (a_1+b_1Acc+c_1Acc^2+d_1Acc^3) + (a_2+b_2Acc+c_2Acc^2+d_2Acc^3)S + (a_3+b_3Acc+c_3Acc^2+d_3Acc^3)S^2 \qquad \textbf{(3-4c)}$$

(Model L)

$$F_L = (a_1+b_1Acc+c_1Acc^2+d_1Acc^3) + (a_2+b_2Acc+c_2Acc^2+d_2Acc^3)S + (a_3+b_3Acc+c_3Acc^2+d_3^3)^2 + (a_4+b_4Acc+c_4Acc^2+d_4Acc^3)S^3 \qquad \textbf{(3-4d)}$$

Table 3-1 provides a summary of all the statistical models that were considered in selecting a best model to capture the fuel consumption and emission rates. Table 3-1 includes the number of parameters, and the sum of squared errors and correlation coefficients used as measures of effectiveness (MOEs). The sum of squared errors returns the sum of the squares of the differences of corresponding values (i.e. the raw data and the predicted value). The equation for the sum of squared differences is:

Sum of squared errors = $\sum(x_i - y_i)^2$ **(3-5)**

where

x_i = predicted values (gal/hr or millgram/s) of fuel consumption and emission model

y_i = raw data values (gal/hr or millgram/s)

The equation to estimate the correlation coefficient is:

$$\rho_{xy} = \frac{COV(X,Y)}{\sigma_x \sigma_y} \qquad \textbf{(3-6)}$$

where :

$-1 \leq \rho_{xy} \leq 1$

and:

$$COV(X,Y) = \frac{1}{n}\sum_{i-1}^{n}(x_i - \mu_x)(y_i - \mu_y) \qquad \textbf{(3-6a)}$$

where:

σ_x, σ_y : standard deviation of the predicted values and the raw data

x_i, : predicted values (gal/hr or millgram/s) of the fuel consumption and emission model

y_i : raw data values (gal/hr or millgram/s)

μ_x, μ_y : mean of the predicted values and the raw data

Table 3-1 Summary of the Fuel Consumption Modeling Results of Regression I.

Method	No. of Parameters	Sum of Squared Errors	Correlation Coefficient
Model A	333	N/A	N/A
Model B	444	N/A	N/A
Model C	9	44.15979	0.996904
Model D	12	53.67932	0.996334
Model E	12	33.33944	0.997619
Model F	16	52.46797	0.996831
Model G	45	1857.388	0.942227
Model H	60	1960.971	0.932148
Model I	9	66.59052	0.995358
Model J	12	3434.103	0.828656
Model K	12	70.96154	0.995098
Model L	16	1837.55	0.928849

As inspection of Table 3-1 indicates that Model E is the best fuel consumption model among all Regression I analysis models, judging by the sum of squared errors and correlation coefficients. This regression produced an acceptable correlation coefficient (0.998), and the lowest sum of squared errors (33.340). Among the decision criteria, the number of parameters is also very important from the computational effort point of view. According to the computing time criteria, Model C provided a reasonable sum of squared errors and a correlation coefficient with a small number of regression coefficients.

Figures 3-6 and 3-7 describe the predicted fuel consumption and the raw data.

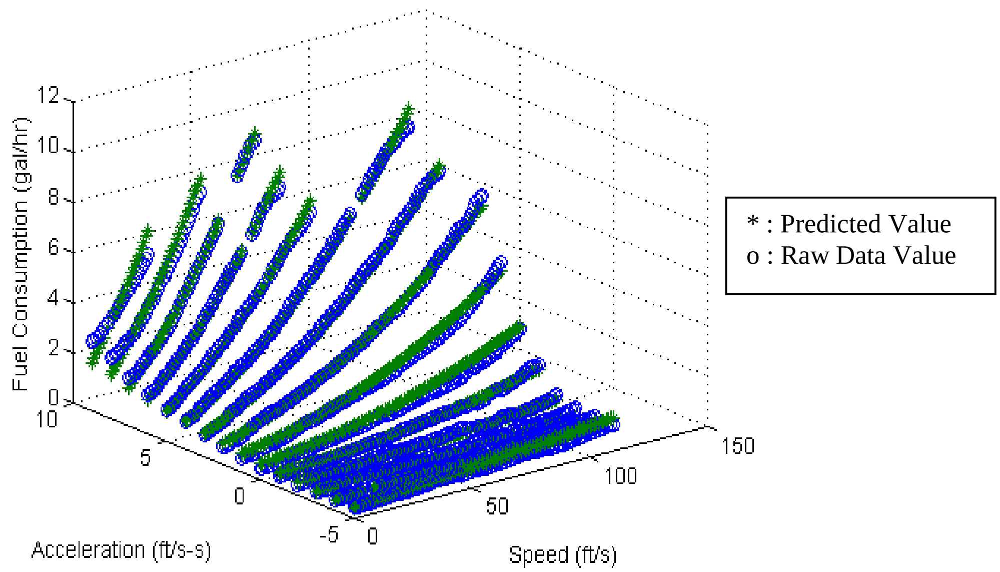

Figure 3-6 Predicted Fuel Consumption for Model C.

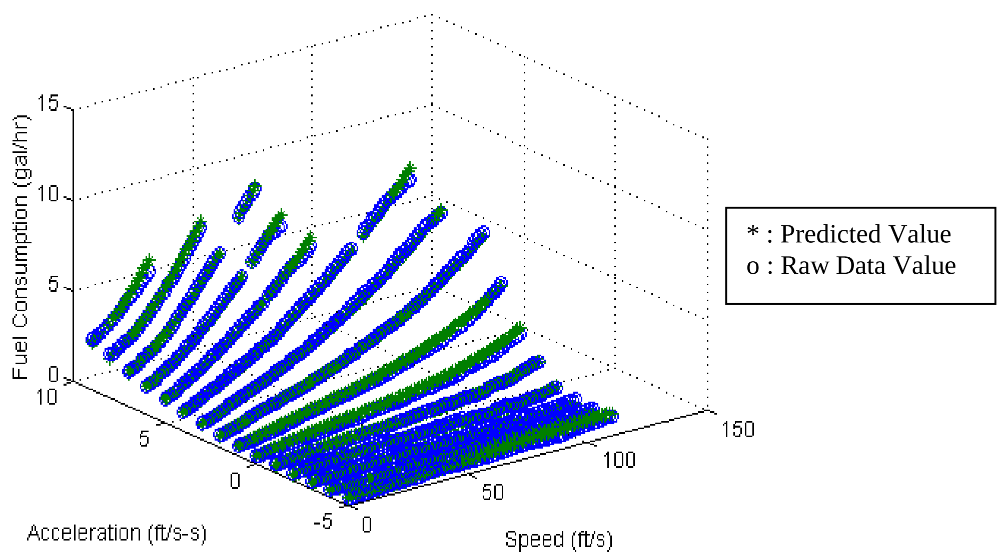

Figure 3-7 Predicted Fuel Consumption for Model E.

Using Models C and E, the CO emissions rate data of a composite vehicle were fitted. The summary of the results are shown in Table 3-2. Parameters are found in Appendix B.

Table 3-2 Summary of the Emission (CO) Modeling Results of Regression I.

Method	No. of Parameters	Sum of Squared Errors	Correlation coefficient
Model E	12	87376723	0.933079
Model C	9	77159193	0.943977

Both models produced reasonable correlation coefficients that determine the relationship of the predicted values and the CO data. However, it was found that some predicted values were negative, a very undesirable condition. This analysis was later corrected with the introduction of natural logarithms in the modeling process. In order to reduce the sum of squared errors, other attempts were initiated.

Figures 3-8 and 3-9 describe the predicted CO emission rates and the raw data.

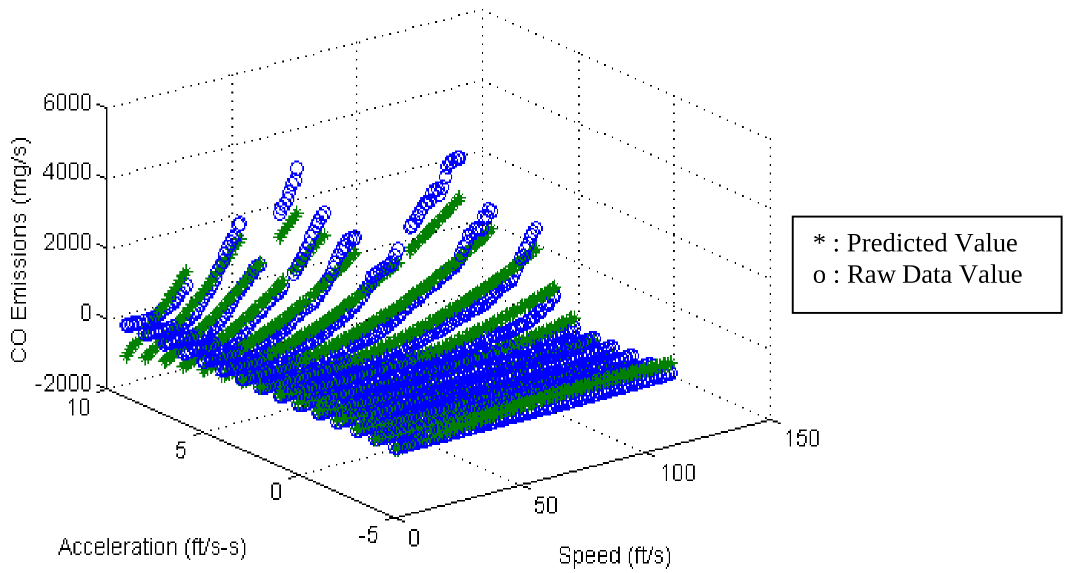

Figure 3-7 Predicted CO Emission Rates of Model C.

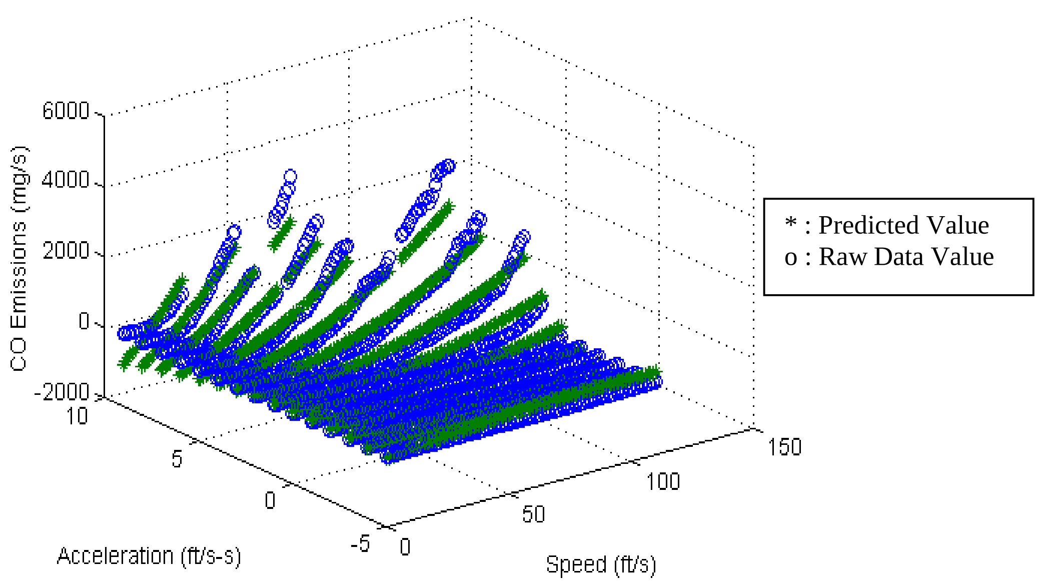

Figure 3-8 Predicted CO Emission Rates of Model E.

3.3.2 Regression Model II

In the previous section, integrated multiple regression models were developed to predict the fuel consumption and emission rates. In this section, a polynomial regression technique was attempted to predict the fuel consumption and emission rates.

Each raw data point is a function of acceleration and speed. Using this concept, the following polynomial equation was established.

(Model M)

$$F=a+bA+cA^2+dA^3+eS+fS^2+gS^3+hAS+iAS^2+jAS^3+kA^2S+lA^2S^2+mA^2S^3+nA^3S+oA^3S^2+pA^3S^3 \quad \textbf{(3-7)}$$

where

F : fuel consumption or emission rates (gal/hr or milligram/s)

a : intercept

$b,c,\ldots,p$: coefficients

A : acceleration (ft/s^2)

S : speed (ft/s)

A summary of this regression model is presented in Table 3-2. The results shown in Table 3-2 are the output of the model fitted to predict fuel consumption and CO emission rate data for a composite vehicle.

Table 3-3 Summary of Fuel Consumption and CO Emission Rate Model Results (Model M).

	Fuel Consumption Results	CO Emission Results
Correlation Coefficient	0.998	0.993
Sum of Squared Errors	25.975	8652558

The table shows that this model (Model M) predicted a better estimate of the raw data than Model E in terms of the correlation coefficient and the sum of squared errors. This fuel consumption model produced a satisfactory sum of squared errors. Nevertheless, the predicted values of the CO model still produced some negative values. In order to remove negative emission rates, a data transformation technique was adopted.

Figures 3-10 and 3-11 compare the predicted values and the raw data.

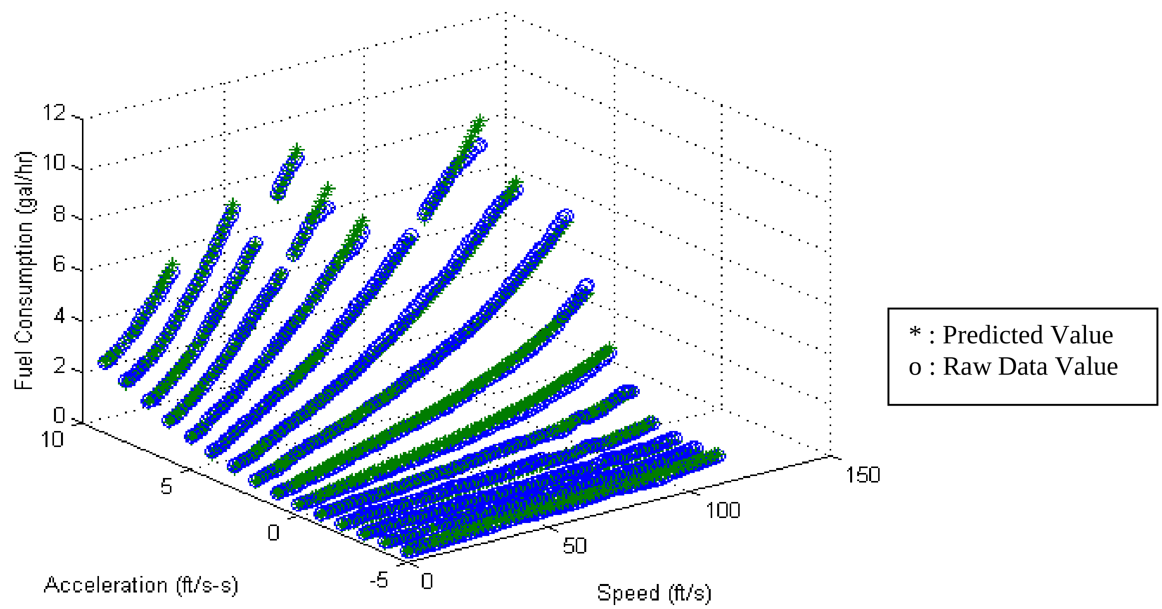

Figure 3-10 Predicted Fuel Consumption of Model M.

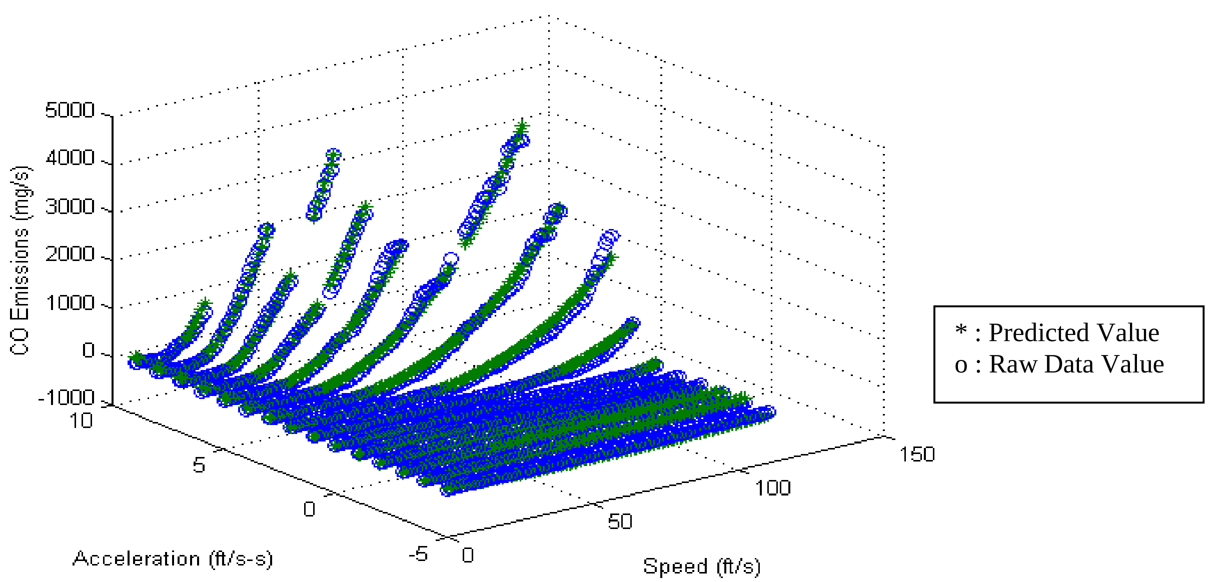

Figure 3-11 Predicted CO Emission Rates of Model M.

3.3.3 Regression Model III

The main drawback of the previous models was the generation of negative numbers for some dependent variables. This situation is both undesirable and unrealistic. In order to overcome this weakness, a data transformation technique using a log function was adopted. First, the data were transformed using the natural log. Second, a regression model using the same characteristics as the previous model (Model M) was fitted to the transformed data. Finally, the predicted values were transformed by the exponential function. Using this concept, the following logarithmic polynomial equation was established:

$$\log(MOE_e) = \sum_{i=0}^{3}\sum_{j=0}^{3}(k_{i,j}^{e} * s^{i} * a^{j}) \qquad \textbf{(3-8)}$$

where

MOEe = fuel consumption or emissions rates (l/hr or mg/s)

k = model regression coefficients

s = speed (m/s)

a = acceleration (m/s^2)

The first attempt at modeling the CO emission rates produced an unsatisfactory sum of squared errors (712,671,321), but included some statistically insignificant terms. After the removal of the two insignificant terms, this model reduced the sum of squared errors significantly (i.e., 92,099,193).

A summary for this model (Model N) is provided in Table 3-4.

Table 3-4 Summary of Fuel Consumption and CO Emission Rate Model Results (Model N).

	Fuel Consumption Results	CO Emission Results
Correlation Coefficient	0.997603	0.9493807
Sum of Squared Errors	33.65873	92099193

As shown in Table 3-4, this model did not improve the measures of effectiveness significantly. Nevertheless, the CO model did not generate negative emission rates, so it improved the predictive capabilities of previous models.

This model uses the polynomial variables derived from speed and acceleration variables, which can result in multi-collinearity. However, removing the variables to reduce the variance inflation (VIF) which is a measure of multi-collinearity, reduces the model's performance. Therefore, this model reserves the polynomial variables despite problems with multi-collinearity. Figure 3-12 illustrates the model's performance with or without multi-collinearity.

Figures 3-13 and 3-14 compare the predicted values using this model and the raw data. The errors of this model are shown in Appendix B.

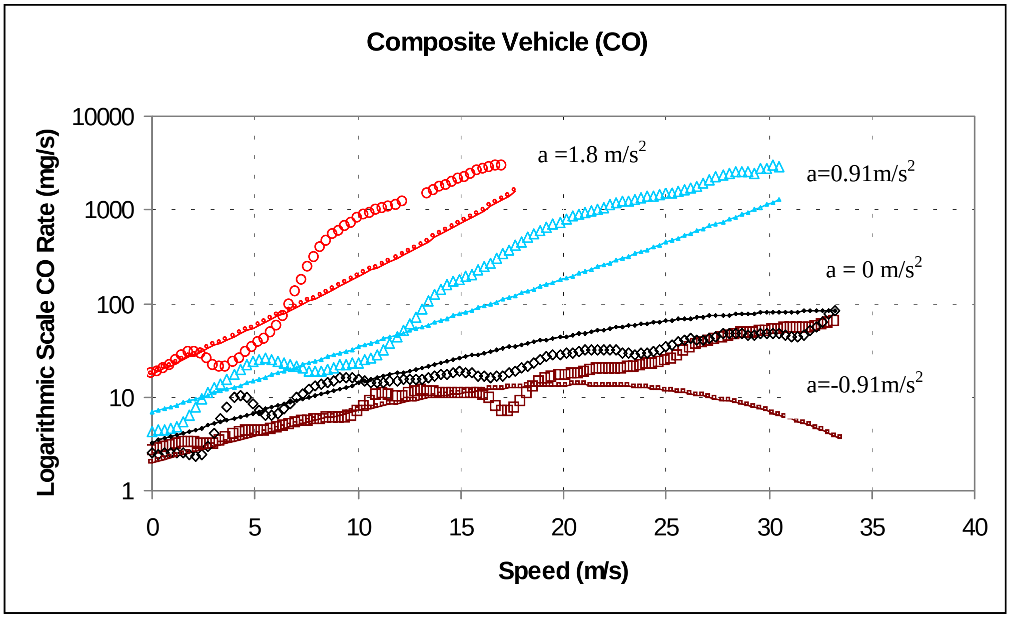

Predicted CO of Regression Model with Eight Variables (No Multi-Collinearity)

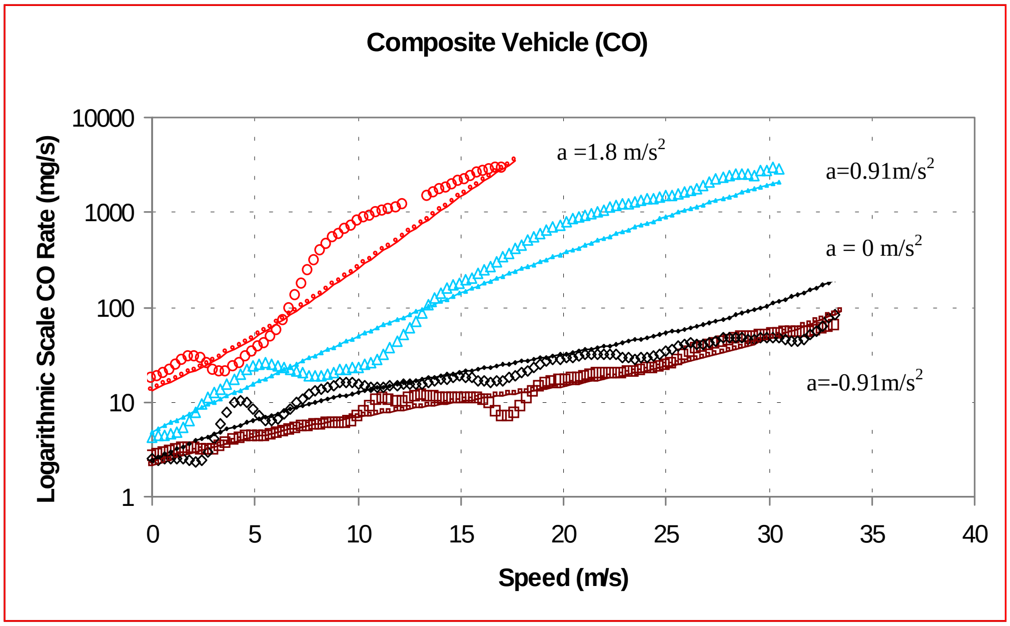

Predicted CO of Regression Model with Sixteen Variables

Figure 3-12 CO Predictions of Regression Models with and without Multi-Collinearity.

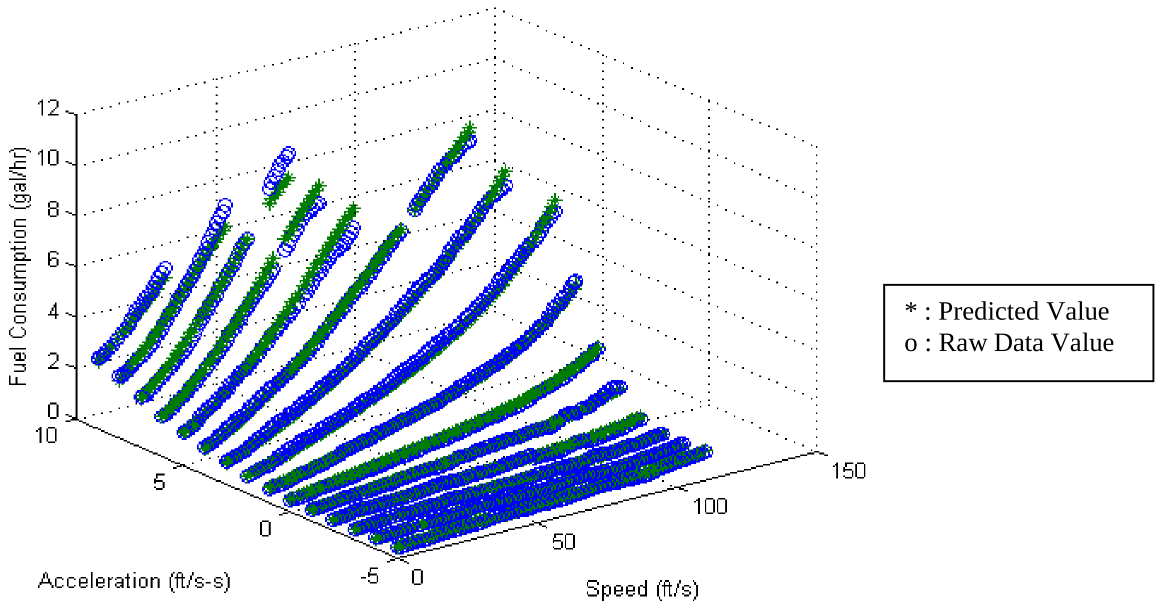

Figure 3-13 Predicted Fuel Consumption of Model N.

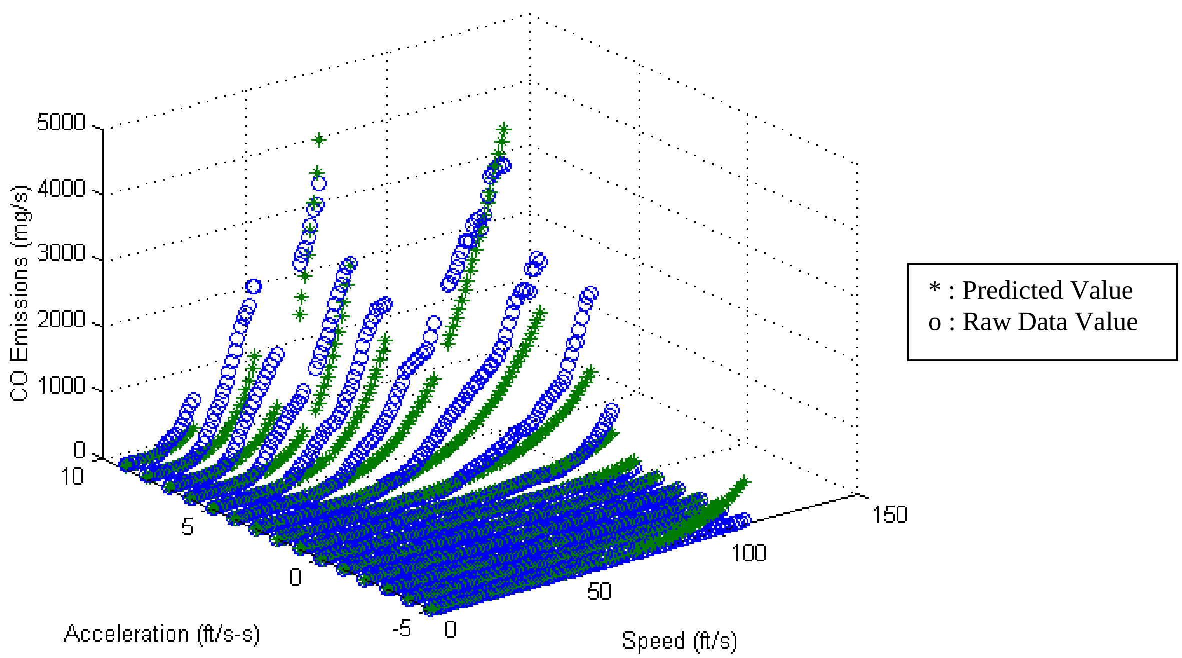

Figure 3-14 Predicted CO Emission Rates of Model N.

3.3.4 Neural Network Model

Neural networks are composed of many simple elements supporting an information processing system that has special characteristics. These elements are motivated by human biological nervous systems. The network function is determined by the connections between elements. This function is decided by a training step which is a significant process in the neural network modeling. In other words, the neural network is trained to perform a particular function by adjusting the values of the connections among elements. Trained networks tend to produce reasonable answers when presented with inputs that they have never experienced. A new input will produce an output similar to the collected output data for a corresponding input vector. Consequently, the trained neural networks tend to predict the expected data in a reasonable error range.

A neural network might be a good candidate to estimate fuel consumption and emission rates, due to the following arguments:

- Data is heavily nonlinear with several oscillations along the speed axis.
- Data needs to be fitted with a fast computational procedure for later implementation in micro-simulation models.
- The accuracy of the algorithm needs to be sufficient to support second-by-second simulations.

In order to predict the fuel consumption and emission rates, a neural network was trained to mimic the raw data. The MATLAB Neural Network Toolbox was used to perform the neural network training analysis. MATLAB is a general mathematical package produced by the Mathworks Company [Mathworks, 1997]. This tool is very efficient in handling matrices, and was used throughout this research project to handle data manipulation tasks and neural network computations.

Throughout this research project, several programs or 'templates' were developed in MATLAB to perform the following neural net computations:

- Network training/learning.
- Testing and evaluation of a trained network.
- Implementation to estimate car emissions.

For any given car, learning data sets are used to train the neural network to recognize patterns. Each template requires the following inputs:

- Number of inputs.
- Value for the learning coefficient.
- Number of processing elements (neurons) in the hidden and output layers.
- Maximum number of cycles (epochs) for each run.
- Required accuracy in the training procedure (i.e., sum of the squared errors for each run).

Backpropagation, which is the one of many training methods available in neural network analysis, was used for this modeling. Backpropagation for multiple-layer networks and nonlinear differentiable functions is simply a gradient descent method to minimize the sum of squared errors of the weights and biases produced by the neural network. Based on the analysis performed with several transfer function algorithms of backpropagation techniques the Levenberg-Marquardt algorithms (trainnlm: Matlab function) have been found to be an efficient and reliable training method to be used for this study [Trani and Wing-Ho 1997]. The design of an appropriate neural network topology involves: choosing the appropriate neurons' transfer functions, basic decisions about the amount of neurons to be used in each layer, and selecting the amount of hidden layers.

The best topology for car fuel consumption and emission rates comprises three layers with one hyperbolic tangent sigmoid and two log sigmoid transfer functions joining them. In neural network topology design, there are tradeoffs between numerical complexity and prediction performance. In general, the simplest neural network topology that produces good results should be selected. A mathematical form representing a three-layer neural network is shown in Equation 3-9.

$$\mathbf{MOE_e=F^3(W^3F^2(W^2F^1(W^1p+b^1)+b^2)+b^3)} \qquad \mathbf{(3\text{-}9)}$$

where:

MOEe = fuel consumption or emissions rates (l/hr or mg/s)

$W^{1,}$, W^2 and W^3 = model coefficients

b^1, b^2 and b^3 = bias matrices

p = an input vector containing pairs of (speed, acceleration) used as predictor variables

F^1 = nonlinear transfer function (hyperbolic tangent sigmoid, $F = \frac{1}{1+e^{-n}}$)

F^2 and F^3 = nonlinear transfer functions (logarithmic sigmoid, $F = \frac{e^n - e^{-n}}{e^n + e^{-n}}$)

Figure 3-15 illustrates a general neural network applied to fuel consumption and emissions function prediction. As shown in Figure 3-15, three nonlinear transfer functions (F), model coefficients (W), and bias matrices (b) are utilized to obtain an MOEe. Model coefficients and bias matrices are generated by a MATLAB Neural Network function (trainnlm) after a network training. Once an input vector (p) is multiplied to model coefficients (W^1) with a matrix form, the matrix (W^1p) is added to with a bias matrix (b^1), which is a training output, and forms another matrix form (W^1p+b^1). Then, this matrix is transformed by a nonlinear transfer function (F^1). These procedures are iterated three times to acquire a predicted MOEe.

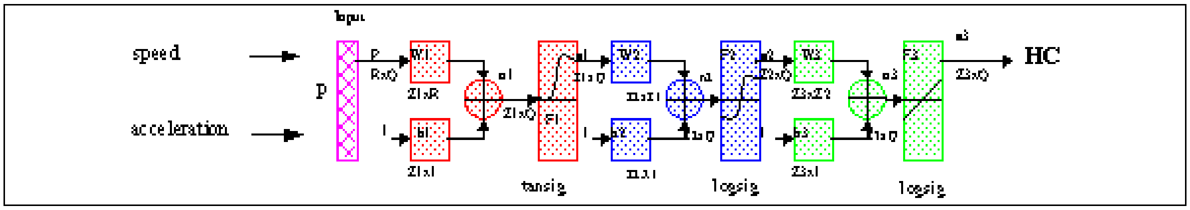

Figure 3-15 General Three-Layered Neural Network .

The source code of this neural network model (Model O) is provided in Appendix C, and the summary of the results of the model for the composite vehicle are shown in Table 3-5.

Table 3-5 Summary of Fuel Consumption and CO Emission Rate Model Results (Model O).

	Fuel Consumption Results	CO Emission Results
Correlation Coefficient	0.9998	0.9996
Sum of Squared Errors	3.3046	548620

As shown in Table 3-5, it was found that this neural network model (Model O) correlated well with the raw data presented. These models produced very high correlation coefficients (0.999, 0.999) and low sums of squared errors (3.3, 548620), which are the best values obtained so far. However, due to the neural network characteristic that traces the trained results, it is difficult to identify this as the best model. Therefore, further evaluations are considered.

Figures 3-16 and 3-17 compare the predicted values and the raw data. The errors between predicted values and the raw data are shown in Appendix B.

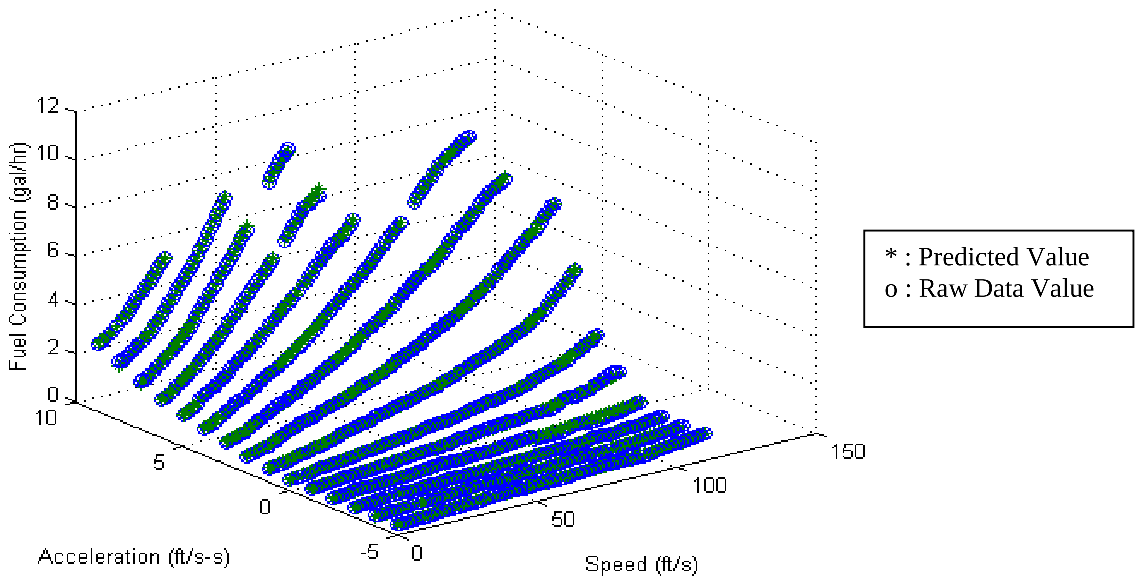

Figure 3-16 Predicted Fuel Consumption of Model O.

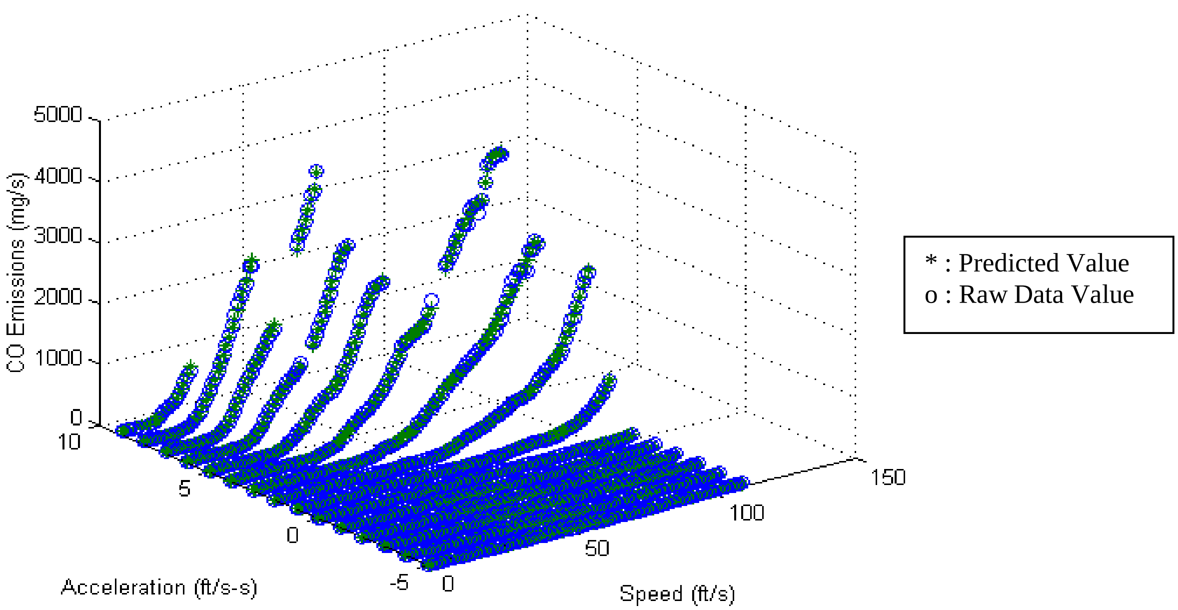

Figure 3-17 Predicted CO Emission Rates of Model O.

3.4 Model Verification

In the previous section, several models were developed that capture the fuel consumption and emission rates for individual vehicles. Before we implemented these models into micro-simulation ITS applications, it was necessary to validate the model based on the raw data collected.

In order to test the models developed, three test methods were adopted:

- FTP cycle test
- US06 cycle test
- Generalization test

3.4.1 FTP Cycle Test

The Federal Test Procedure (FTP) is the vehicle test procedure used by the environmental protection agency (EPA). This procedure is commonly used for light duty vehicle testing. The FTP is used to test vehicle emissions performance on a “typical” driving schedule, using a dynamometer to simulate actual road conditions.

The FTP is characterized by a 11.04 mile trip, consuming 1874 seconds, and traveling at an average speed of 21.2 mph. The cycle consists of three distinct segments: (a cold-transient phase, a stabilized phase, and a hot-transient phase). Because the mass emissions from each of the three segments are collected in separate bags, the three operating modes are often referred to in terms of "bags" (DOT, 1994). A complete FTP is comprised of:

- a cold-start or cold-transient phase ("Bag 1”), corresponding to the first 3.59 miles (505 seconds in length);
- a stabilized phase ("Bag 2"), which is the final 3.91 miles (867 seconds in

length); and

- a hot-start or hot-transient phase ("Bag 3"), corresponding to the first 3.59 miles .

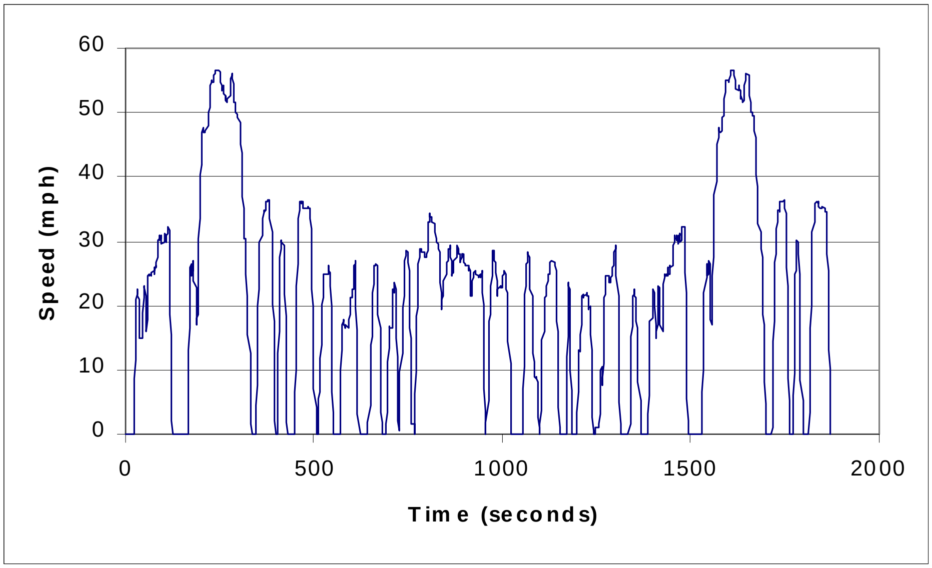

Figure 3-18 Speed Profile of the FTP Cycle.

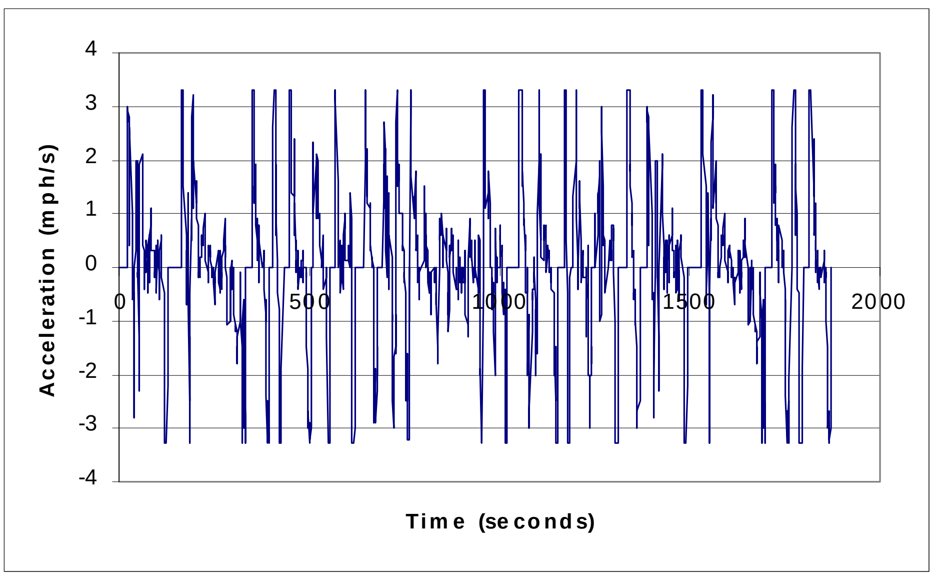

Figure 3-19 Acceleration Profile of the FTP Cycle.

Speed and acceleration profiles were used for input variables to predict fuel consumption and emission rates. The results of each model were compared to the interpolated raw data. Aggregate total error, the mean of 1 second-based errors, standard deviation, a correlation coefficient and CPU computing time were adopted as measures of effectiveness. The equation for the aggregate total error is:

$$Total\_error(\%) = \frac{abs(X - Y)}{Y} \times 100 \qquad \textbf{(3-10)}$$

where

X = sum of the predicted values during the entire FTP cycle

Y = sum of the interpolated values of the raw data during the entire FTP cycle

The one second-based error is computed according to the following expression,

$$Second - based\_error(\%) = \frac{abs(x - y)}{y} \times 100 \qquad \textbf{(3-11)}$$

where

x = predicted values for one second

y = interpolated values for one second

The results of five measures of effectiveness for Models C, E, M, N and O are shown in Table 3-6. This table shows the measures of effectiveness for the fuel consumption measure. Graphical results of fuel consumption errors are shown in Appendix D.

Table 3-6 Summary of FTP Cycle Test of Fuel Consumption Models for Composite Vehicle.

	Regression Models				Neural Net Model
	Model C	Model E	Model M	Model N	Model O
CPU Time (seconds)	0.0056	0.0162	0.0315	0.0306	0.0884
Total Error	6.26	4.6306	4.1949	0.5758	2.3707
1-s Based Error	14.1	9.3541	8.6548	5.5316	4.2164
Standard Deviation	0.75	0.78	0.784	0.72478	0.7239
Correlation Coefficient	0.985	0.989	0.994	0.995	0.992

As shown in Table 3-6, all the models produced reasonable MOEs. In terms of computation time, Model C exceeded the other models at least twice though it ranked in the last place among most MOEs. After thorough inspection of the table, it was found that Model N produced the most acceptable MOEs among the models.

A summary of CO models is presented in Table 3-7.

Table 3-7 Summary of FTP Cycle Test for CO Emission Rate Models for Composite Vehicle.

	Regression Models				Neural Net Model
	Model C	Model E	Model M	Model N	Model O
CPU Time (seconds)	0.0055	0.0157	0.0306	0.0315	0.0890
Total Error	140	86.55	39.44	3.4618	19.8668
1-s Based Error	739.99	477.22	119.58	16.8691	47.8774
Standard Deviation	96.72	86.55	52.9349	26.1308	43.2809
Correlation Coefficient	0.77	0.80	0.9145	0.90067	0.98609

As shown in Table 3-7, Models C, E and M did not generate satisfactory results. Though Model M produced a higher correlation coefficient than Model N, the former generated higher errors than the latter. One possible reason for this behavior is that Model M generated a large amount of negative values in a low acceleration regime. However, Models N and O produced acceptable results. Model N produced an acceptable aggregate and one second average errors (3.46% and 16.87% respectively). The neural network model (Model O) produced the highest value for a correlation coefficient (0.986) among all the models.

Figures 3-20 through 3-27 show the FTP cycle outputs of CO modeling for Models N and O.

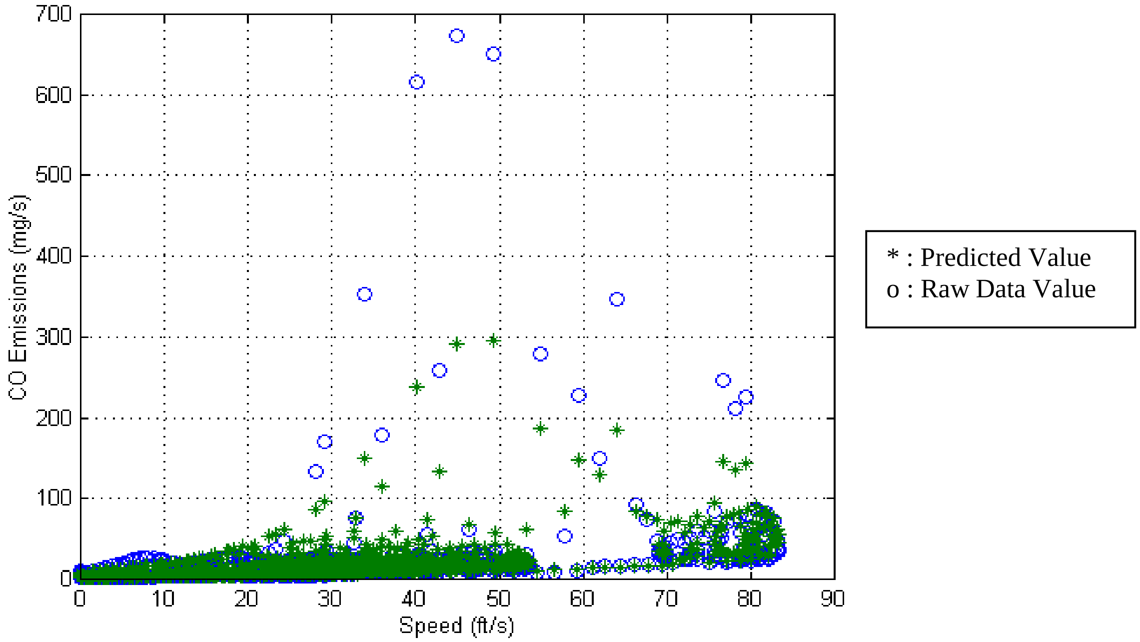

Figure 3-20 FTP Cycle CO Emission Rates for Model N (Speed Based).

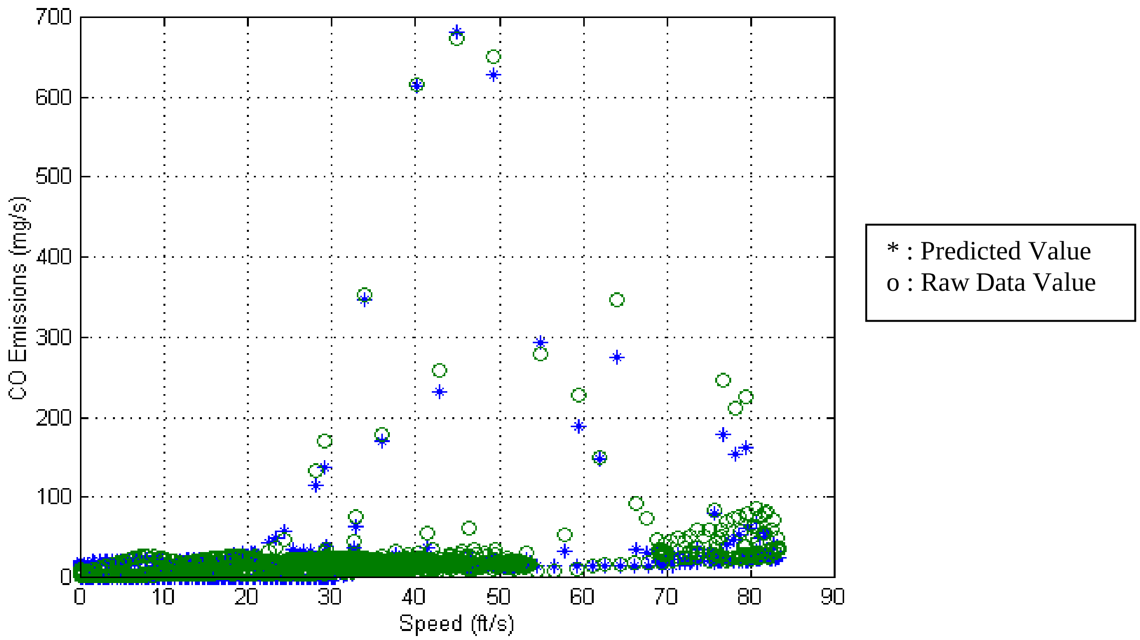

Figure 3-21 FTP Cycle CO Emission Rates for Model O (Speed Based).

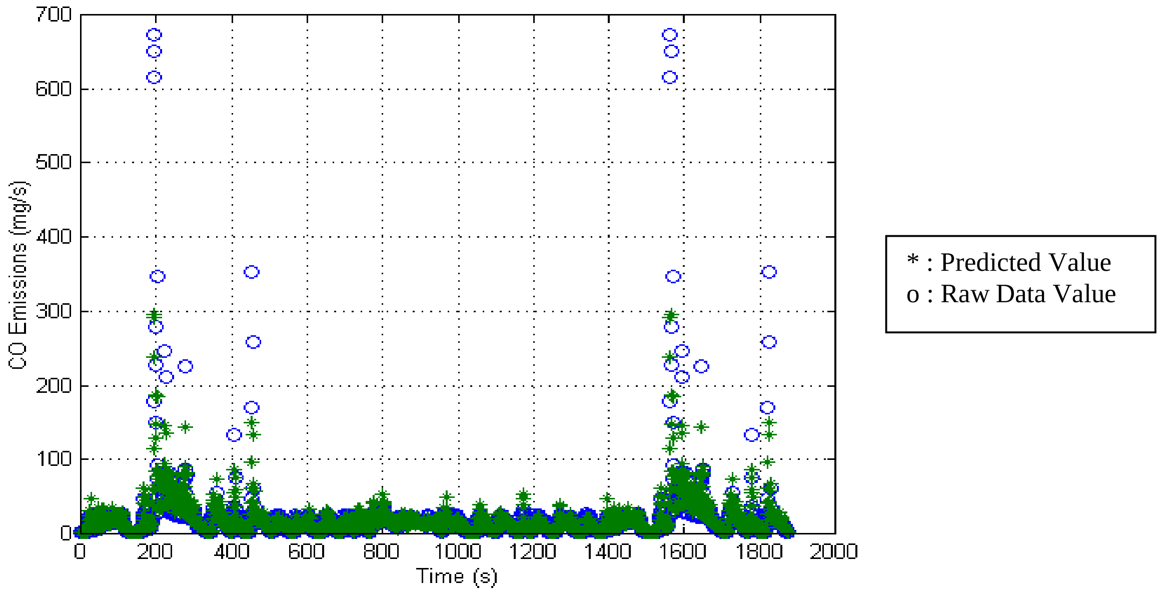

Figure 3-22 FTP Cycle CO Emission Rates for Model N (Time Based).

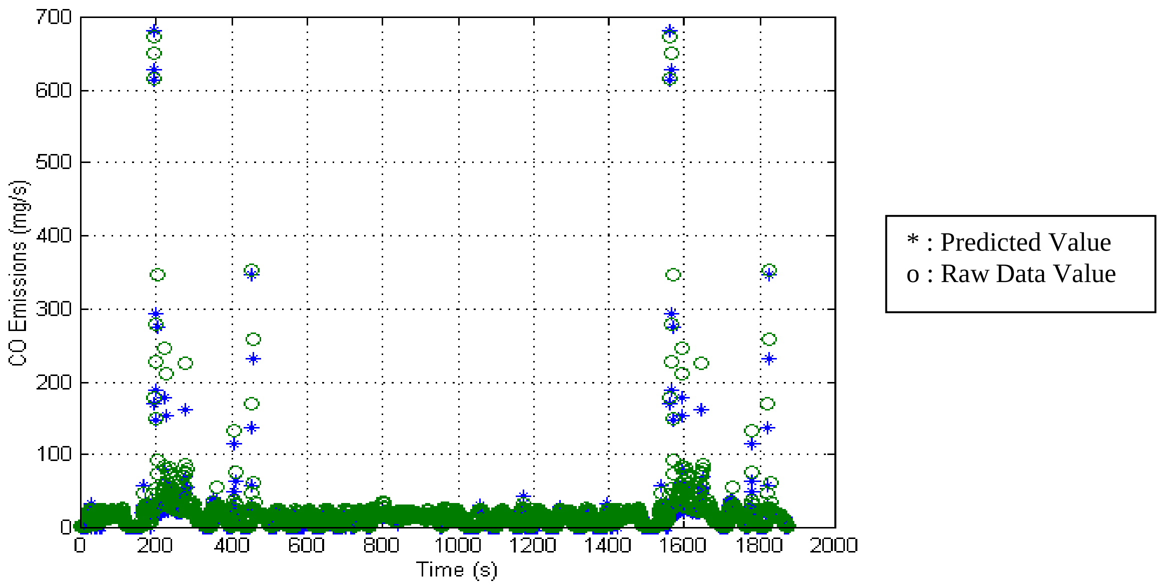

Figure 3-23 FTP Cycle CO Emission Rates for Model O (Time Based).

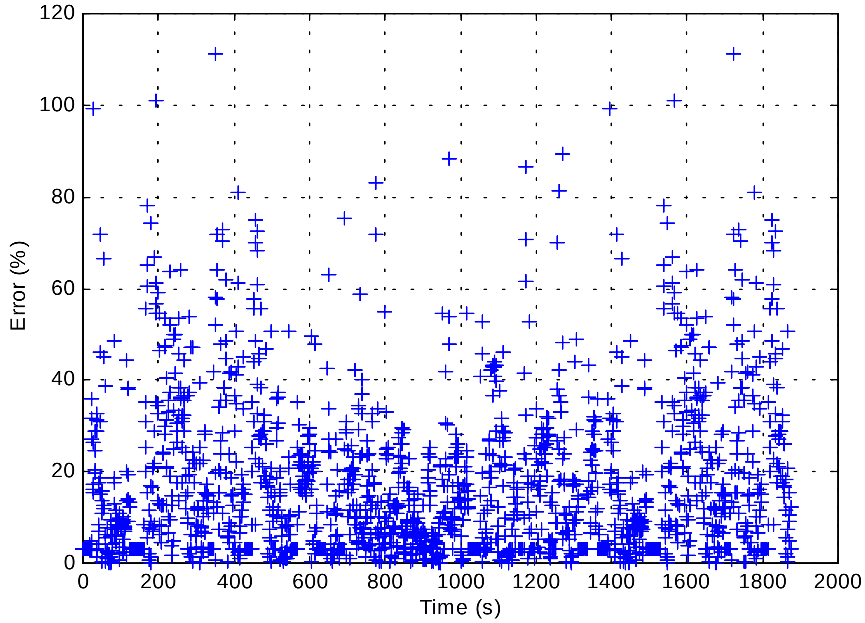

Figure 3-24 FTP Cycle Errors of CO Emissions for Model N (Time Based).

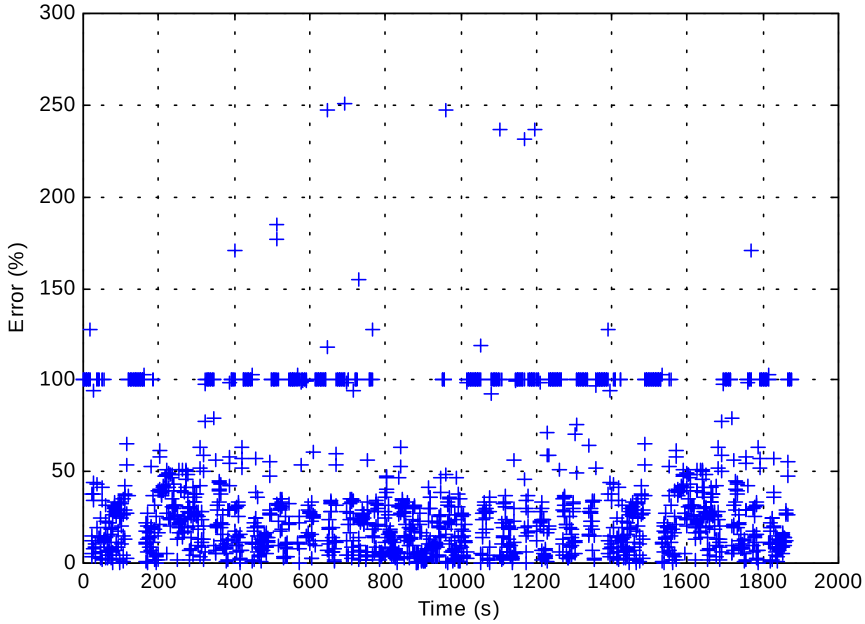

Figure 3-25 FTP Cycle Errors of CO Emissions for Model O (Time Based).

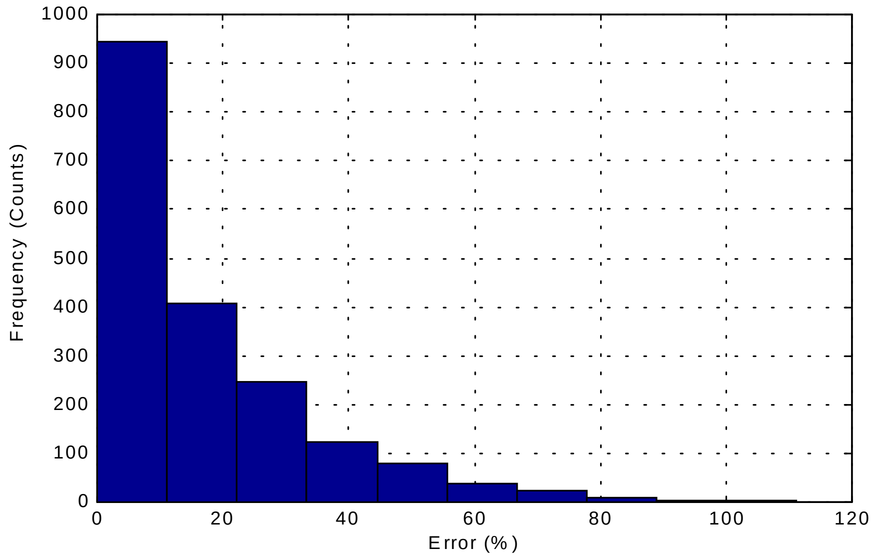

Figure 3-26 FTP Cycle Error Distribution of CO Emissions Rate for Model N.

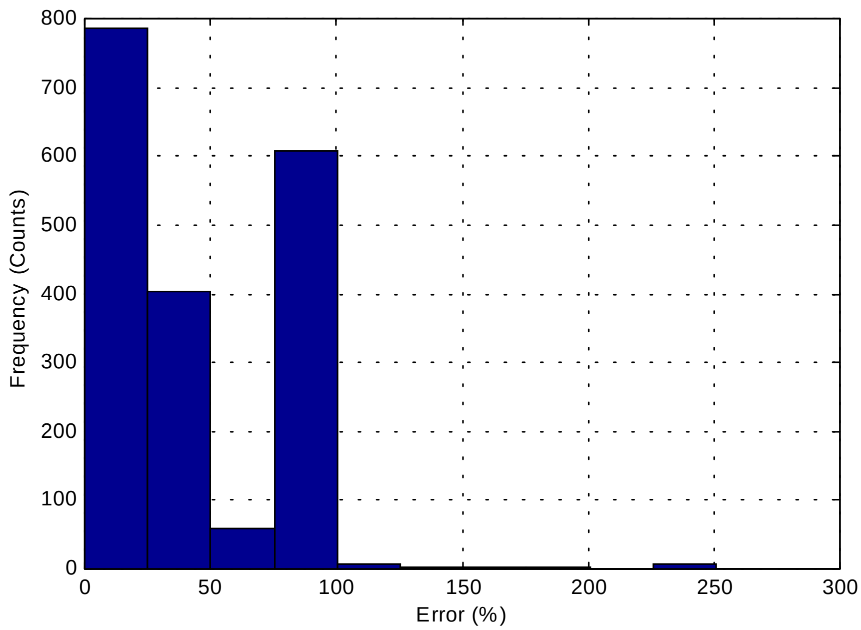

Figure 3-27 FTP Cycle Error Distribution of CO Emissions Rate for Model O.

As shown in Figures 3-20 and 3-22, the expected CO emission rates of Model N underestimated the high emission rate data. Nevertheless, it was found that Model N produced smaller errors than Model O (see Figures 3-24 through 3-27). Model N is a good predictor of emission rates in the low speed and acceleration regime, whereas Model O fits well at higher emission rates.

3.4.2 US06 Cycle Test

The US06 cycle used for the second test is a high acceleration aggressive driving schedule that is often recognized as a "Supplemental FTP" driving cycle. This Supplemental Federal Test Procedure (SFTP) was designed to address shortcomings with the current FTP in the representation of aggressive (high speed and/or high acceleration) driving behavior, rapid speed fluctuations, and driving behavior following startup. This cycle represents a new set of requirements designed to more accurately reflect real road forces on the test dynamometer.

This EPA defined cycle has an average speed of 47.97 mph over a distance of 8.01 miles. The complete cycle takes 600 seconds. The speed and acceleration variation is shown in Figures 3-28 and 3-29.

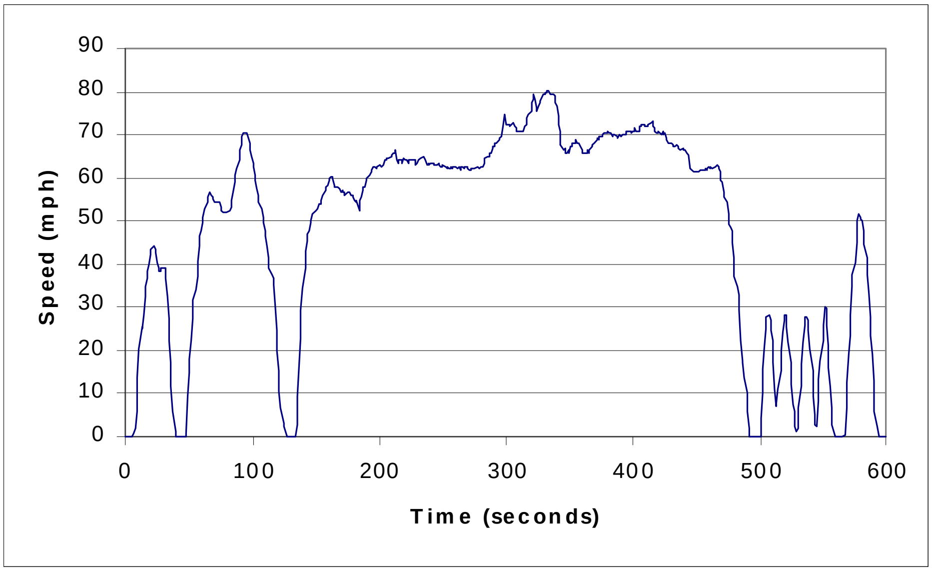

Figure 3-28 US06 Cycle Speed Profile.

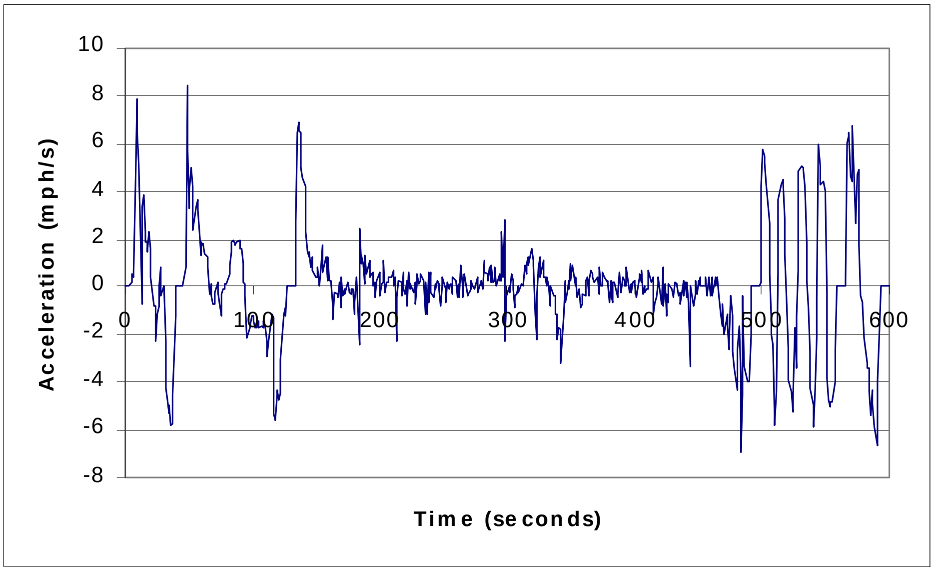

Figure 3-29 US06 Cycle Acceleration Profile.

In this US06 cycle test, speed and acceleration profiles were used as input variables. However, due to the high acceleration and speed characteristic of this cycle, some speed and acceleration profiles exceed the boundary of the raw data (thirteen times out of 596 seconds). Accordingly, it was unfeasible to obtain the precise interpolated value of the raw data. In order to minimize the differences between the interpolated values and the real values of the US06 cycle, the speed and acceleration profiles that surpass the boundary of the raw data were replaced by the maximum value or minimum value of the raw data.

A summary of the US06 cycle for Models N and O, which have produced acceptable results until now, is presented in Table 3-8.

Table 3-8 Summary of US06 Cycle Test for Composite Vehicle.

	Fuel Consumption Modeling		CO Emissions Modeling	
	Model N	Model O	Model N	Model O
CPU Time(seconds)	0.0118	0.032	0.0125	0.0331
Total Error	2.1662	2.0857	16.7923	33.4787
1-s Based Error	4.4050	14.0092	39.1142	41.0706
Standard Deviation	2.0144	1.9084	1845.5897	514.2616
Correlation Coefficient	0.97605	0.97042	0.65669	0.94192

As shown in Table 3-8, both models yield reasonable outputs for fuel consumption modeling. In terms of CO emissions rate modeling, Model N produced lower error values than Model O, while Model O generated a higher correlation coefficient value. Figures 3-30 through 3-36 illustrate the two behaviors of these models.

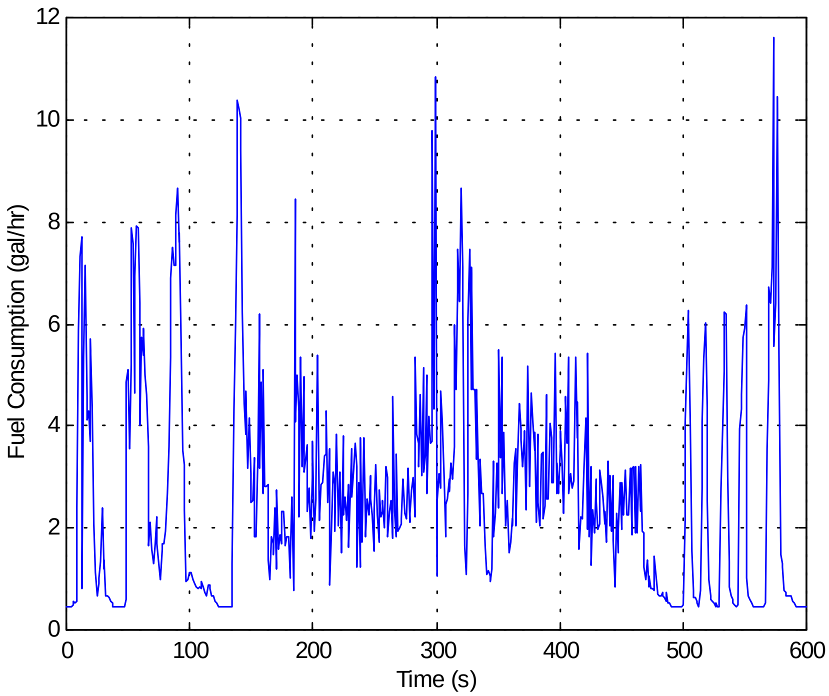

Figure 3-30 Interpolated Fuel Consumption (Composite Vehicle, US06).

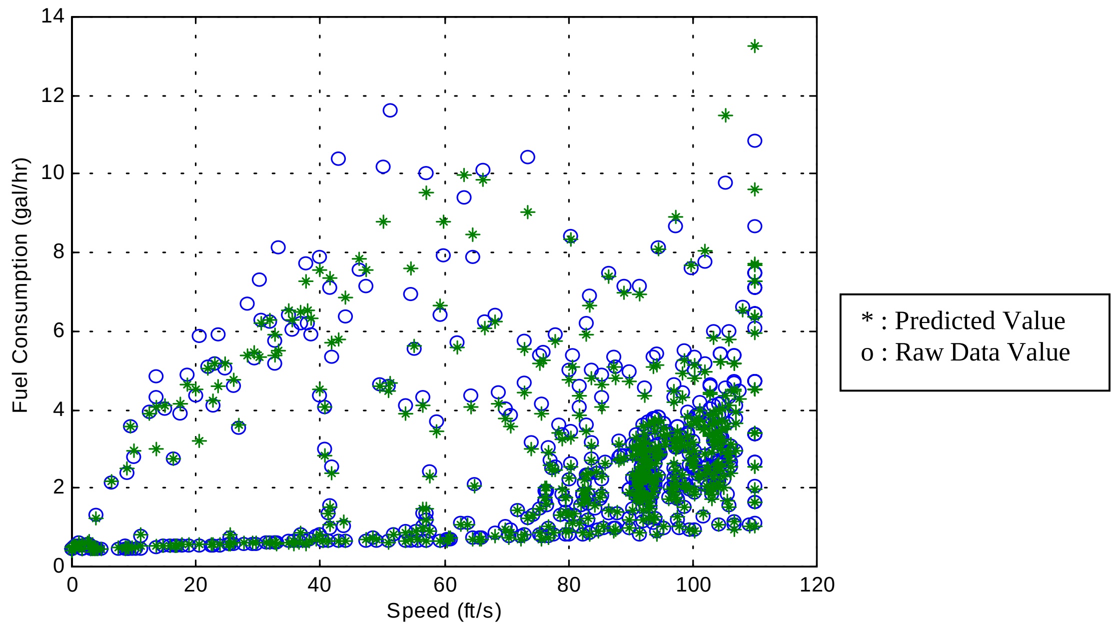

Figure 3-31 US06 Cycle Fuel Consumption Results for Model N (Speed Based).

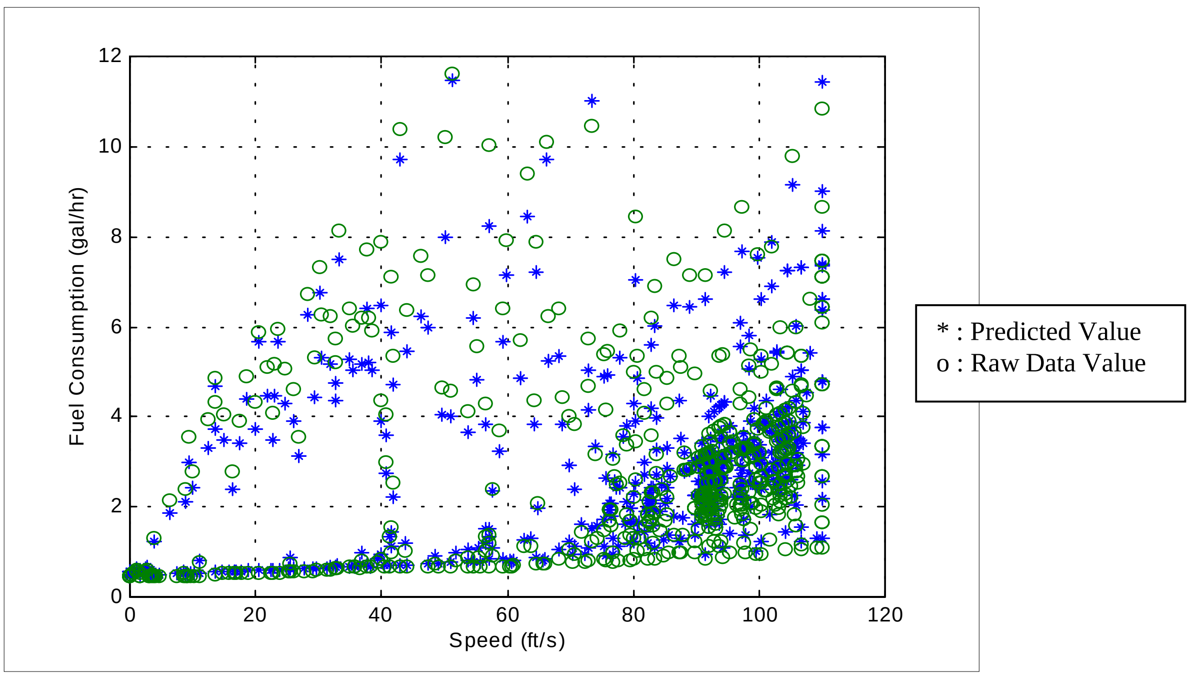

Figure 3-32 US06 Cycle Fuel Consumption Results for Model O (Speed Based).

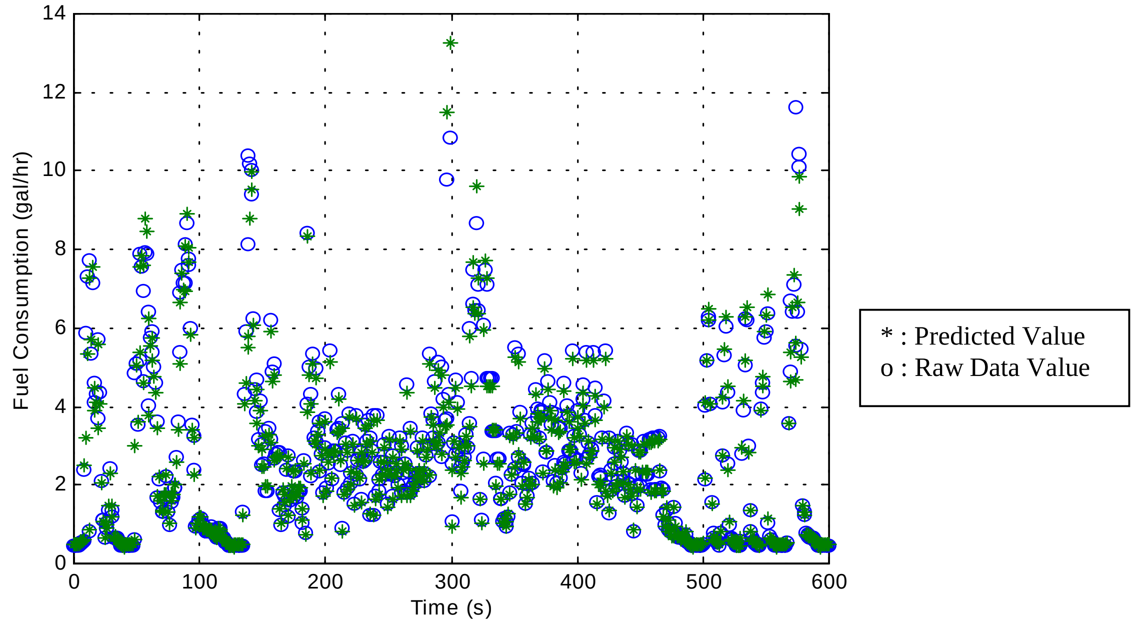

Figure 3-33 US06 Cycle Fuel Consumption Results for Model N (Time Based).

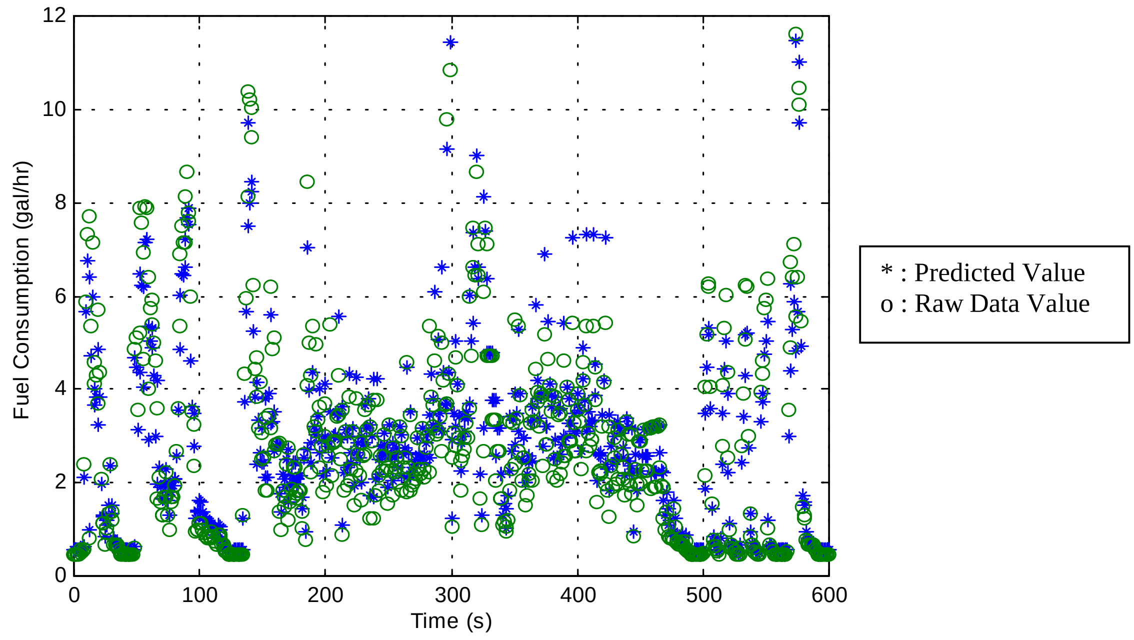

Figure 3-34 US06 Cycle Fuel Consumption Results for Model O (Time Based).

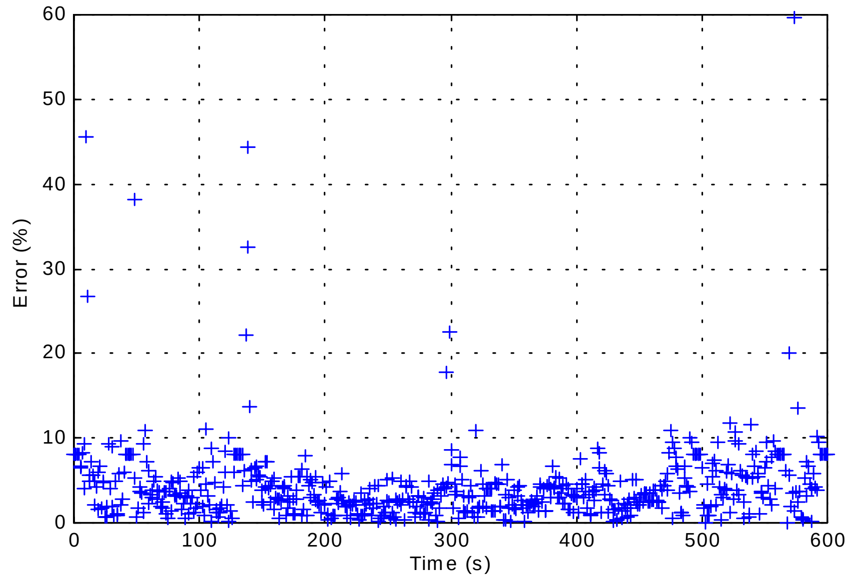

Figure 3-35 Fuel Consumption Errors for Model N (US06 Cycle).

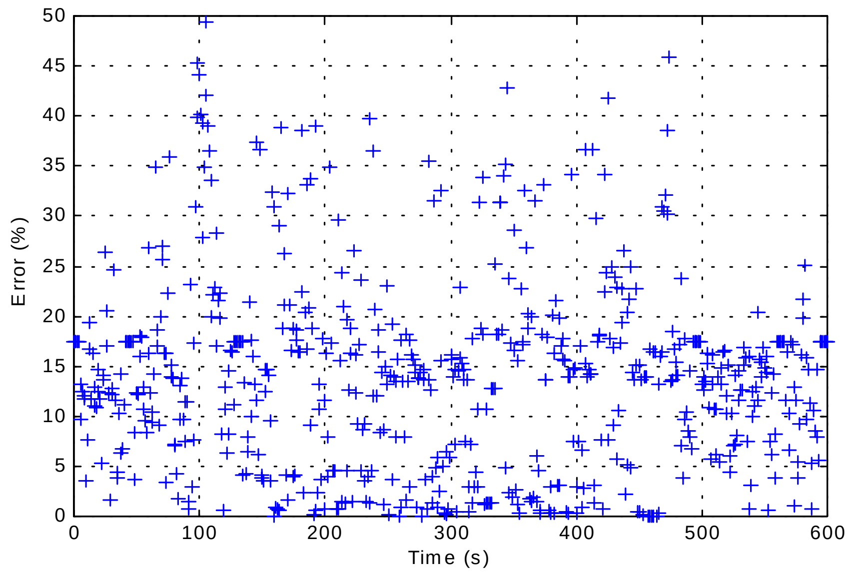

Figure 3-36 Fuel Consumption Errors for Model O (US06 Cycle).

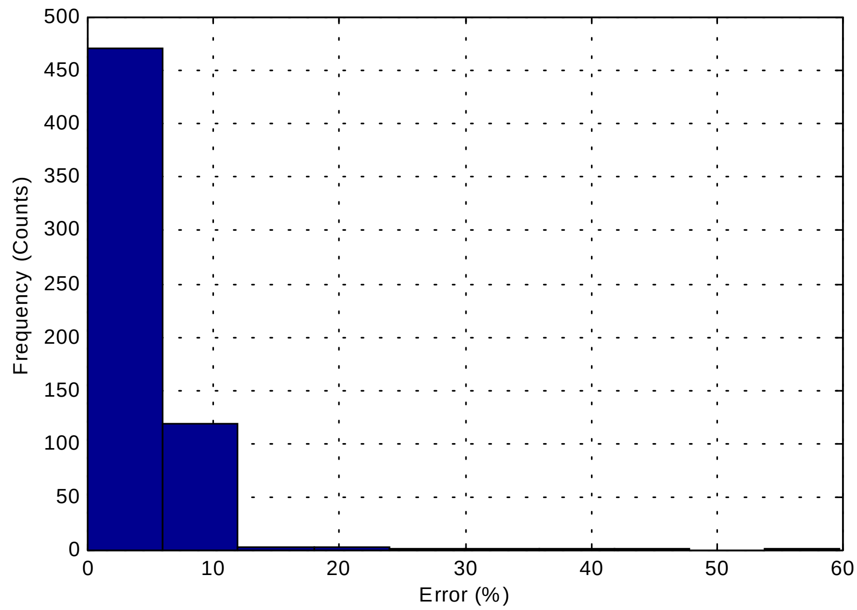

Figure 3-37 Error Distribution of Fuel Consumption for Model N (US06 Cycle).

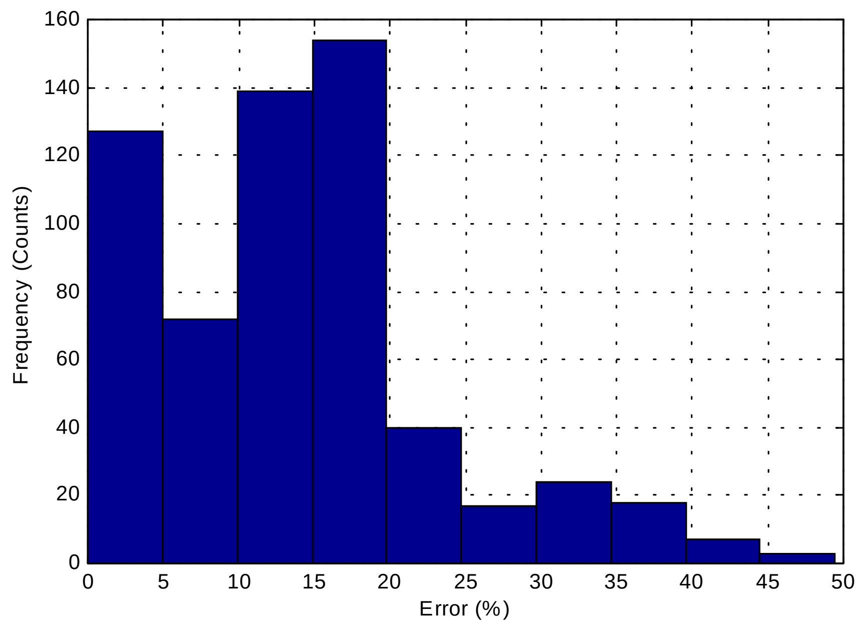

Figure 3-38 Error Distribution of Fuel Consumption for Model O (US06 Cycle).

Figure 3-30 represents the interpolated fuel consumption of raw data using the US06 cycle. Figures 3-31 through 3-34 compare the accuracy of the two models showing the difference between the interpolated and predicted values for speed and time series using the US06 cycle. Figures 3-35 through 3-38 show the errors between the interpolated and predicted values.

As shown in the previous figures, the variance of error for fuel consumption modeling of Model N is smaller than that of Model O. Most of the errors in model N are within 10%, while those for Model O are dispersed up to 40%.

Figures 3-39 through 3-47 illustrate the US06 test outputs of CO emissions rate modeling for Model N and Model O.

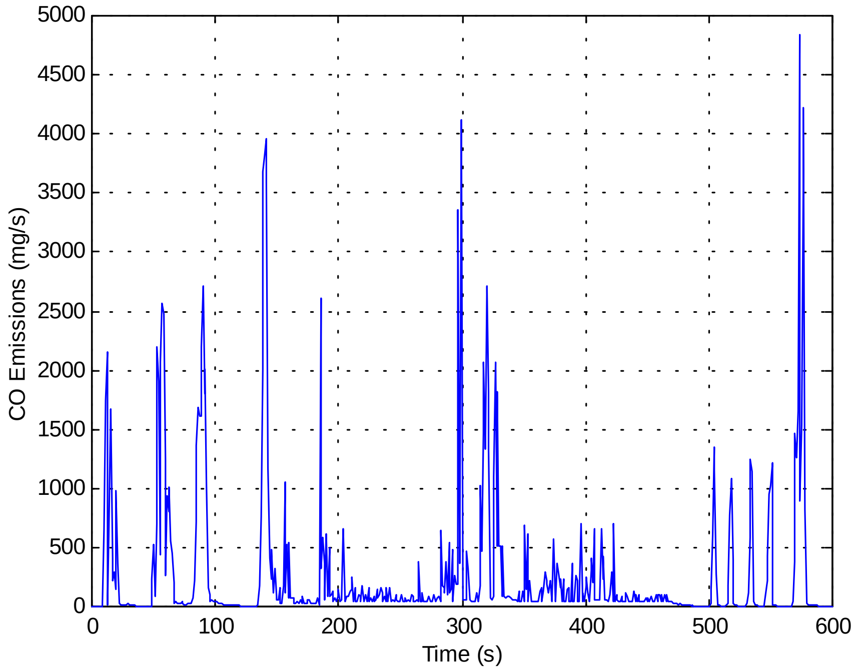

Figure 3-39 Interpolated CO Emission Rates (Composite Vehicle, US06).

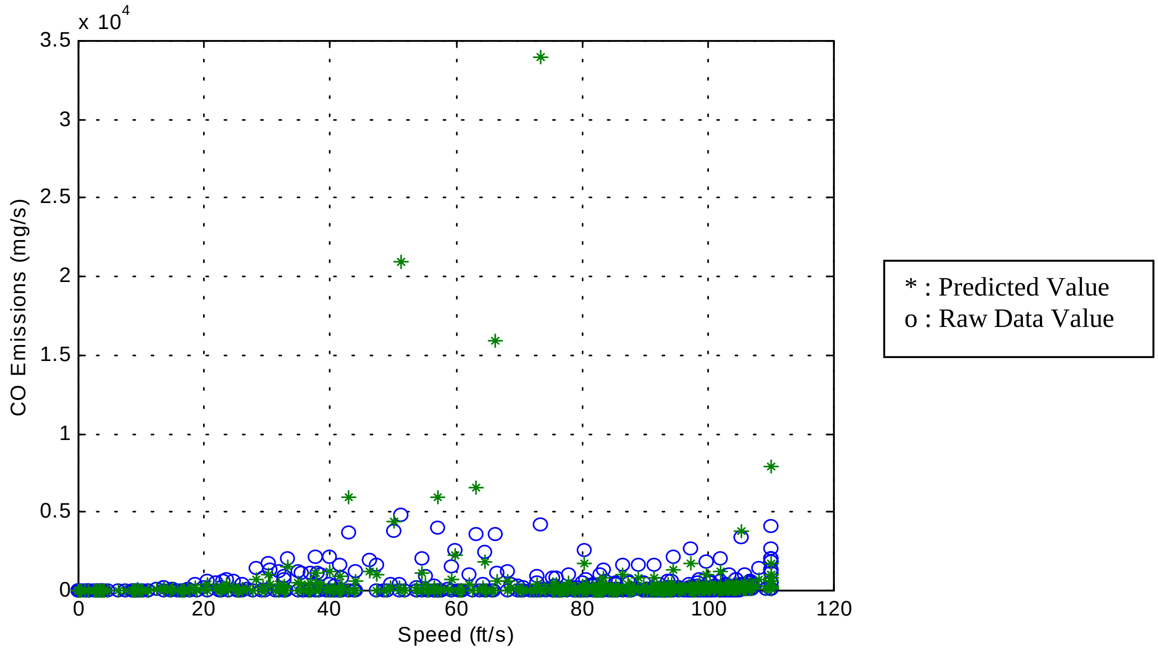

Figure 3-40 Speed Trace of CO Emission Rates (US06 Cycle) for Model N.

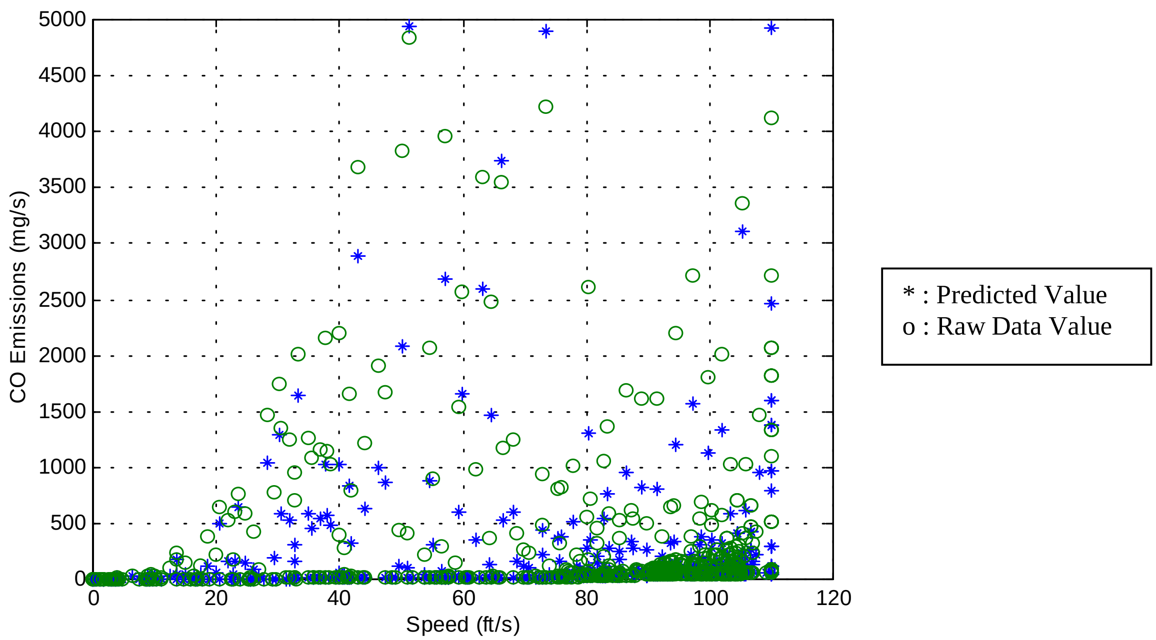

Figure 3-41 Speed Trace of CO Emission Rates (US06 Cycle) for Model O.

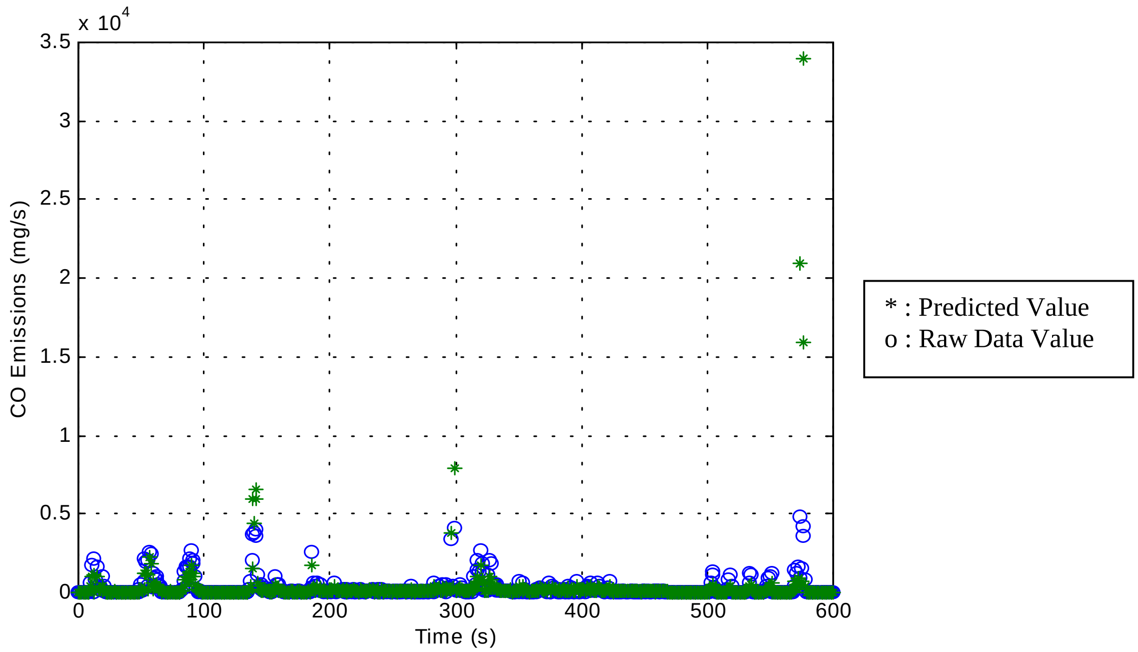

Figure 3-42 Time Trace of CO Emission Rates (US06 Cycle) for Model N.

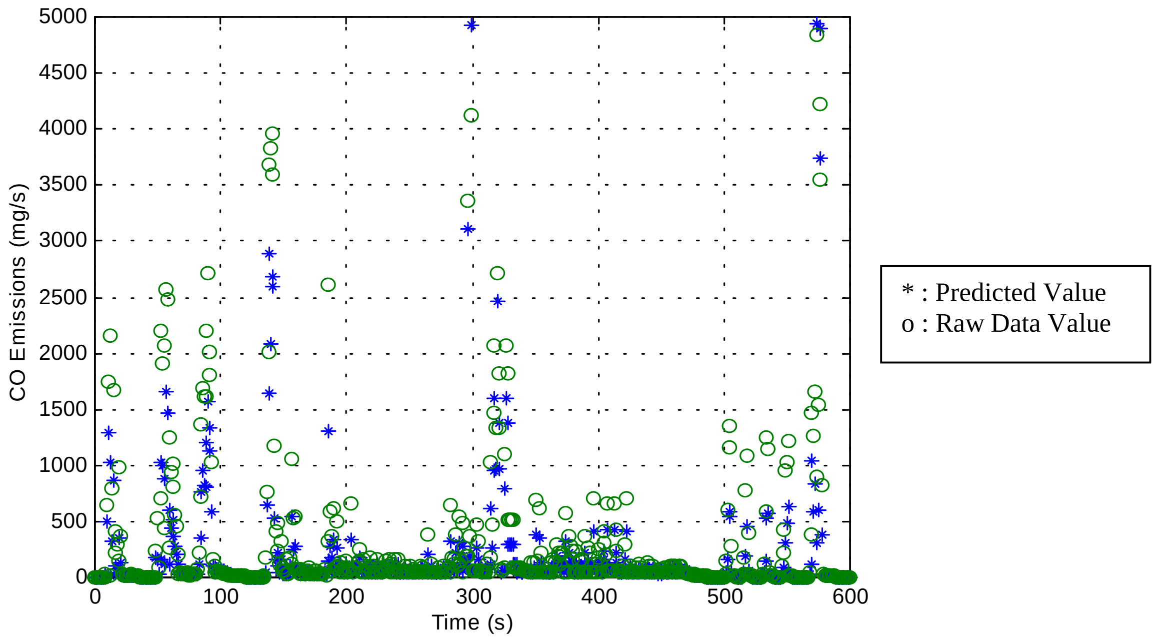

Figure 3-43 Time Trace of CO Emission Rates (US06 Cycle) for Model O.

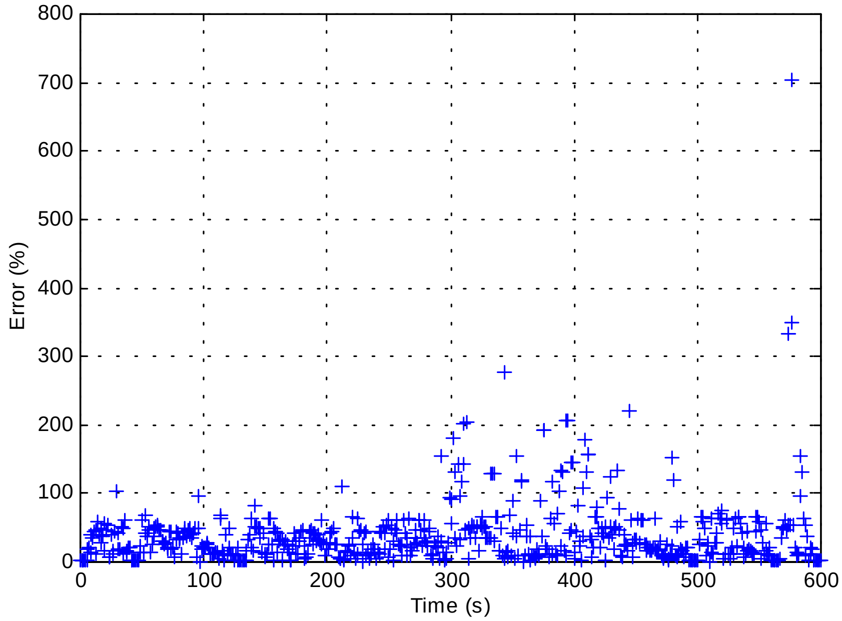

Figure 3-44 CO Emission Error (US06 Cycle) for Model N.

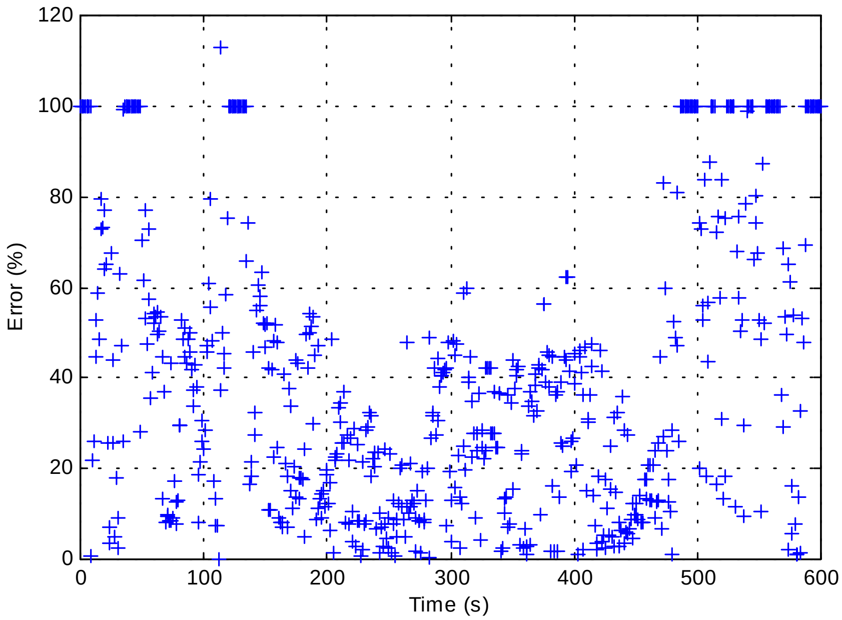

Figure 3-45 CO Emission Error (US06 Cycle) for Model O.

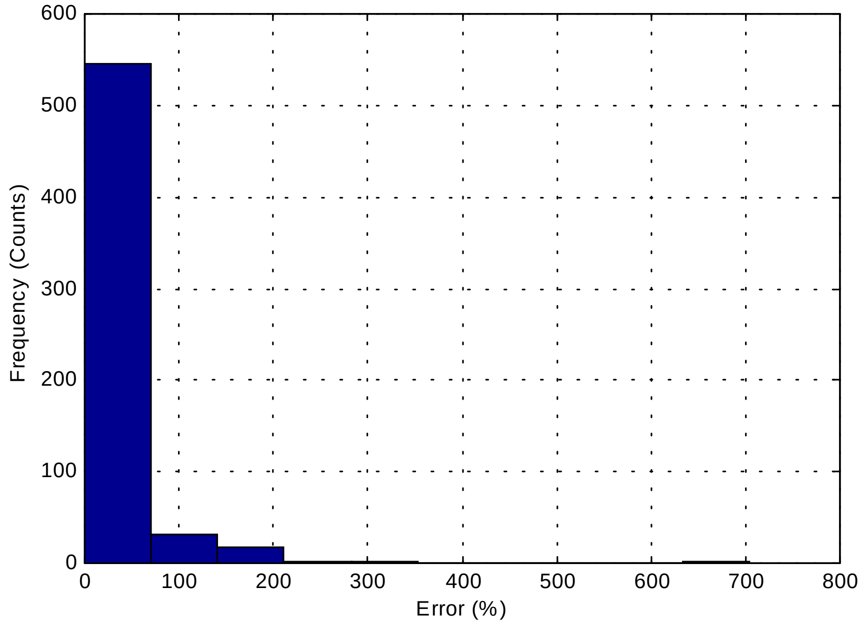

Figure 3-46 Error Distribution of CO Emission for Model N (US06 Cycle).

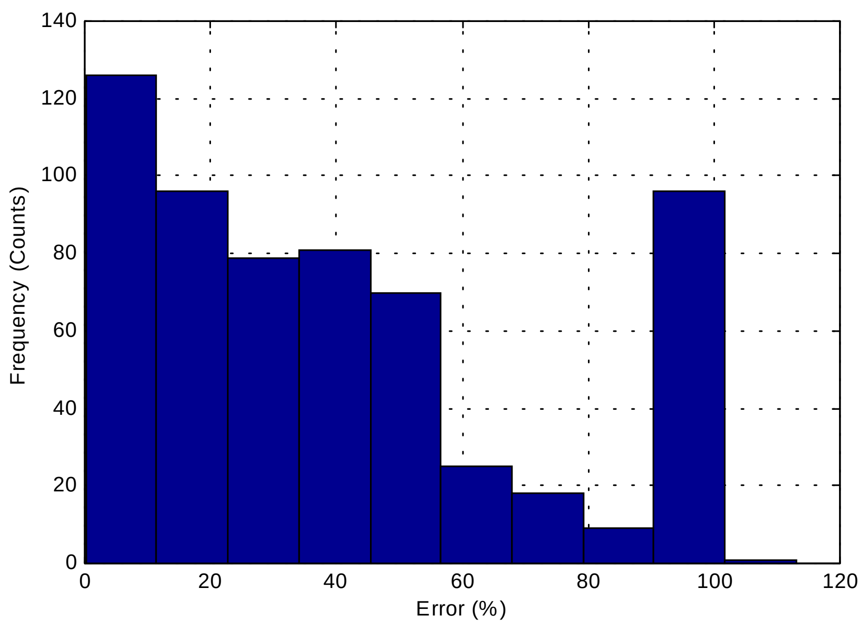

Figure 3-47 Error Distribution of CO Emission for Model O (US06 Cycle).

As shown in the previous figures, it was found that Model N overestimated some CO data points located at the end of the cycle. This results in a standard deviation of error (1845.59), which is three and a half times the standard deviation for Model O (514.26). An inspection of Figure 3-43 reveals that many of the predicted values of Model O underestimate the interpolated CO emission rate values of the US06 cycle.

3.4.3 Generalization Test

A generalization technique was used to verify the accuracy of these models. In the neural network model, the outputs of a supervised neural network come to approximate the target values, given the inputs in the training set. The ability to predict the trained inputs may be useful in itself. But more importantly, a neural net should be generalized to have model outputs approximate target values given inputs that are not in the training set (Sarle,1997).

In order to use generalization, a total of 10,000 random numbers (100 random acceleration and 100 random speed) were generated. These 10,000 random numbers were used as input variables into the neural network model (Model O) and the regression model (Model N).

The output of the generalization test is presented in Table 3-9.

Table 3-9 Summary of Generalization Test for Composite Vehicle.

	Fuel Consumption Modeling		CO Emissions Modeling	
	Model N	Model O	Model N	Model O
CPU Time(seconds)	0.1603	3.5534	0.1642	3.5212
Total Error	0.5931	0.5985	36.6104	6.1426
1-s Based Error	7.0271	6.3676	31.1767	34.5944
Standard Deviation	64.6656	61.6378	32.1231	38.3163
Correlation Coefficient	0.988	0.989	0.9626	0.992

As shown in Table 3-9, both Models N and O produced good results in fuel consumption modeling. In terms of CO emissions rate modeling, the total error for Model O was about six times smaller than for Model N, whereas the CPU time consumption for Model O was notably greater than that of Model N.

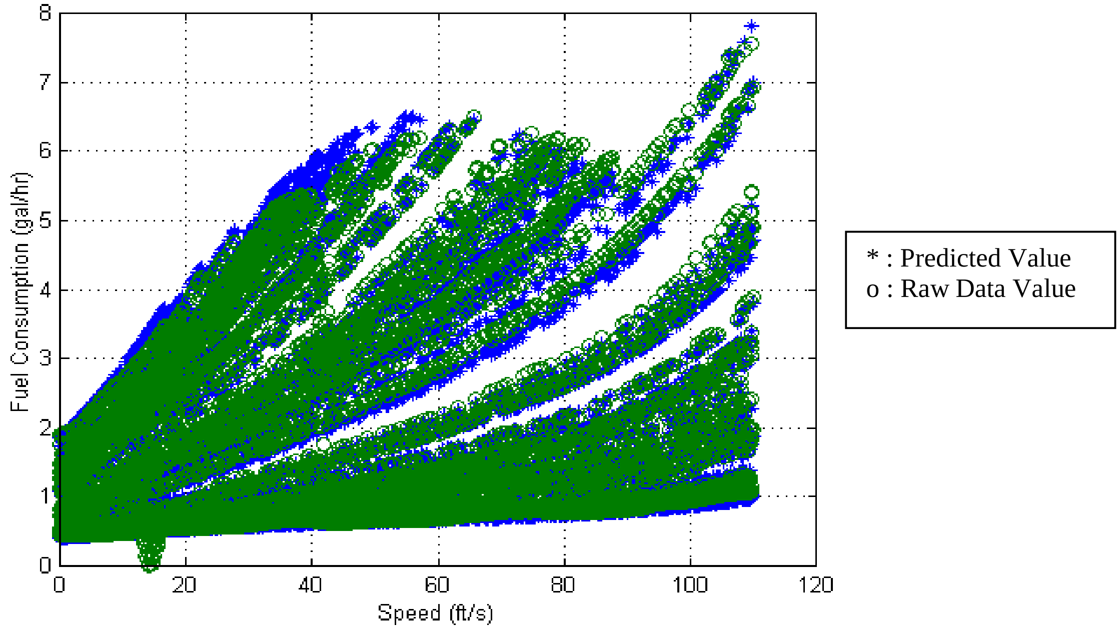

Figure 3-48 Predicted Fuel Consumption of Model N in Generalization Test.

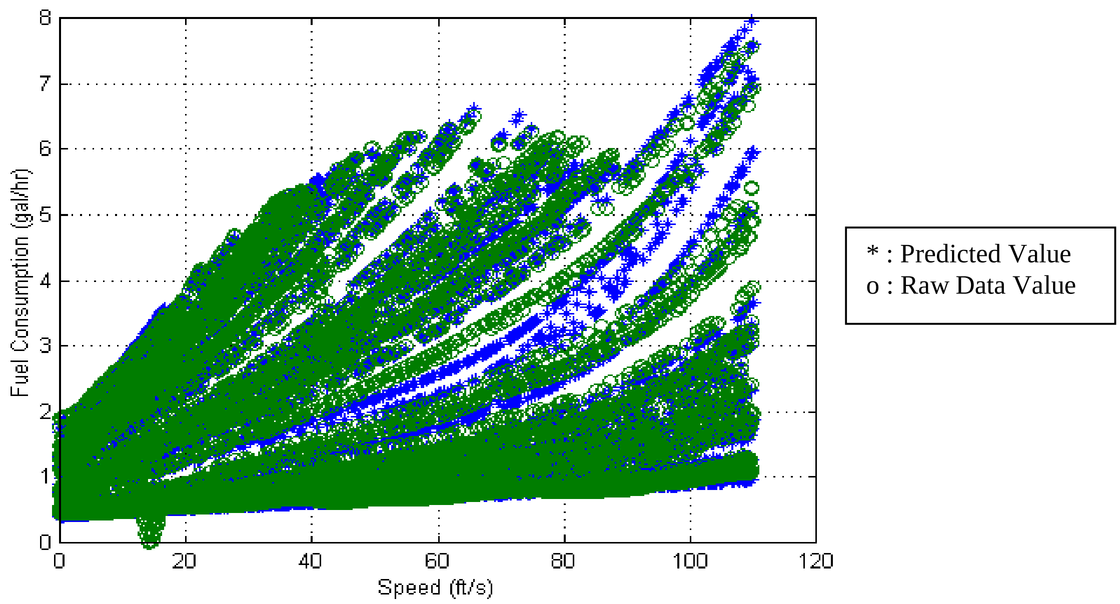

Figure 3-49 Predicted Fuel Consumption of Model O in Generalization Test.

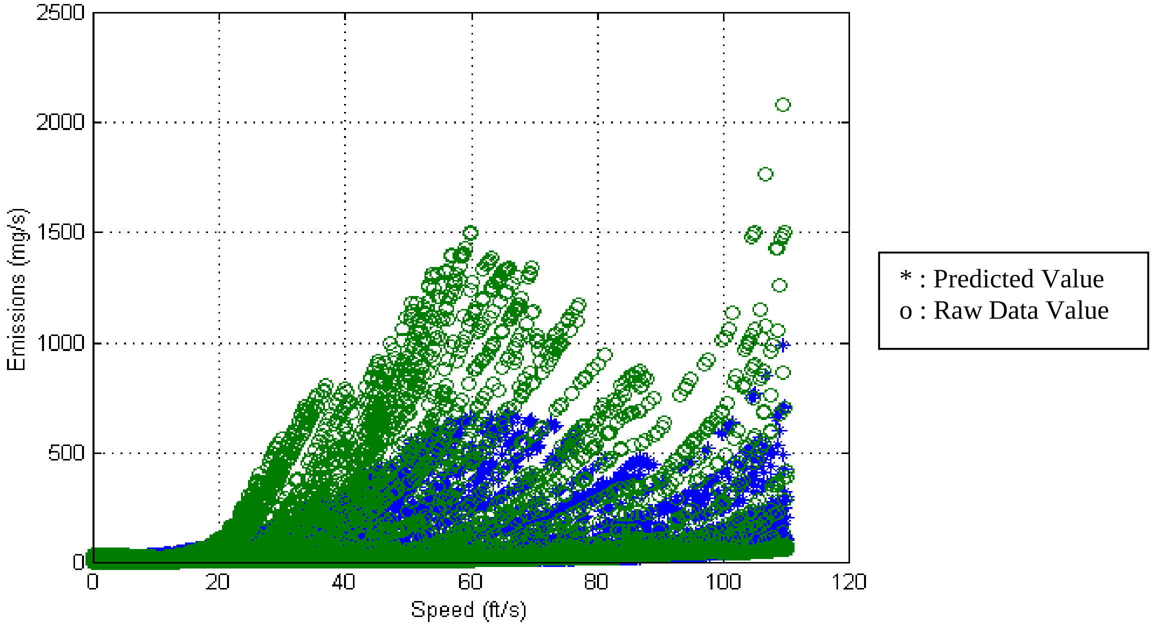

Figure 3-50 Predicted CO Emission Rates of Model N in Generalization Test.

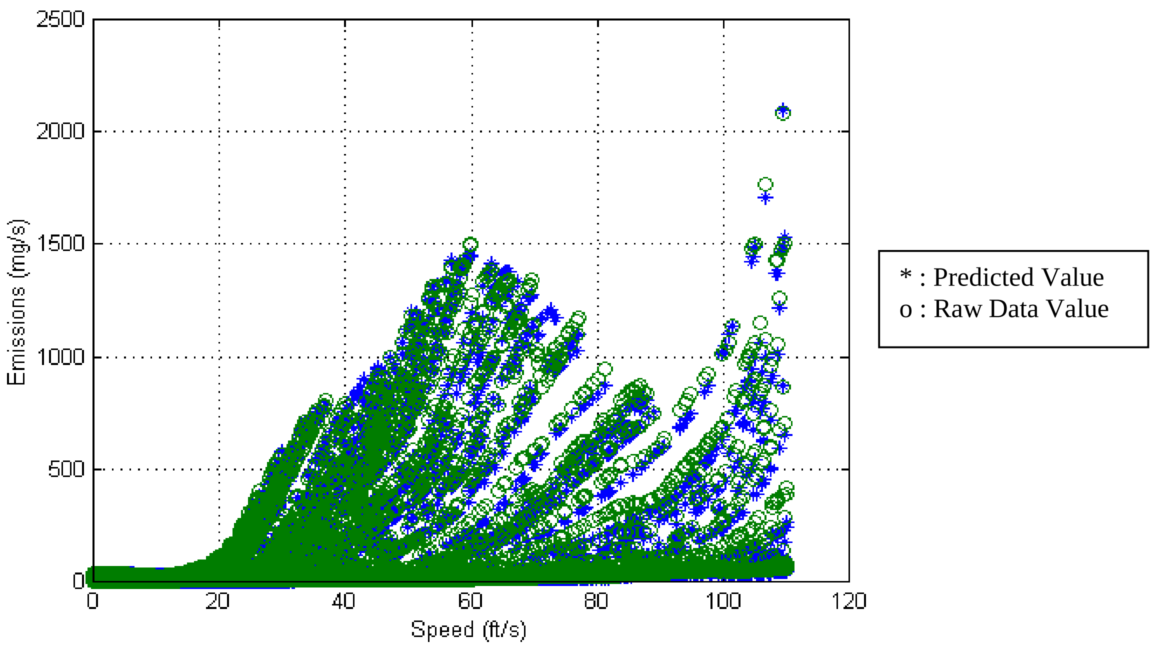

Figure 3-51 Predicted CO Emission Rates of Model O in Generalization Test.

3.5 Summary of Chapter 3

This chapter discussed the Oak Ridge National Laboratory data and several mathematical models that predict the MOEs based on individual vehicle speed and acceleration profiles.

In order to obtain a regression equation, many experimental combinations of speed and acceleration using linear, quadratic, cubic, and quartic terms are modeled. A regression model was developed to predict vehicle fuel consumption and emission rates using a combination of linear, quadratic, and cubic speed and acceleration terms.

Backpropagation, one of many training methods available in neural network analysis, was used for this modeling. Backpropagation for multiple-layer networks and nonlinear differentiable functions is simply a gradient descent method that minimizes the sum of squared errors of the weights and biases produced by the neural network training process. Based on the analysis performed with several transfer function algorithms and various backpropagation techniques, the Levenberg-Marquardt algorithm (trainnlm: Matlab function) was found to be an efficient and reliable training method and consequently used in this study.

Currently, the models do not consider ambient temperature, start emissions, road grade, and accessory use. Sample varification results are included for two vehicle-driving cycles and generalization tests. The models presented estimate vehicle fuel consumption to within 2.5% of their actual measured values. Vehicle emission rate errors fall in the range of 3-33% with correlation coefficients ranging between 0.94 and 0.99.

Chapter 4. Sample Model Application

4.1 Introduction

A mathematical model has been developed to describe and explain the first order contribution of vehicle speed and acceleration on energy and emissions. In order to provide an adequate description of system behavior, it was necessary for the model to be validated. In fuel consumption and emissions modeling, a number of reasonable tests are available to test the model. In this section, the general issues concerning model testing are reviewed, and sensitivity analyses are conducted to validate the models developed.

The model developed has been applied to a signal coordination and an incident management problem. This model was implemented into a micro-simulation model INTEGRATION and applied to typical networks for model testing. The composite vehicle was used throughout the entire testing model.

4.2 Signal Coordination

In this section, three scenarios are tested to check the energy economy and environmental effects of several signal control strategies which are typical of real networks. The three scenarios are:

- No control
- Stop sign control
- Traffic signals control

4.2.1 No Control Test

This scenario is tested to find out the least fuel consumption and the least emissions speeds. Consider a typical suburban corridor, which has three intersections and four links. Each link length is 1 km, and the same constant free-speeds are applied to the entire network. The complete network is 4 km in length. In order to estimate the most fuel efficient speed, a single vehicle traverses the network at 10 km/hr speed increments from 10 km/hr to 100 km/hr in the simulation model. The simulation runs are executed assuming no vehicle acceleration. Figure 4-1 represents the network configuration used in the simulation.

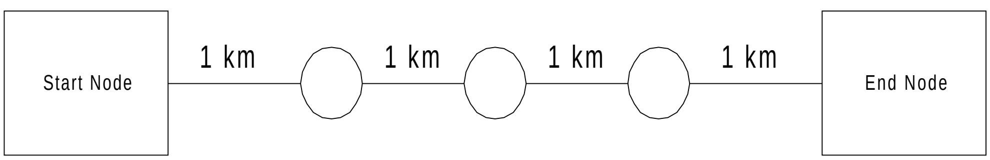

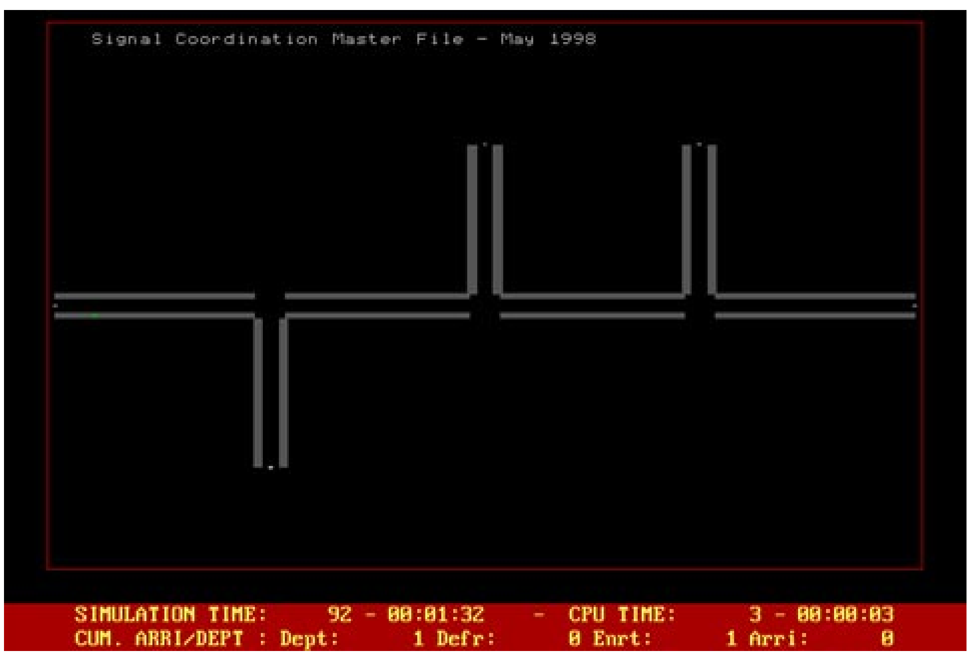

Figure 4-1 Simulation Screen Capture.

Figure 4-2 shows a time-speed diagram showing the total travel time for each run. From this figure we observed that although fuel consumption and emissions are generally small at lower speeds for one second, the total fuel consumption and emissions also depend on the total travel time. As vehicle speeds increase, travel time decreases, thus resulting in an optimum fuel and emissions economy speed. Table 4-1 shows the one second fuel consumption and emission rates and the total travel time in the network for every speed.

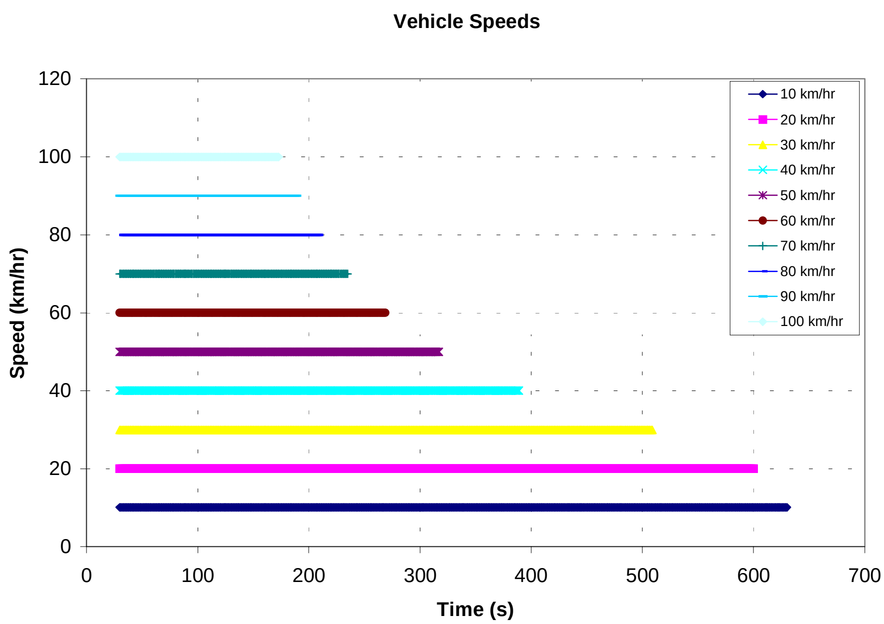

Figure 4-2 Vehicle Speeds and Total Travel Time.

Table 4-1 One-Second Fuel Consumption and Emission Rates.

Speed (km/hr)	Fuel Consumption (liters/s)	HC (mg/s)	CO (mg/s)	NOx (mg/s)	Total Travel Time (s)
10.1	0.00072	0.62	4.87	0.56	630
20	0.00091	0.77	8.3	0.88	600
30	0.00111	0.94	12.65	1.34	509
40	0.00131	1.15	17.81	1.98	389
50	0.00152	1.41	24.02	2.86	317
60	0.00174	1.79	32.19	4.06	269
70	0.00201	2.37	44.48	5.67	235
80	0.00236	3.32	65.69	7.84	209
90	0.00284	5.02	107.61	10.78	189
100	0.00356	8.3	202.78	14.8	173

As shown in Table 4-1, the fuel consumption and emission rates increase as speeds increase, while total travel time decreases. Figures 4-3 and 4-4 represent the total fuel consumption and emissions for every speed.

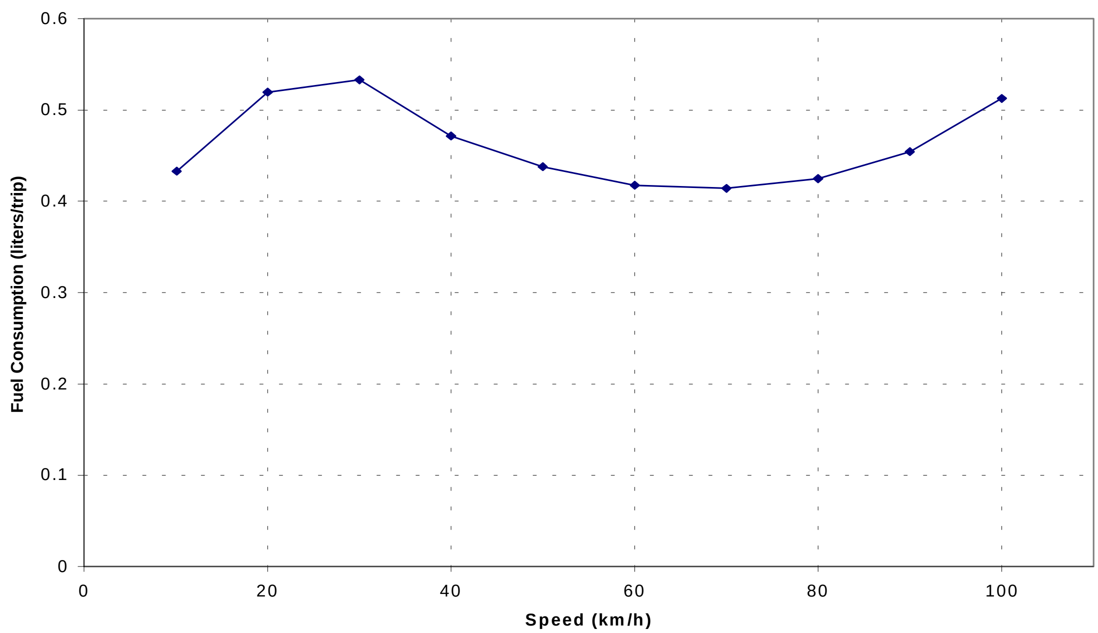

Figure 4-3 Fuel Consumption vs. Constant Speed.

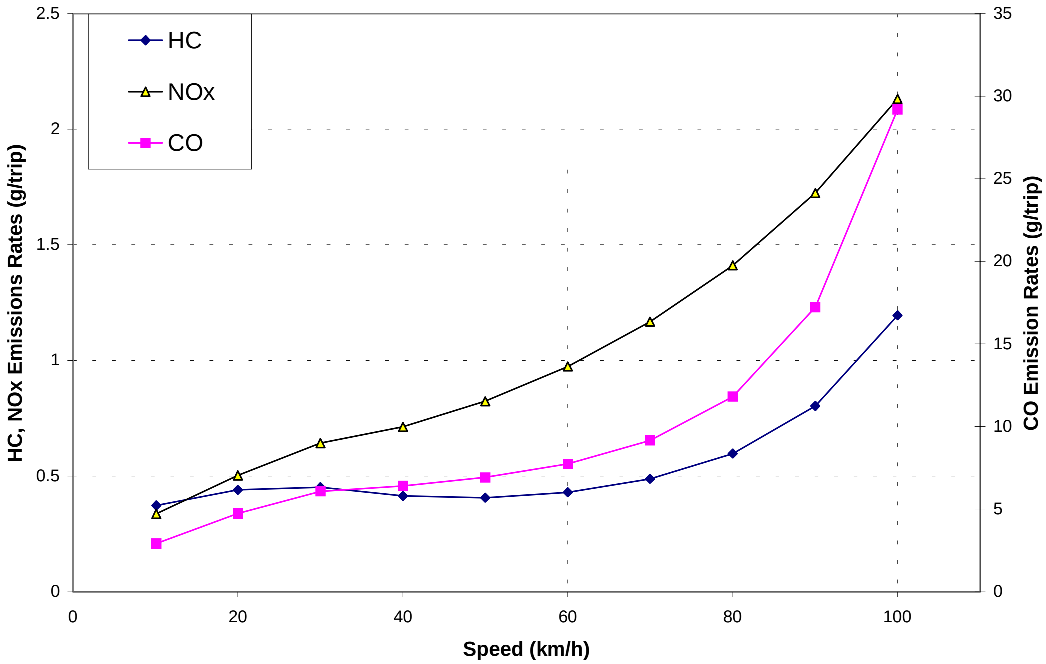

Figure 4-4 Emissions vs. Constant Speed.

Careful examination of Figures 4-3 supports that the best fuel economy speed is around 70 km/hr. In case of emissions, their characteristics are different from those of fuel consumption. Usually total emissions increase as speed increases, except HC. According to the results, the minimum total HC emission (0.406 g) is found to be around 50 km/h. In the case of CO and NOx, emissions increase as speed increases. Under real driving conditions, a constant speed along network links is not possible. As mentioned in the previous chapter, acceleration variations influence fuel consumption and emissions. Therefore, the next scenario examines the impact of acceleration and average speed on the same network.

4.2.2 Average Speeds Test

Two main emission models commonly used in the United States are the Environmental Protection Agency's (EPA's) MOBILE model and the California Air Resources Board's (CARB's) EMFAC model. In both models, emission rates highly depend on the vehicle's average speed. As shown in Chapter 3, the vehicle emission rates are dependent on acceleration as well. Therefore, this section investigates how the same average speed can generate different fuel consumption and emission rates using the simulation model.

In order to simulate a typical scenario, exactly the same network is used as described before (No Control Test). The first vehicle is driven at 36 km/h at a constant speed, and the second vehicle starts the first link at 25 km/h and drives at 75 km/h, 25 km/h and 75 km/h in the second, third and fourth links, respectively. Figure 4-5 represents the trajectories of vehicle speed.

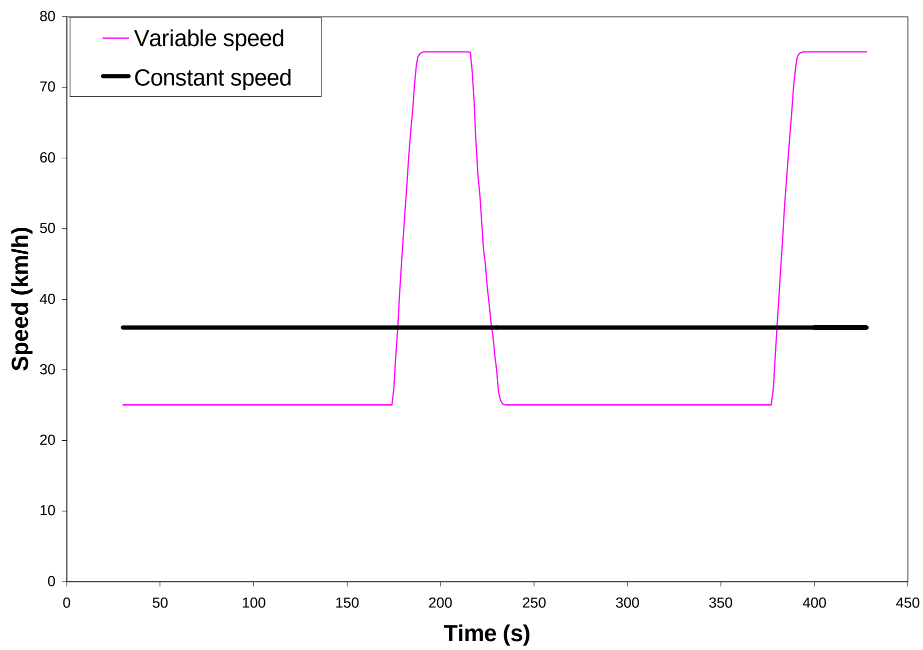

Figure 4-5 Speed Profiles for Average Speed Tests

Both of the two vehicles finish their trip at the same average speed, 36 km/h. Figure 4-6 represents the variation in acceleration of the variable speed vehicle. The total fuel consumption and emission rates after complete trips, are presented in Table 4-2.

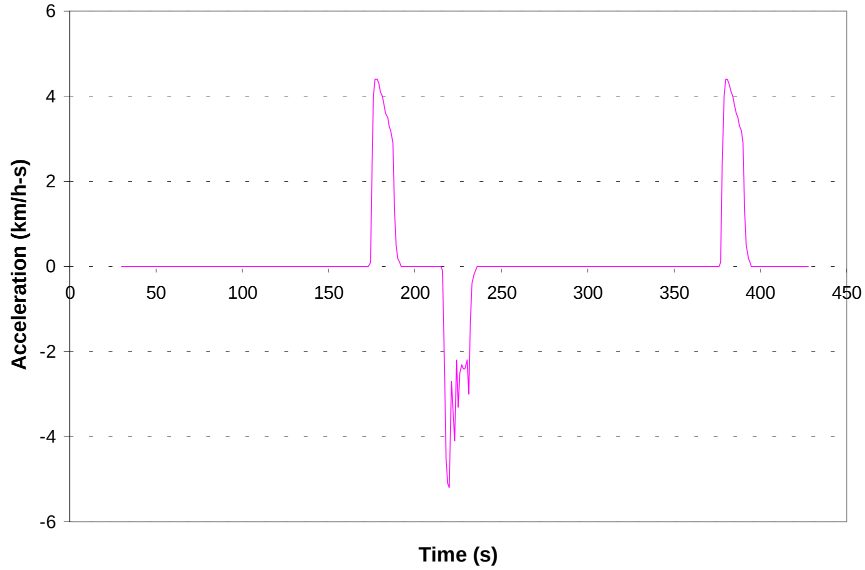

Figure 4-6 Variation in Acceleration for Average Speed Test.

Table 4-2 Summary of Average Speed Test.

	Fuel Consumption (liters/s)	HC (mg/s)	CO (mg/s)	NOx(mg/s)
Variable Speed	0.619	1119.69	23033.24	1732.6
Constant Speed	0.492	424.00	6256.03	680.0

Table 4-2 shows that the variable speed trip consumes more fuel than the constant speed trip as expected. In the case of emissions, the emission rates of the variable speed trip for all three emissions surpass those of the constant speed trip, also. This phenomenon, in which a variable speed trip exceeds a constant speed trip, can be explained by the impact of vehicle acceleration. As mentioned in Chapter 3, fuel consumption and emissions rates are generally high in the positive acceleration mode.

Therefore, whenever the speed of a vehicle changes during a trip, high rates of fuel consumption and emissions are consumed and/or emitted. Figures 4-7 and 4-8 represent the second-by-second variations in fuel consumption and HC rates during the entire test trip.

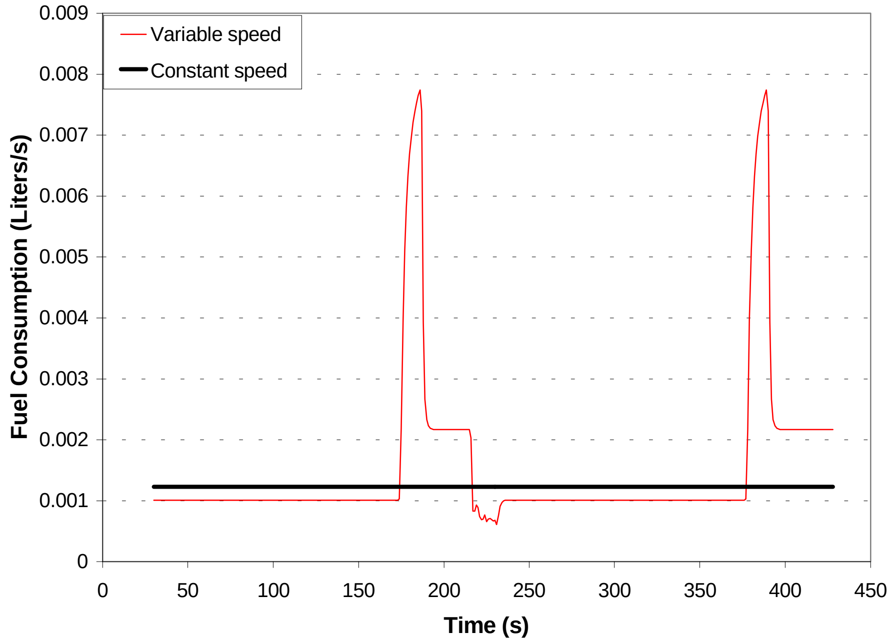

Figure 4-7 Variations in Fuel Consumption Rates.

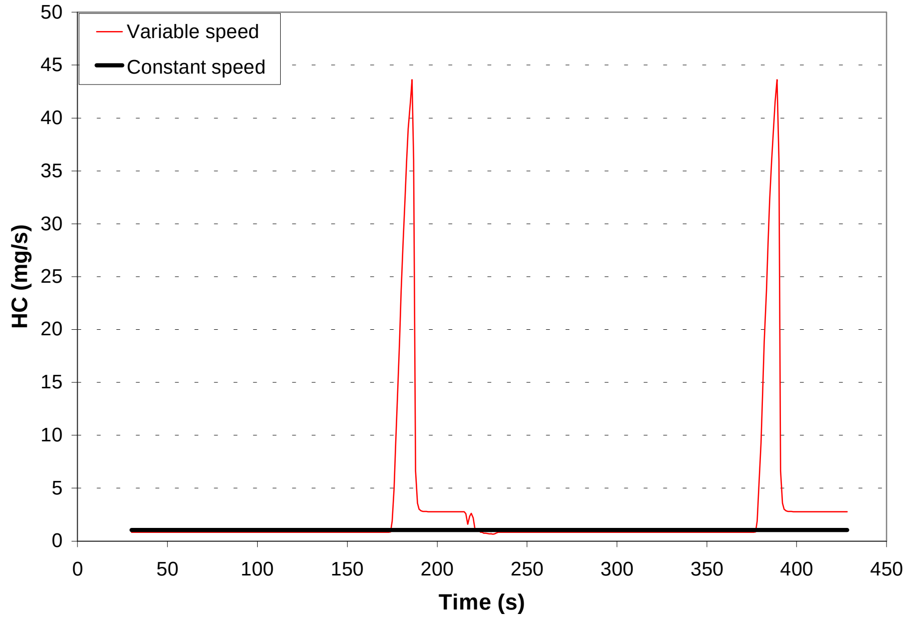

Figure 4-8 Variations in HC Emission Rates.

4.2.3 Stop Sign Control Test

In this section, a stop sign control system is applied to the simulation model. Generally, interrupted driving conditions consume more fuel and emit more emissions than constant speed driving conditions. This test verifies how stop signs affect fuel consumption and emissions rates in a specific network.

In order to simulate the scenario, we use the same network described in Section 4.1.1 (No Control Test), but add three stop signs. The first test vehicle is driven at 50 km/h at a constant speed without any stop signs, and the second test vehicle is driven at 50 km/h with a non-constant speed with three stop signs.

Figure 4-9 represents the variations in fuel consumption rates with stop sign controls. As shown in Table 4-3, fuel consumption rates decrease in front of stop signs and sharply increase after the stop sign implementation.

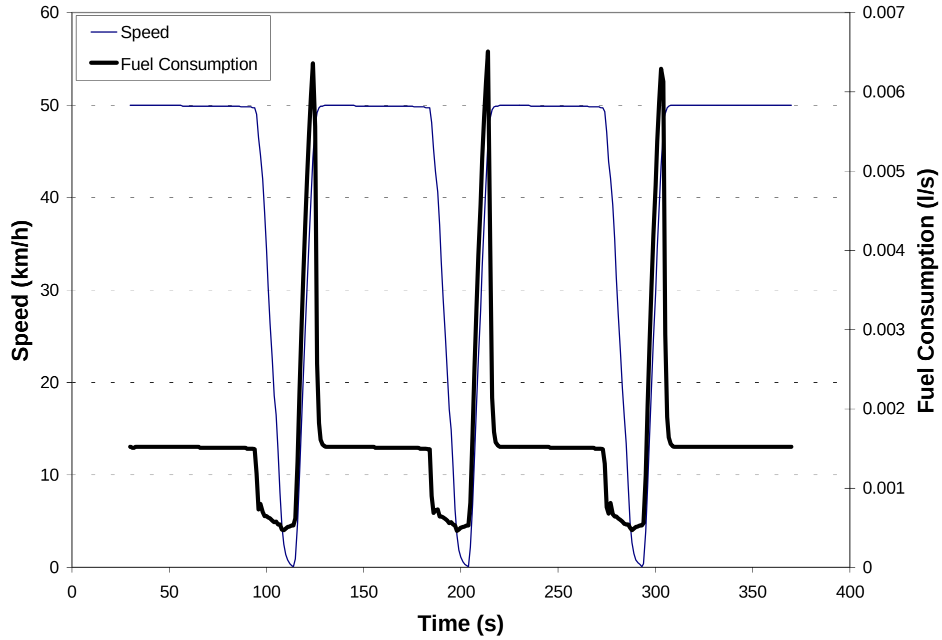

Figure 4-9 Variation in Fuel Consumption with Stop Signs Control Network.

Table 4-3 shows the differences in fuel consumption and emission rates in the simulated corridor with and without stop sign controls.

Table 4-3 Summary of Stop Signs Control Test (50 km/h).

	Fuel Consumption (liters/s)	HC (mg/s)	CO (mg/s)	NOx(mg/s)
No Control	0.43776	406.08	6917.72	823.85
Stop Sign Control	0.54757	640.2	11479.92	1513.97
Relative Difference(%)	0.250845	0.576537	0.659495	0.837677

As shown in the previous table, unessential stop signs provide negative impacts on energy economy and air quality. Especially, in the case of NOx, almost twice the emission of this pollutant is related to three stop signs in a 4 km length network. The severity of the impact can be different according to the prescribed free speeds.

4.2.4 Traffic Signal Control Test

This scenario serves to explain how good signal coordination can affect the fuel consumption and emissions rates in a specific corridor. Signal coordination is one of the basic elements of the Intelligent Transportation System (ITS), and is widely used in many cities in the world. Signal coordination can reduce arterial travel times, increase average travel speed and reduce stopped delay times for vehicles traveling on mainlines and at intersections. This section verifies the impacts of good signal coordination on fuel consumption and emissions.

For this analysis, we consider the same urban corridor with three intersections and four links, as before. Each link length is 0.35 km, which is reasonable for intersection lengths in urban areas. Demand from the start node to the end node is 300 veh/h. The last vehicle injected into the simulation departs 15 minutes from the beginning of the simulation. A free speed of 50 km/h is applied to the entire corridor.

In order to study the effect of signal coordination, four scenarios are adopted: 1) poor fixed-time signal coordination, 2) good fixed-time signal coordination and 3) real-time traffic signal coordination. Figures 4-10 through 4-12 represent second-by-second vehicle trajectories for three signal controls. Each small dot in each figure represents a time-space trace.

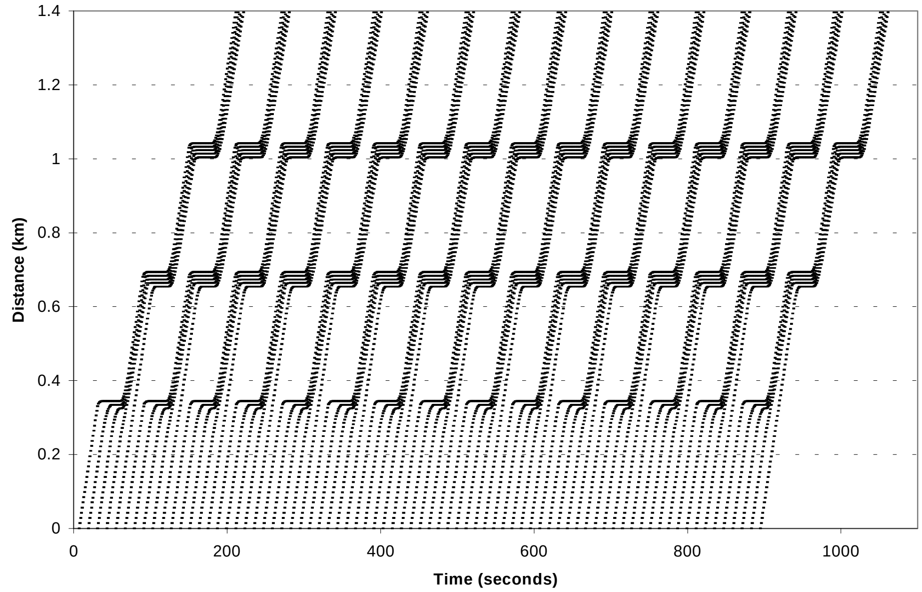

Figure 4-10 Vehicle Trajectory (Poor Fixed-time Signal Coordination).

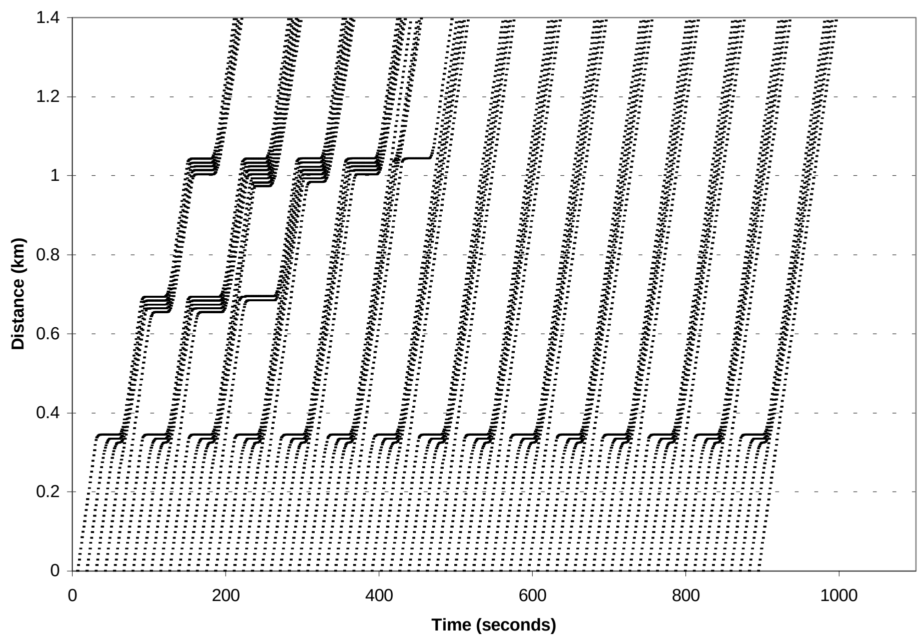

Figure 4-11 Vehicle Trajectory (Real-time Traffic Signal Coordination).

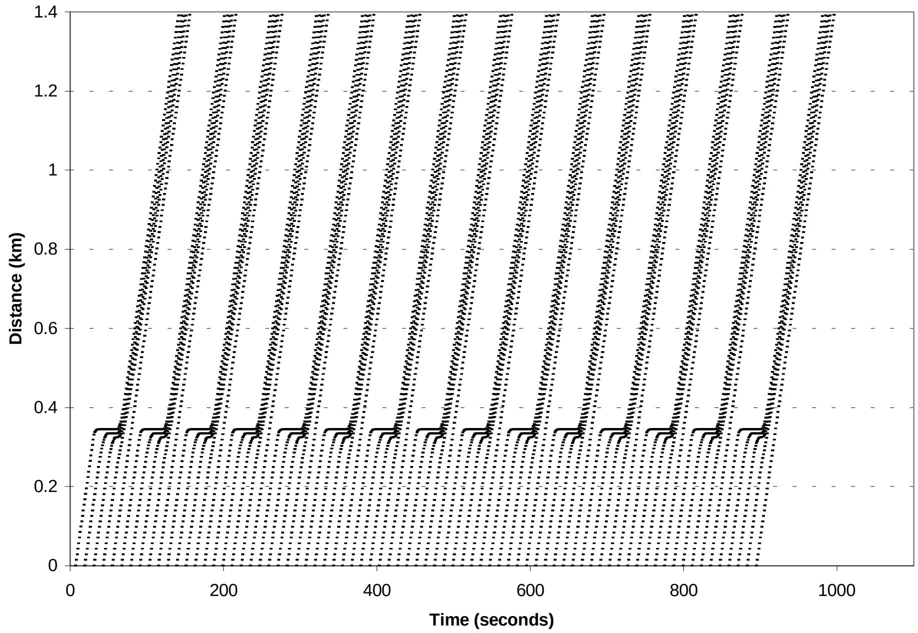

Figure 4-12 Vehicle Trajectory (Good Fixed-Time Signal Coordination).

Figure 4-10 represents the vehicle trajectory for poor fixed-time signal coordination. Each narrow line stands for each vehicle, and the wide lines represent the traffic platoons generated by the signal. As shown in the figure, all vehicles stop at the first, second, and third signals due to the poor signal coordination.

Figure 4-11 represents the vehicle trajectories in a real-time traffic signal coordination implementation. Initially, most of the vehicles stop at the signal but, as time progresses, the signals change their offsets and vehicles progress without stops. Figure 4-12 shows the vehicle trajectories of good fixed-time signal coordination. As shown in the figure, vehicles proceed without a stop after the first signal.

Table 4-4 shows the summary of the delay metrics associated with each strategy.

Table 4-4 Summary of the Delay of Four Signal Control Strategies.

	Total Delay (s)	Average Vehicle Delay (s)
No Signal Control	0	0
Poor Fixed-time Signal Coordination	4210	56.144
Real-time Signal Coordination	1614	21.527
Good Fixed-time Signal Coordination	586	7.823

As discussed in the previous chapter, vehicle fuel consumption and emission rates are highly dependent on vehicle acceleration. Repeated delays and stops result in frequent acceleration behavior. Poor signal control coordination reduces fuel economy and increases the production of emissions. Figure 4-13 depicts the variations in speed and acceleration for a probe vehicle used to access poor signal coordination.

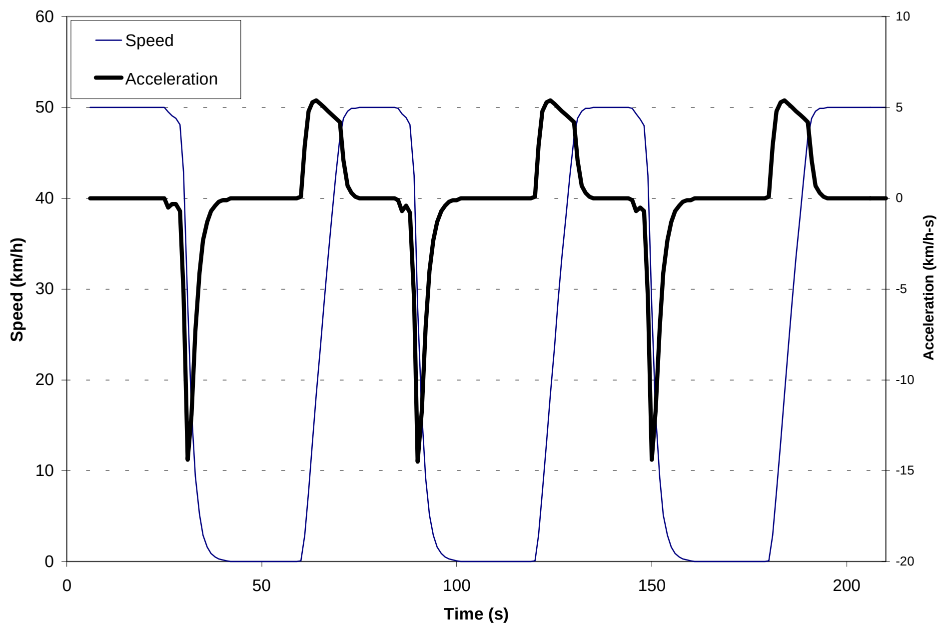

Figure 4-13 Variations in Speed and Acceleration under Poor Signal Coordination.

Figure 4-14 represents the sample emission rates for a probe vehicle under good and poor signal coordination strategies.

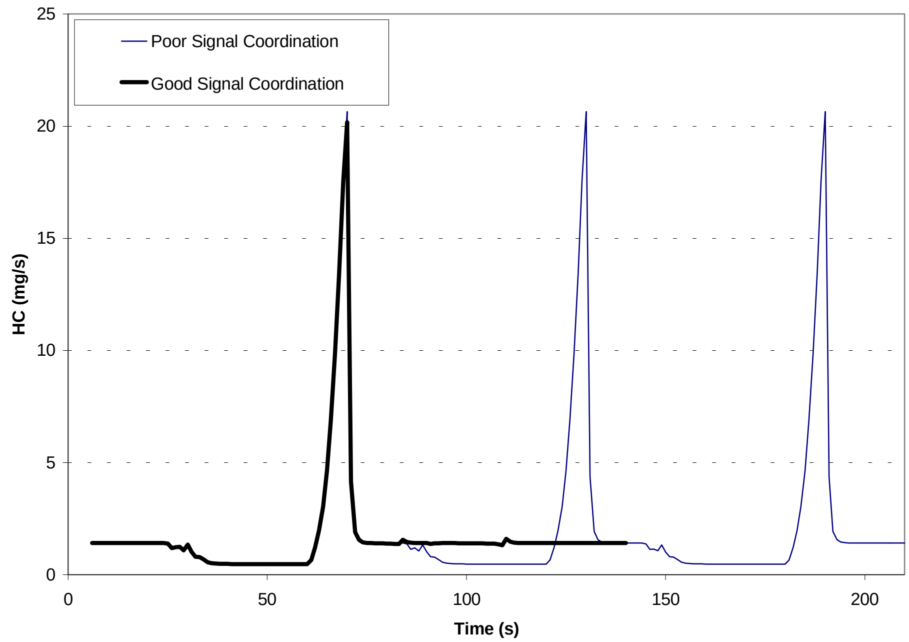

Figure 4-14 HC Emissions for a Probe Vehicle.

As shown in Figure 4-14, stops and acceleration behaviors produce up to ten times more emissions than a constant speed driving behavior. Until the first signal, emission rates are same for the both signal controls. However, it is observed that after the first sharp emission peak, HC rates are almost constant for good signal coordination. This is not the case under poor signal coordination. Table 4-5 and Figure 4-15 show a summary of the fuel consumption and emissions rates for four different signal controls.

Table 4-5 Summary of Total Fuel Consumption and Emissions.

	Fuel Consumption (liters)	HC (g)	CO (g)	NOx (g)
No Signal Control	11	10	180	21
Poor Signal Coordination	19	21	350	54
Real-time Signal Coordination	15	15	260	36
Good Signal Coordination	13	13	227	30

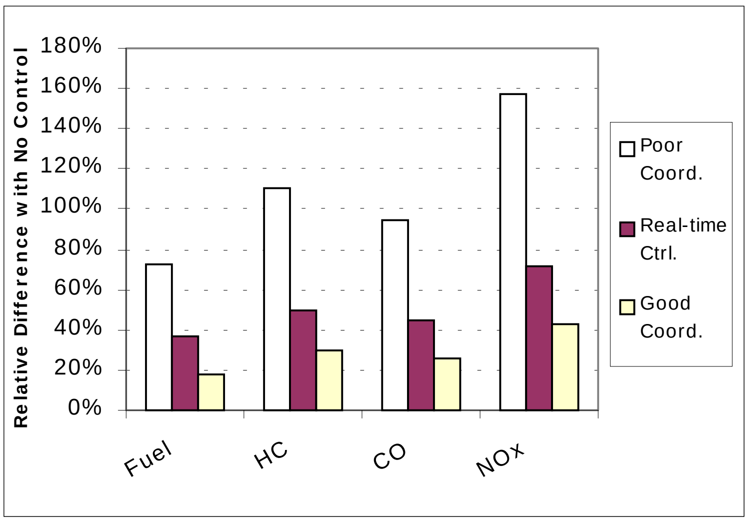

Figure 4-15 Relative Difference with No Control.

As shown in Figure 4-15, poor signal control coordination produces the NOx pollutant up to increments of 157% than is the case with those observed under no signal control. However, Figure 4-16 shows possible pollutant reductions using various signal control strategies.

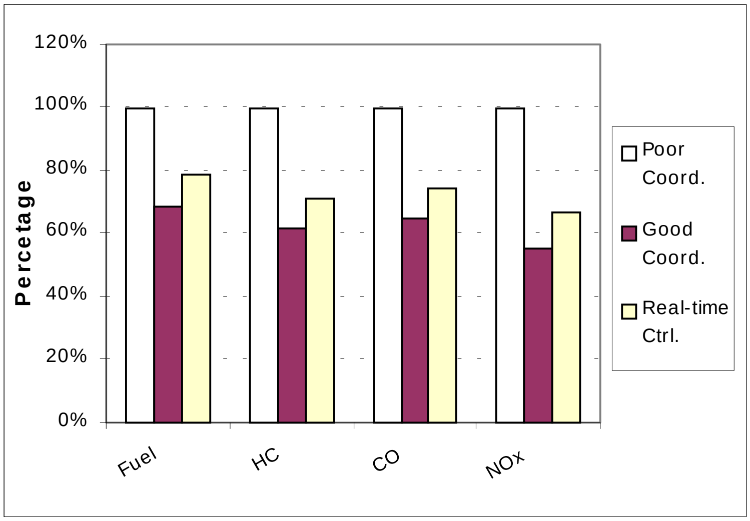

Figure 4-16 Comparison of Fuel Consumption and Emissions for Various Signal Controls.

Figure 4-16 suggests that good signal coordination and real-time signal controls can increase fuel economy and reduce the pollution metrics. Furthermore, good signal coordination can reduce NOx pollutants up to 45 %, compared with poor signal coordination.

4.3 Incident Delay Impact

An incident is any non-recurrent event that causes a temporary reduction in roadway capacity. Incidents are one of the main elements that affect highway delays. Incident management, which is one of most popular ITS techniques, has been established in urban areas nationwide to help reduce the magnitude of incident induced congestion.

Incident management improves the incident control capabilities of transportation and public safety systems, implements a response to minimize the effects on traffic, and helps public and private organizations to identify incidents quickly. Generally, incident management has five stages: incident detection, incident verification, incident response, incident clearance, and motorist information.

In this section, it was investigated how reduced incident recovery time and motorist information affect fuel consumption and emissions. In order to simulate a real incident condition, the INTEGRATION software was used.

4.3.1 Variable Incident Duration Test

A 25 km length section of one lane highway is used to test energy and emissions under incidents. There is no exit on this section, and the free speed is 100 km/h, the jam density is 90 veh/h, and the saturation flow rate of this section is 2250 veh/h. The departure rate is 900 veh/h (v/c ratio = 0.4), and incident duration times increases from 0 to 1200 seconds with a 300 seconds interval.

In order to simulate the scenarios, we assume that,

1. The first and the last times that vehicles enter the network is 0 and 1800 seconds, respectively. Also, simulations continue by 3000 seconds in order to clear all the vehicles entering the network. All the estimates of measures of effectiveness (MOEs) are the output of 1800 seconds of simulation.
2. All the incidents block 100 percent of the lane capacity. And, after clearance, the lane capacity is fully recovered.
3. The incident occurs at 900 seconds from the start of the simulation, and it occurs on the 19.75 km point from the departure location.

Figure 4-17 illustrates total delays for each incident duration time. Total Delay increases exponentially as incident duration lengthens.

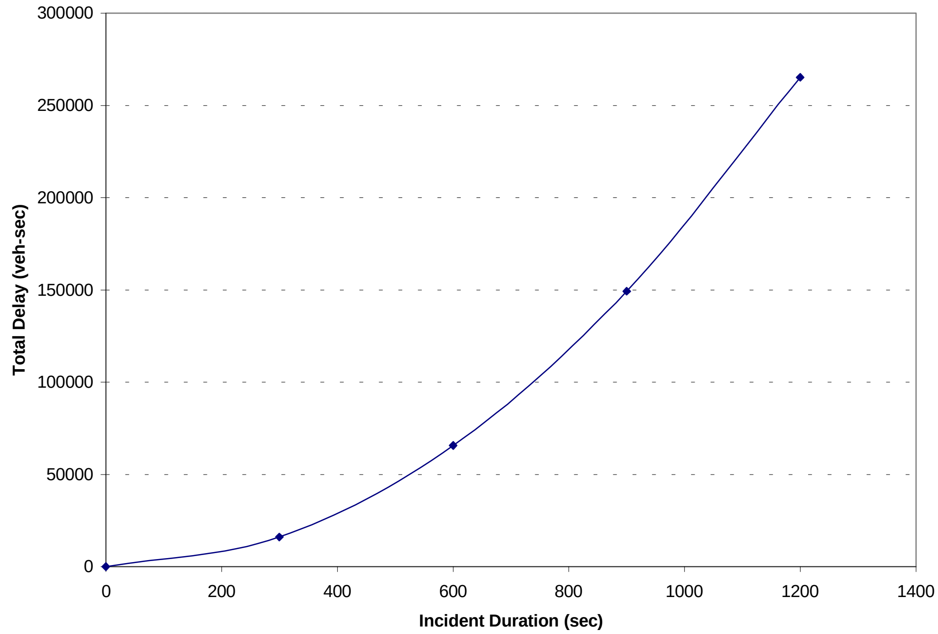

Figure 4-17 Total Delays for Various Incident Duration Times.

Figure 4-18 represents the total fuel consumption and emission rates produced during each simulation time. As shown in Figure 4-18, the changes in incident duration do not affect the total fuel consumption and emissions rates significantly. The figure illustrates that the total emissions of HC and NOx does not change much according to changes in incident duration, while total CO emission rates increase about 15% after the reduction in incident length (1200 to 0 seconds).

The results can be explained in that although there was no incident on the highway, individual vehicles generated sufficiently large emissions to account for this outcome. The free flow speed of these simulations was 100 km/h, which is known to produce good amount of emissions. Also, vehicles produce very small amounts of emissions during idling condition. And, in this case, the effect of acceleration, which is the main factor affecting fuel consumption and emissions, was relatively small.

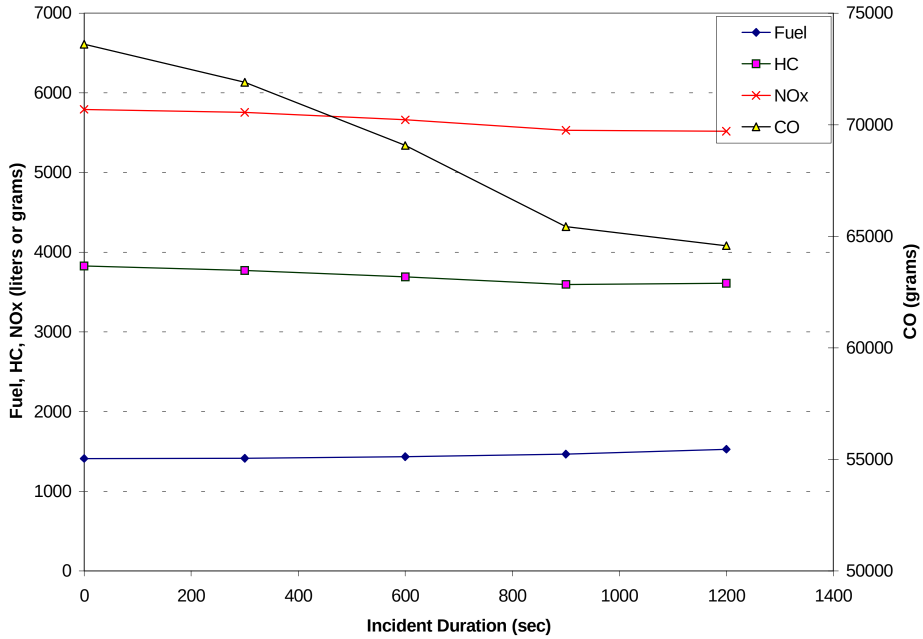

Figure 4-18 Fuel Consumption and Emission Rates for Various Incident Duration.

4.3.2 Route Diversion Strategy Test

The simulation network used for route diversion test is shown in Figure 4-19.

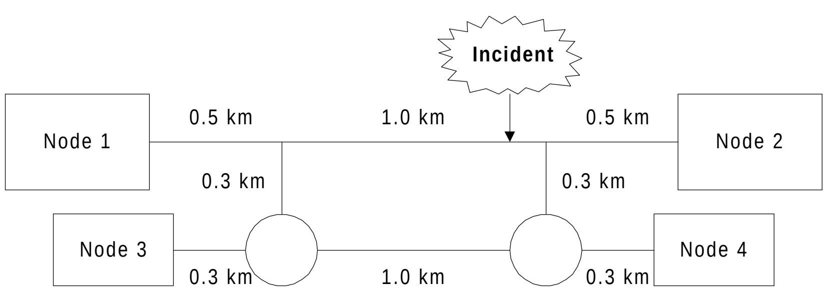

Figure 4-19 The Sample Network for Route Diversion Test.

The network has four nodes, including two signalized intersections. Two signals on the arterial have two phases, and the signal time is optimized by INTEGRATION itself. To simplify the analysis, one side of the highway and the arterial are considered for simulations. The incident occurs at the 1.3 km point from the starting node of the highway and blocks two out of three lanes. This incident starts at 150 seconds and ends 600 seconds from the start of the simulation. In the case of the diversion test, real-time traffic information is provided to the vehicles on the highway while 20 percent of error rates are applied.

The following parameters are used in all the simulations.

- Total Simulation Time: 1200 seconds
- Vehicle Departure Time: 0 to 900 second
- Total network length: 4.8 km (8.8 lane-km)
- Number of Vehicles Entered: 650 vehicles (600 on hwy. and 50 art.)
- Free Flow Speed: 100 km/h on the highway and 60 km/h on the arterial
- Jam Density: 80 veh/km
- Capacity: 2000 veh/hr
- Number of Lanes: Three lanes on the highway and one lane on the arterial

Table 4-6 illustrates the simulation results of diversion, no-diversion, and the no-incident tests.

Table 4 - 6 Summary of Diversion Technique Results.

	Diversion	No Diversion	No Incident
Total Delay (veh-secs)	33053	51799	4574
Veh-stops	859	838	93
Fuel (l)	228.09	225.95	158.71
CO (g)	22589.77	20507.15	11315.21
HC (g)	2989.38	3356.51	1773.76
NOx (g)	891.59	850.63	626.76

The results of the test support the following findings:

1. Diversion technique reduces 35 percent of the total delay.
2. Diversion technique increases fuel consumption, CO and NOx emission rate slightly.
3. Diversion technique does not affect the fuel consumption and emissions rates significantly.

Even though the diversion technique reduced the total vehicle delay, it did not reduce the fuel consumption and emission rates. This may be explained in that the total delay caused by an incident is dominated by idle conditions (stopped delay), the fuel consumption and emission rates in idling condition are relatively low. This might be the main reason why the diversion technique does not reduce fuel consumption and emissions rates.

Recently, many cities have adopted signal coordination techniques and incident management techniques and would like to know how these techniques affect fuel economy and emissions. According to these case studies, the signal coordination technique reduces pollutants significantly and also saves energy, while incident management does not decrease fuel consumption and emission rates. However, these results can be vary according to the network conditions, flow characteristics, traffic signal control types, and simulation scenarios.

4.4 Summary of Chapter 4

This chapter has demonstrated how the combined use of a microscopic vehicle dynamic model, together with a microscopic vehicle energy and emission model, can be utilized to evaluate alternative ITS and non-ITS applications. The microscopic energy and emission models were implemented into the INTEGRATION traffic simulation model and applied to a typical networks for model testing. As a test of feasibility, this tool was utilized to evaluate alternative types of traffic control and incident management problem.

The study demonstrated that for steady-state conditions (no vehicle accelerations), the tool predicted vehicle fuel consumption and emissions consistently with field data that were obtained from ORNL. Furthermore, the study demonstrated that vehicle fuel consumption and emissions are more sensitive to the level of vehicle acceleration than they are to the vehicle speed (difference of up to ten-fold). In addition, this study has demonstrated that the use of the average trip speed to estimate vehicle fuel consumption and emissions (as is the case in MOBILE5) fails to capture these important differences in acceleration levels. Finally, the study demonstrated that incident management techniques did not affect the energy and emissions rates notably.

Chapter 5. Conclusions

5.1 Summary of the Thesis

This thesis demonstrates some preliminary modeling results of microscopic fuel consumption and emission rate models and their applications. Key input variables to these models are vehicle speed and acceleration. The results of this modeling study support the following conclusions:

- For a composite vehicle, modeling results demonstrate a good agreement between the raw data and the model predictions;
- The accuracy of both models in predicting fuel consumption appears to be reasonable, with correlation coefficients of above 0.99;
- The accuracy (correlation coefficient: 0.85-0.95) of both models in predicting CO, NOx, and HC emissions rates is acceptable for traffic impact assessment, including the assessment of ITS technology impacts on the environment.

The development of these models attempts to bridge the existing gap between traffic model simulator outputs, traditional transportation planning models, and environmental impact models. The models presented in this thesis are general enough to be incorporated in any existing or planned model where vehicle kinematics are explicit enough to include speed and acceleration variables. This model was implemented into a micro-simulation model INTEGRATION and applied to a typical network for model testing. The model developed has been applied to a signal coordination and an incident management problem. The composite vehicle is used throughout the entire model testing. The summary of the case studies support the following conclusions:

- Vehicle fuel consumption and emissions are more sensitive to the level of vehicle acceleration than to vehicle speed.

- Under constant speed driving condition, the best fuel economy speed is found at around 70 km/h. Emissions generally increase as speed increases, while the minimum total HC emission is found at around 50 km/h.
- Even for vehicle trips that have the same average speeds, their fuel consumption and emissions rates are significantly different. A variable speed trip consumes and emits more fuel (25 %) and emissions (300 to 400 %) than a constant speed trip.
- Good real-time signal coordination can reduce the fuel consumption and emission rates more significantly than can poor signal coordination.
- However, a reduction in incident duration does not reduce the amount of pollutants while this decreases the fuel consumption slightly.
- Also, the diversion technique does not affect fuel consumption and emission rates significantly in the case study.

5.2 Model Limitations

Like any mathematical model, there are some limitations in the use of the models developed. These limitations include the following:

- Start up emissions (cold-start vs. hot-start) and ambient temperature are not considered in the current models. Work is needed to develop models that are sensitive to the ambient temperature.
- Models cannot be applied beyond the vehicle speed and acceleration boundaries that were used in their calibration.

The first point arises because all data from ORNL were collected under hot-stabilized engine conditions. Recent second-by-second data obtained from the EPA have proven valuable in determining the differences between hot-running and cold-started engines. A model is being developed to add this contribution as an external additive function to the models presented here.

The second limitation results from the inherent limitation of any model to extrapolate response values beyond the boundaries used in the model calibration procedure. While most vehicles can travel faster than 110 ft/s (upper limit of the testing boundary), it is impossible to establish a reliable forecasting pattern at high speeds due to the heavy nonlinear nature of the response curves. No data is available to verify energy and emissions rates.

5.3 Further Research

The following areas of research are currently being pursued to expand the applicability of the models developed in the context of microscopic traffic simulation:

- Aggregate start-up vehicle emissions and microscopic start-up emission models must be added to the microscopic fuel consumption and emissions model, including cold-start, hot-start, and soak-time functions.
- The environmental impact of heavy-duty vehicles cannot be ignored in the modeling process. Heavy-duty gasoline and diesel engines should be modeled separately.
- Vehicle composition and its analysis are important considerations in the modeling process. Additional vehicle data including high emitters must be added to the model.
- More data are required to extend the boundaries of the data and to include more vehicles.
- Currently, only three air pollutants (CO, HC, and NOx), in addition to fuel consumption, are modeled. Two important pollutants, particulate matters and CO2, will be added to the model.

References:

Akcelik, R. (1985) An Interpretation of the parameters in the Simple Average Travel Speed Model of Fuel Consumption, *Australian Road Research No. 15*, Melbourne.

Akcelik, R. (1989) Efficiency and Drag in the Power-Based Model of Fuel Consumption, *Transportation Research 23B*, 376-385.

An, F., and M. Ross (1993a) Model of Fuel Economy with applications to Driving Cycles & Traffic Management, *Transportation Research Record*, Washington, D.C.

An, F., and Ross, M. (1993b) A Model of Fuel Consumption and Driving Patterns, SAE Paper No. 930328.

Baker, M. (1994) *Fuel Consumption and Emission Models for Evaluating Traffic Control and Route Guidance Strategies*, Mater thesis, Queen's University, Kingston, Ontario, Canada

Barth, M., An, F., Norbeck, J., and Ross, M. (1996) Model Emission Modeling: A Physical Approach, *Transportation Research Record, No. 1520*, Washington, D.C.

Barth, M., Norbeck, J., Ross, M. (1998) National Cooperative Highway Research Program Project 25-11: Development of a Comprehensive Modal Emissions Model, Presented at the 77th Annual Meeting of the Transportation Research Board, Washington, D.C.

Davis, S.C. (1994) *Transportation Energy Data Book: Edition 14. ORNL-6798.* Center for Transportation Analysis, Energy Division, Oak Ridge National Laboratory, Tenn.

DOT and EPA (1993) Clean Air Through Transportation: Challenges in Meeting National Air Quality Standards. Aug.

Ennsm, P., J. German, and J. Markey (1993) EPA's Survey of In-Use Driving Patterns: Implications for Mobile Source Emission Inventories. Office of Mobile Sources, U.S. Environmental Protection Agency.

EPA (1993a) Automobile and Carbon Monoxide, U.S. Environmental Protection Agency Report No. EPA 400-F-92-005. January

EPA (1993b) Federal Test Procedure Review Project: Preliminary Technical Report. Office of Air and Radiation, May

EPA (1994a) Automobile Emissions: An Overview, U.S. Environmental Protection Agency Report No. EPA 400-F-92-007. August

EPA (1994b) Milestones in Auto Emissions Control, U.S. Environmental Protection Agency Report No. EPA 400-F-92-014. August

Fisk, C. S. (1989) The Australian Road Research Board instantaneous model of fuel consumption *Transportation Research 23B,* 373-376.

Guensler, F., S. Washington, and D. Sperling (1993) A Weighted Disaggregate Approach To Modeling Speed Correction Factors. *Transportation Research Record*, Washington, D.C., 44pp.

Guensler, R. et al. (1998) Overview of the MEASURE Modeling Framework, *Transportation Research Record*, Washington, D.C.

Horowitz, J.L., (1982) *Air Quality Analysis for Urban Transportation Planning*. MIT Press, Cambridge, Mass., 387 pp.

Johnson, J.H. (1988) Automotive Emissions. *Air Pollution, the Automobile, and Public Health*. Health Effects Institute. National Academy Press, Washington, D.C.

LeBlanc, D., M.D. Meyer. F.M. Saunders, and J.A. Mulholland (1994) Carbon Monoxide Emissions from Road Driving: Evidence of Emissions due to Power Enrichment. Presented at the *Transportation Research Record*, Washington, D.C., 23pp.

Mobile 5A User Guide (1993) Environmental Protection Agency, Ann Arbor, Michigan

Murrell, D. (1980) *Passenger Car Fuel Economy: EPA and Road*. U.S. Environmental Protection Agency, Jan., 305 PP

National Research Council (NRC) (1995) *Expanding Metropolitan Highways: Implications for Air Quality and Energy Use*, National Academy Press, Washington, D.C.

Nizich, S.V., T.C. McMullen, and D.C. Misenheimer (1994). *National Air Pollutant Emissions Trends*, 1900-1993. EPA-454/R-94-027. Office of Air Quality Planning and Standards, Research Triangle Park, N.C., Oct,. 314 PP.

Neural Network Toolbox for Use with Matlab Users Guide Version 3 (1998), Mathworks Inc., Ntick, MA.

Post K et al. (1984) Fuel consumption and emission modeling by power demand and a comparison with other model. *Transportation Research 18A*, 191-213.

Richardson, A.J., and Akcelik, R. (1981) Fuel consumption Models and Data Needs for the design and Evaluation of Urban Traffic System, Australian Road Research Board, Report No. ARR 124, September

Van Aerde, M. (1998) *INTEGRATION Release 2.10 for Windows: User's Guide-Volume I, Fundamental Model Features*, Blacksburg, VA

Ward's Automotive Yearbook (1996), 58th Edition, Ward's Communications, Southfield, MI, Intertec Publishing.

Ward's Automotive Reports (1995), Ward's Communications, Vol. 70, No. 51, December, Southfield, MI, Intertec Publishing.

West, B., McGill, R., Hodgson, J., Sluder, S., Smith, D. (1997) Development of Data-Based Light-Duty Modal Emissions and Fuel consumption Models, Society of Automotive Engineers Paper No. 972910

Appendix A

Table A-1 Test Vehicle and Industry Average Specifications.

Year	Make/Model	Engine	Transmission	Curb Weight lbs (kg)	Rated hp
Light-Duty Cars					
1988	Chevrolet Corsica	2.8L pushrod V6,PFI	M5	2665(1209)	130
1994	Oldsmobile Cutlass Supeme	3.4L DOHC V6, PFI	L4	3290(1492)	210
1994	Oldsmobile 88	3.8L pushrod V6, PFI	L4	3360(1523)	170
1995	Geo Prizm	1.6L OHC I4, PFI	L4	2460(1116)	105
1993	Subaru Legacy	2.2L DOHC flat 4, PFI	L4	2800(1270)	130
	5-car average	2.8L, 5.2 cyl.		2915(1322)	149
1995	LDV industry average	2.9L, 5.4 cyl.		2900(1315)	
Light-Duty Trucks					
1994	Mercury Villager Van	3.0L pushrod V6, PFI	L4	4020(1823)	151
1994	Jeep Grand Cherokee	4.0L pushrod I6, PFI	L4	3820(1732)	190
1994	Chevrolet Silverado Pickup	5.7L pushrod V8, TBI	L4	4020(1823)	200
	3-truck average	4.2L, 6.7 cyl		3953(1793)	180
1995	LDT industry average	4.6L, 6.5 cyl			
	8-vehicle average	**3.3L, 5.8 cyl**		3300(1497)	160
1995	**LDC+LDT, industry avg.**	**3.5L, 5.8 cyl**			

Source: West et al. 1997

Appendix B

B-1 Error Plot of Model N

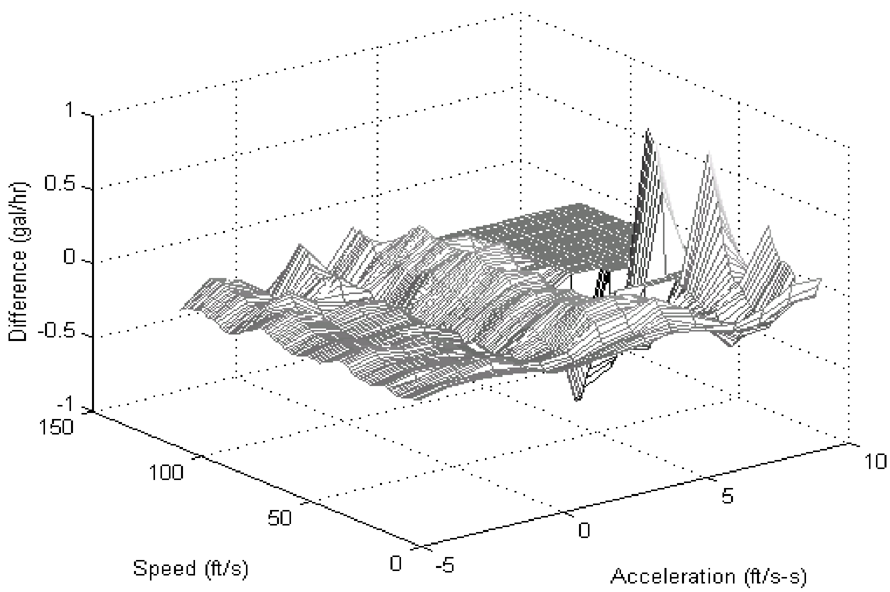

Figure B-1 Differences between the Predicted Fuel Consumption Values and the Raw Data in Model N.

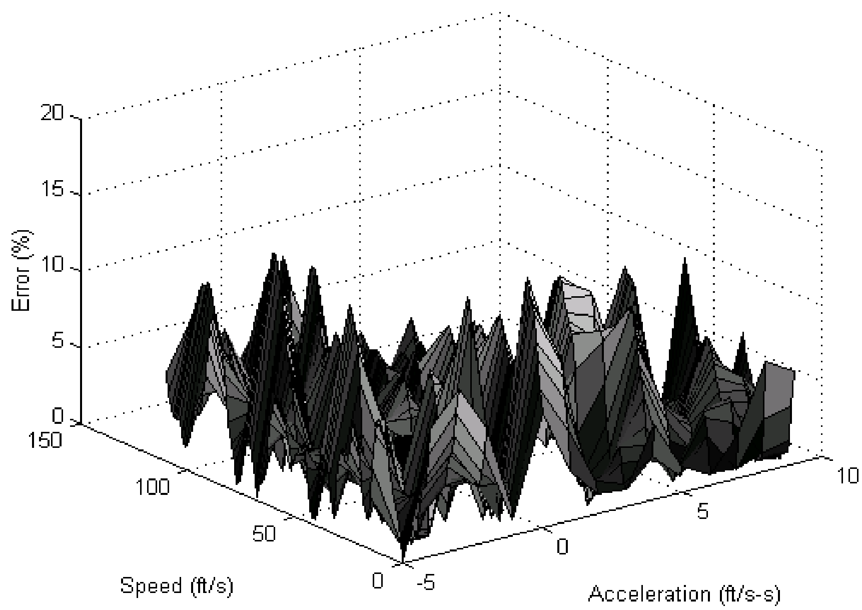

Figure B-2 Error Plot of Fuel Consumption Model for Model N.

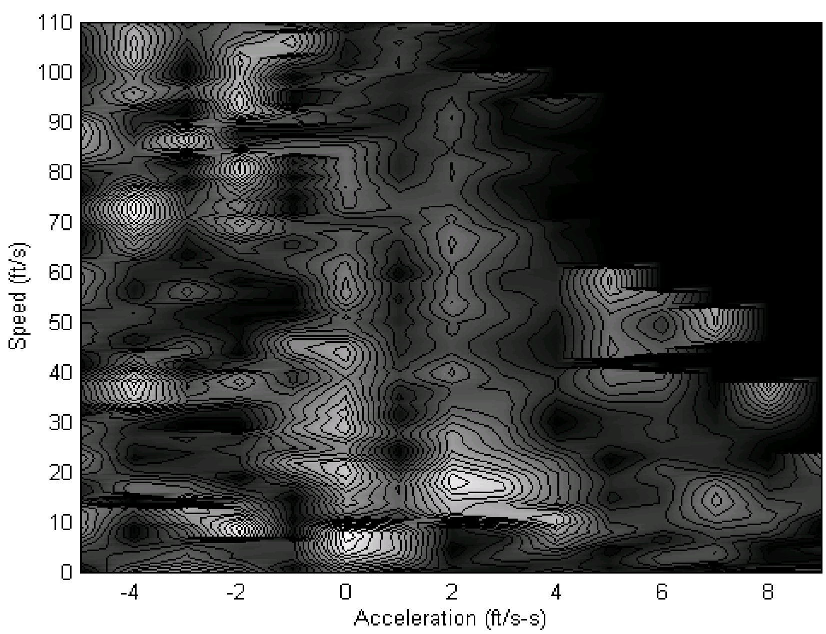

Figure B-3 Contour Plot of Fuel Consumption Error of Model N.

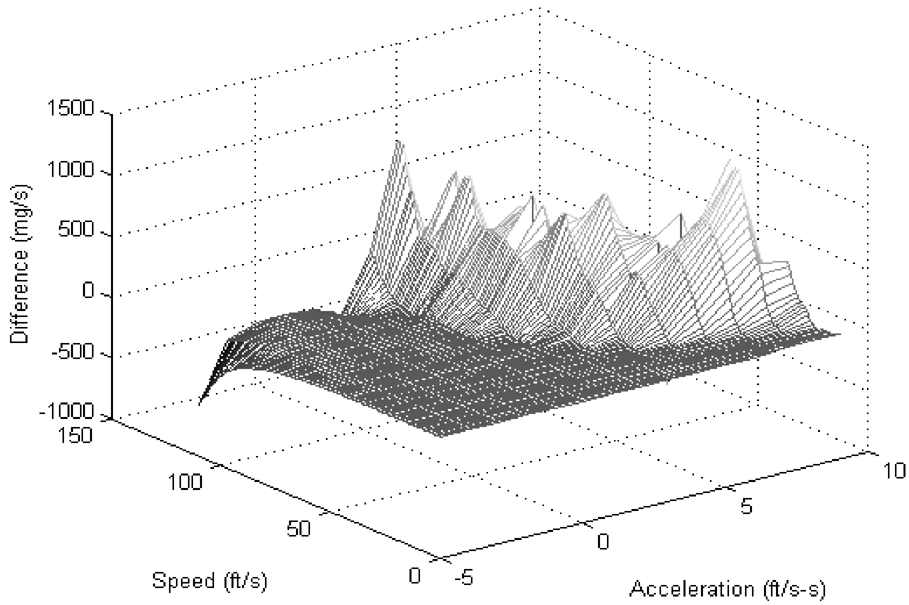

Figure B-4 Differences between the Predicted CO Values and the Raw Data in Model N.

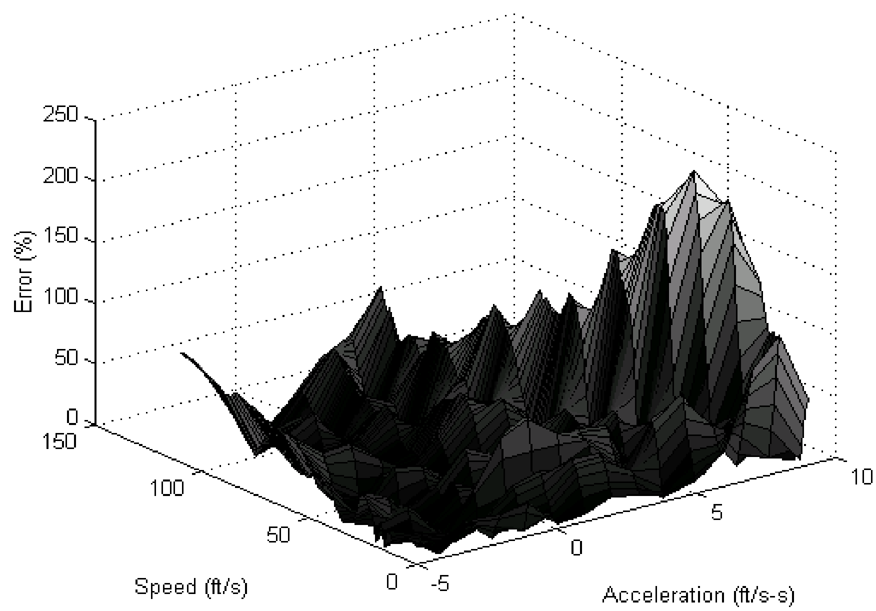

Figure B-5 Error Plot of CO Model for Model N.

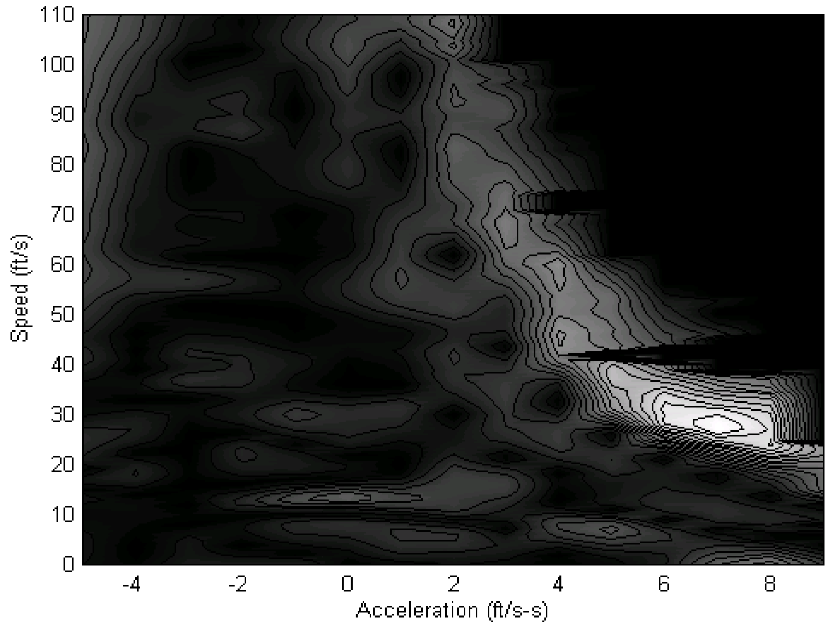

Figure B-6 Contour Plot of CO Error of Model N.

B-2 Error Plot of Model O

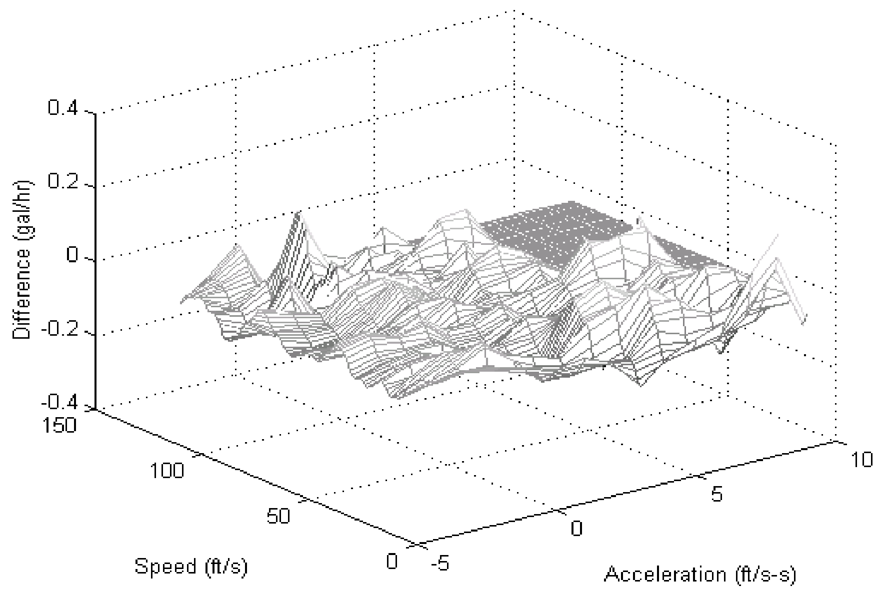

Figure B-7 Differences between the Predicted Fuel Consumption Values and the Raw Data in Model O.

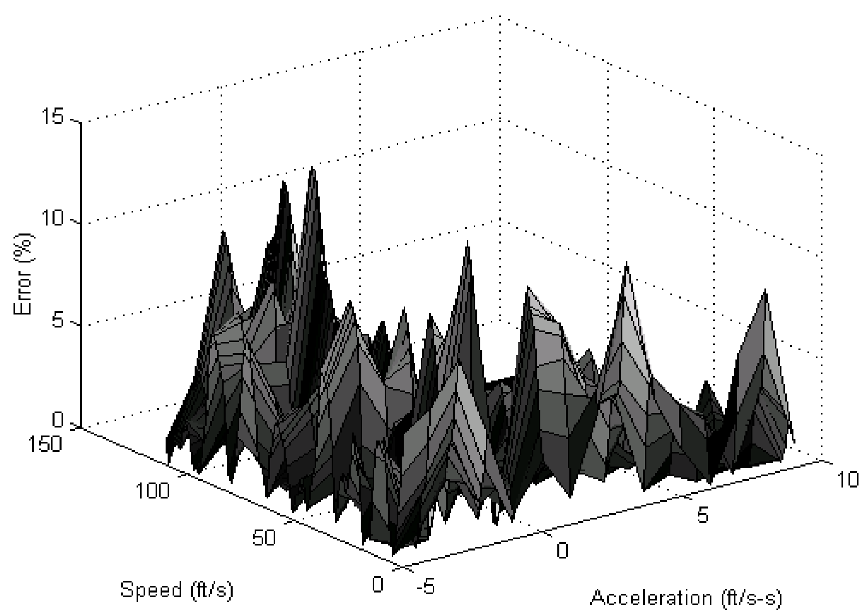

Figure B-8 Error Plot of Fuel Consumption Model for Model O.

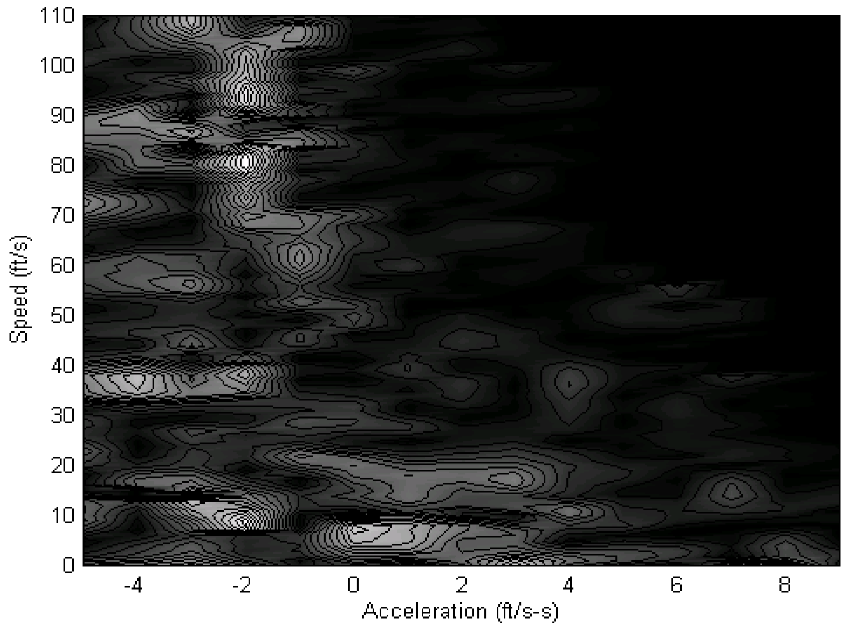

Figure B-9 Contour Plot of Fuel Consumption Error of Model O.

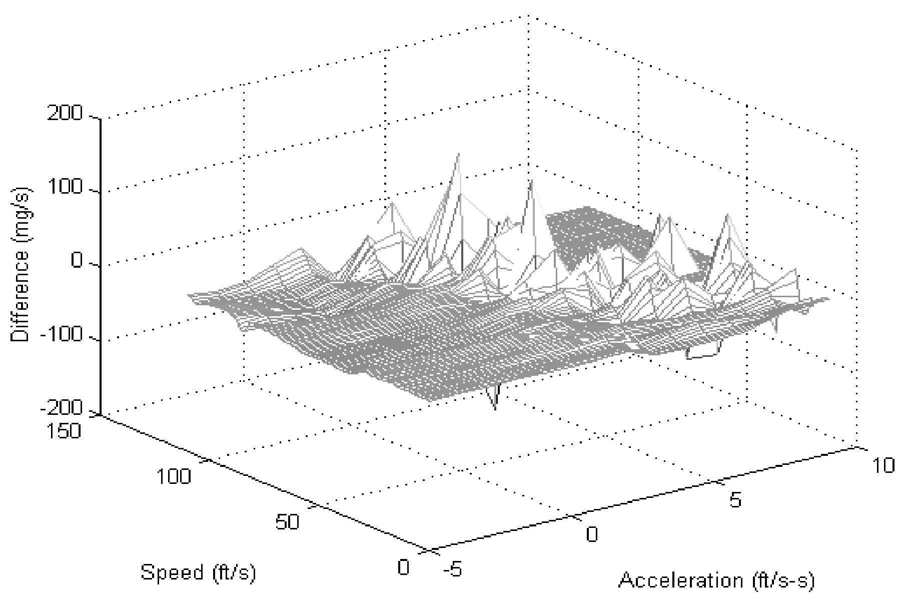

Figure B-10 Differences between the Predicted CO Values and the Raw Data in Model O.

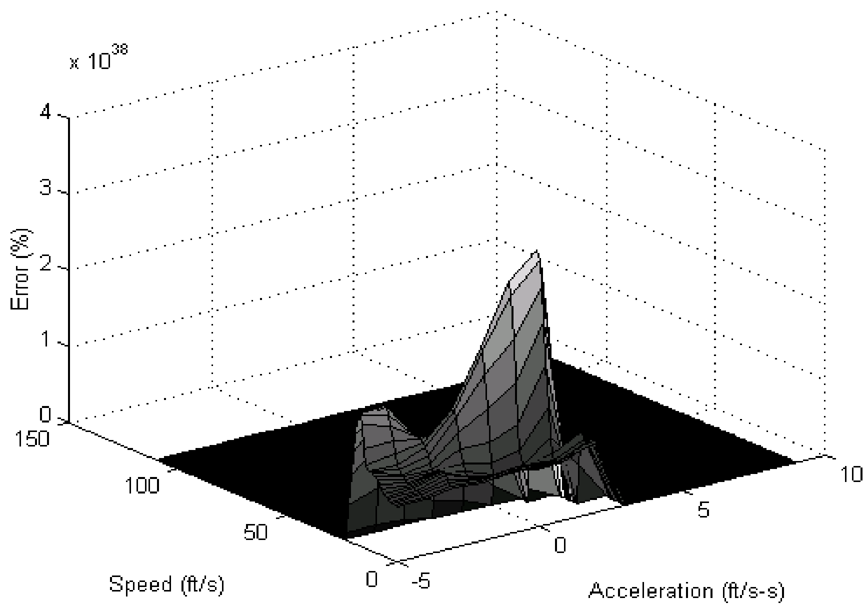

Figure B-11 Error Plot of CO Model for Model O.

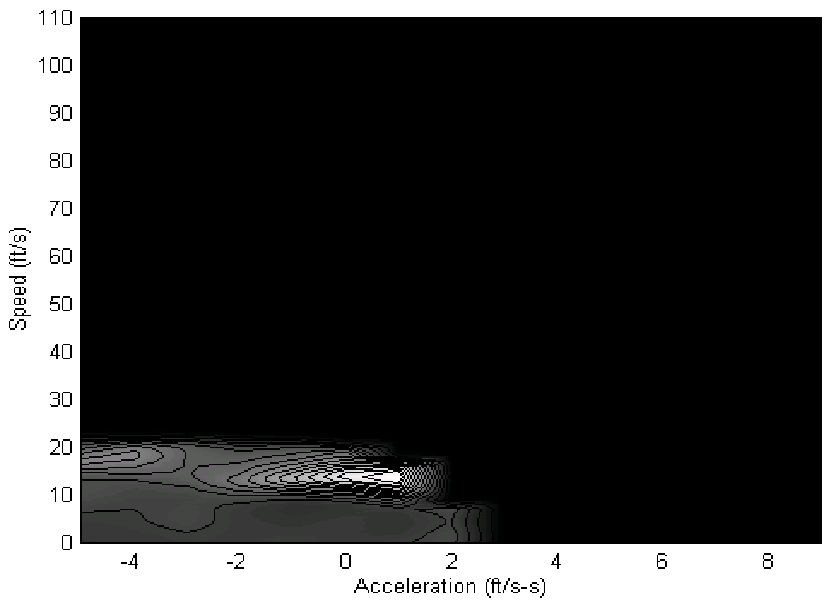

Figure B-12 Contour Plot of CO Error of Model O.

Appendix C

C-1 Matlab source code (Neural network training)

```
% NEURAL NETWORKS TRAINING FOR CAR EMISSIONS
% DEVELOPED BY DR. ANTONIO TRANI and KYOUNGHO AHN
% Revision 2 : Mar/10/1998


% Data input (file with velocity, acceleration and HC emissions
profiles)


% Copy the data(only data) to a new sheet
% Save excel data file as lotus wk1 type
% (EX) corf.wk1


% Save the data as matrix 'emi1'
% Change the worksheet

emi1 = wk1read('com2no.wk1',1,1);

k=0;

[row,col] = size(emi1);

% Assign three column vectors for speed, acceleration and emissions

for j = 1:col
    for i = 1:row
        if emi1(i,j) ~= 0

        k = k + 1;
             emi2(k) = emi1(i,j);
             speed1(k) = i - 1;
             acc1(k) = j - 6;

        end
    end
end

% Transpose the data

emi = emi2;
speed = speed1;
acc = acc1;


[ncol,nrow]=size(emi);
```

```
% Data Normalization (necessary to manipulate data)

speedn = speed/max(speed);
emin = emi/max(emi);
accn = acc/max(acc);

max_emi = max(emi);          % Maximum emissions from database


% Set Inputs and Targets

speed_min = min(speedn);
speed_max = max(speedn);
emi_min = min(emin);
emi_max = max(emin);
acc_min = min(accn);
acc_max = max(accn);
P1_cr = [speed_min speed_max; acc_min acc_max];
T1_cr = [emi_min emi_max ] ;

P_cr = [speedn; accn];
Ta_cr = [emin];

% Initialize Traning Parameters

df = 1;           % Frequency of progress displays (in epochs).
me = 10000;       % Maximum number of epochs to train.
eg = 0.03;            % Sum-squared error goal.
tp = [df me eg ];


% Initialize Weights and Biases

nns = 10;  % Number of Neurons in first layer
nns2 = 5;  % Number of neurodes in second layer


%*******************************
%       For HC Emissions       **
%*******************************


[ W31_cr,b31_cr,W32_cr,b32_cr,W33_cr,b33_cr
]=initff(P1_cr,nns,'tansig',nns2,'logsig',T1_cr,'logsig');

% Taining of the neural networks using Lavenberg-Marquardt Alogrithm

[ W31_cr,b31_cr,W32_cr,b32_cr,W33_cr,b33_cr ]=
trainlm(W31_cr,b31_cr,'tansig',W32_cr,b32_cr,'logsig',W33_cr,b33_cr,'lo
gsig',P_cr,Ta_cr,tp);
```

C-2 Matlab source code (Computer Program to Simulate Neural Network Results)

```
% NEURAL NETWORKS TRAINING FOR CAR EMISSIONS
% DEVELOPED BY TONI TRANI and KYOUNGHO AHN
% Revision # 2 (Mar/15/98)

%-------------------------------------------------
% Change the MAT file
%-------------------------------------------------

% Simulates NN results and checks accuracy


% load cr6
% loads a MAT file with cruise variables
% Simulate Traning Results

clear
load com2cocr;

[ncol,nrow]=size(emi);



%*********************   CO Analysis  *****************************
% Speed Normalization

TM3 = speedn;

% Acceleration Normalization

TA3= accn;

P3 = [TM3; TA3 ];

F3
=simuff(P3,W31_cr,b31_cr,'tansig',W32_cr,b32_cr,'logsig',W33_cr,b33_cr,
'logsig');

cal = F3 * max(emi);


%*************************STATISTICS*****************************

% calculate correlation coefficient and sum of squared error
% emi = GENERALIZED DATA
% F3 = normalized predicted data points
% cal = PREDICTED VALUES

correl=corrcoef(cal, emi)
for i=1:nrow;
   sq_er=(cal-emi).*(cal-emi);
end
sse=sum(sq_er)
```

```
% CALCULATING ERRORS and THE AVERGER MEAN

i = 1:nrow;
w(i) = abs(emi(i) - cal(i))./emi(i).*100;
m = mean(w(i))


hist(w,15)
xlabel('Error (%)');
ylabel('Frequency');
grid
pause


% Plot predicted vs actual HC emissions

plot(speed,emi,'o',speed,cal,'*')
xlabel('Speed (ft/s)')
ylabel('CO emissions (mg/s)')
grid

zoom
pause

plot3(speed,acc,emi,'o')
xlabel('Speed (ft/s)')
ylabel('Acceleration (ft/s-s)')
zlabel('CO Emissions (mg/s)')
grid
rotate3d on
```

C-3 Coefficients of Neural Network Models

Fuel consumption model of composite vehicle

W31_cr =

-2.3441	-3.6068
0.545	3.989
-1.1871	15.8267
-1.3359	-34.9685
-2.1817	2.9977
-0.4643	7.1607
-3.3227	0.773
-0.7025	1.0859
2.153	-1.0691
0.0045	0.9987

W32_cr =

9.8395	11.2833	16.8397	9.5135	-3.5567
5.8301	2.0437	-2.6434	-3.213	5.3262
2.7481	-0.2344	0.0405	0.0371	0.151
2.4731	-0.2383	-0.2996	1.1738	-3.9894
2.3906	-4.7423	1.5799	-0.7749	4.9463
10.3784	2.3867	21.6478	-8.2391	-4.5102
7.2281	4.8014	-13.5799	-7.7487	-3.4256
0.7447	0.6302	1.2586	-0.1151	-2.1916
6.4619	-4.224	-0.3685	-1.2051	18.369
-4.7091	8.1266	-27.8927	-6.2155	26.0683

W33_cr =

7.4912	-3.0672	-11.5365	2.608	35.6099

b31_cr	b32_cr	b33_cr
10.7115	16.662	-1.3345
-1.3451	6.8669	
-4.2914	-2.6062	
3.9883	-0.7492	
-0.9202	-5.059	
4.7345		
-1.0774		
-0.625		
-7.7266		
-0.641		

CO model of composite vehicle

W31_cr =

-8.4423	-12.7762
-4.785	0.2371
3.4909	8.971
0.5224	-1.7775
86.9082	89.803
1.6952	7.6344
20.5473	8.9231
-5.7592	-0.4062
-3.6823	-1.2485
-12.5008	-5.6944

W32_cr =

-142.764	327.5209	4.0144	13.5571	261.809
-0.2301	-1.5754	-17.2545	-28.2826	1.749
-23.8516	-26.8318	136.8162	-3.3562	-28.5863
1.7468	-3.3873	0.6608	-1.2107	0.2341
-40.5162	4.4494	-0.8991	-0.1803	151.5329
146.1387	143.6273	-119.696	16.4878	96.7187
3.0532	8.3863	-5.3488	1.4909	13.8055
19.857	20.7904	-5.601	-7.5315	10.0968
-3.1305	-0.7673	2.4445	-1.5547	-0.7736
41.7037	31.8503	-26.3897	26.8465	-2.4561

W33_cr =

1.1297	-1.0327	84.3573	374.648	-257.178

b31_cr =	b32_cr =	b33_cr =
-20.2527	143.224	166.9758
0.4542	-4.0353	
-3.6283	27.6592	
-0.0455	-2.2379	
-112.456	44.5925	
16.5706		
16.5178		
1.7009		
2.1601		
5.8495		

C-4 General Equation to use Coefficients of Neural Network Models

```
% General equation to use the NN parameters
% Developed by Kyoungho Ahn (Mar/19/1998)
%
%-------------------------------------------------------
% 1. Load MAT file
% 2. Input data transform(speed/max_speed, acc/max_acc)
%-------------------------------------------------------

clear
load com2cocr;

[ncol,nrow]=size(emi);


% Input Data Transform

TM3=speedn;       % speedn=speed/max_speed
TA3=accn;     % acc=acc/max_acc


% Input data matrix

P3=[TM3;TA3];


% Input variable for function 1

kk=W31_cr*P3;

for i=1:nrow;
   kk2(:,i)=kk(:,i)+b31_cr;
end

[row1,col1]=size(kk2);


% Calculating Function1(Hyperbolic tnagent)

for i=1:row1;
   for j=1:col1;
%   tanans1(i,j)= tanh(kk2(i,j));
        tanans2(i,j)=(exp(kk2(i,j))-exp(-
kk2(i,j)))/(exp(kk2(i,j))+exp(-kk2(i,j)));
   end
end


% Input variable for function 2

kk3=W32_cr*tanans2;

for i=1:nrow;
   kk4(:,i)=kk3(:,i)+b32_cr;
```

```
end

[row2,col2]=size(kk4);


% Calculating Function2(Log-sigmoid function)

for i=1:row2;
    for j=1:col2;
    logans(i,j)=1/(1+exp(-kk4(i,j)));
    end
end


% Input variable for function 3

kk5=W33_cr*logans;

for i=1:nrow;
    kk6(i)=kk5(i)+b33_cr;
end

[row3,col3]=size(kk6);


% Calculating Function3(Log-sigmoid function)

for j=1:col3;
    logans2(j)=1/(1+exp(-kk6(j)));
end


% Final Output

predicted=logans2*max(emi);
```

Appendix D

D-1 Fuel Consumption Modeling Test of Model N (FTP Cycle)

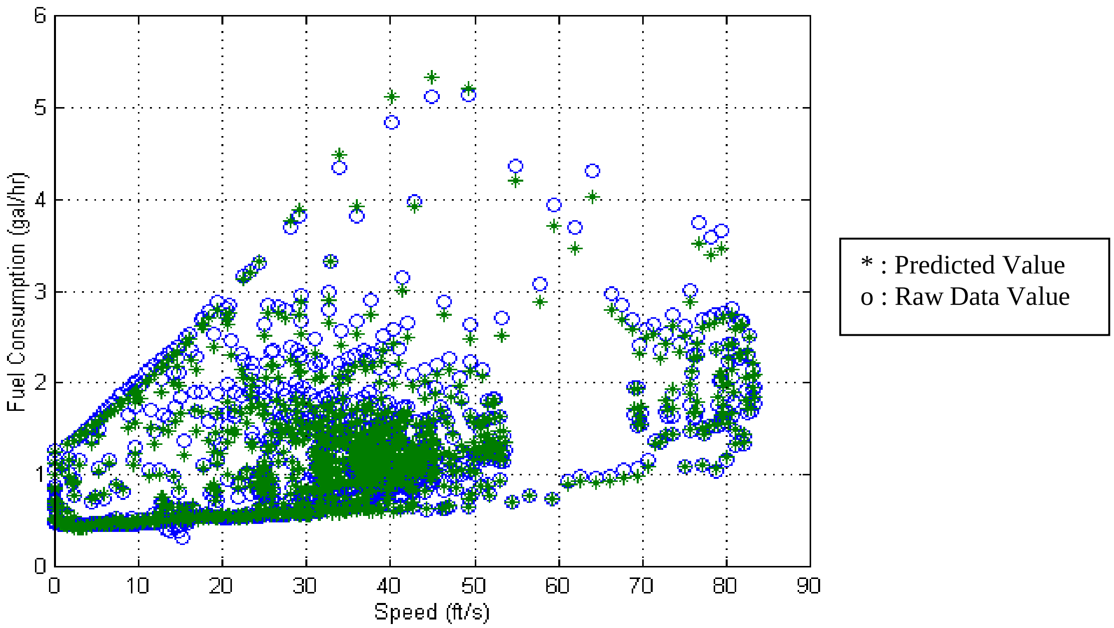

Figure D-1 Fuel Consumption for Model N (Speed Based).

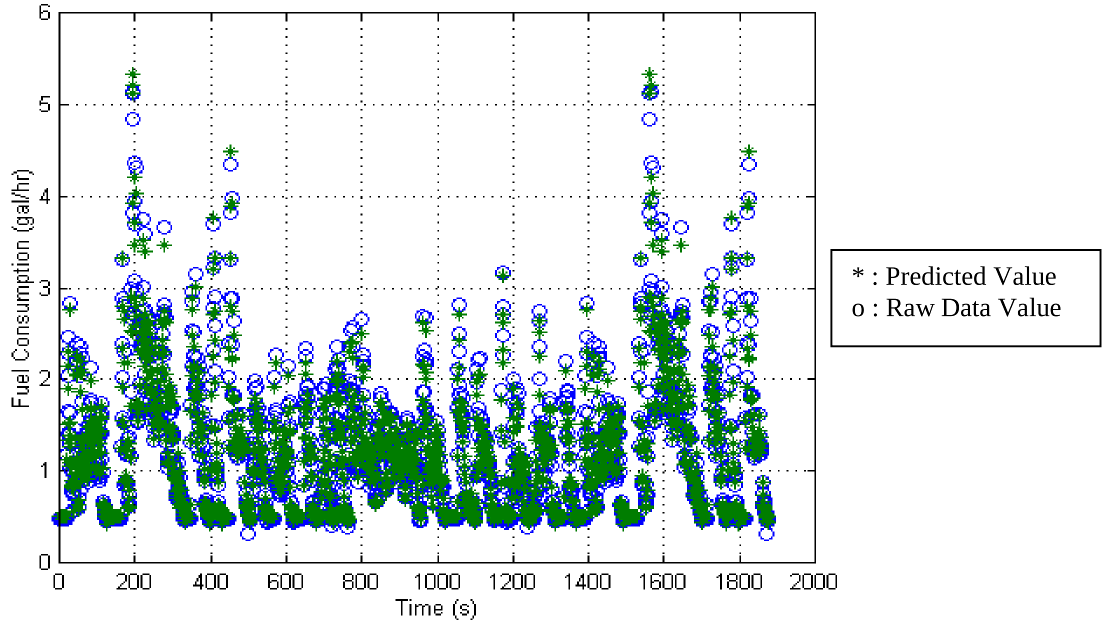

Figure D-2 Fuel Consumption for Model N (Time Based).

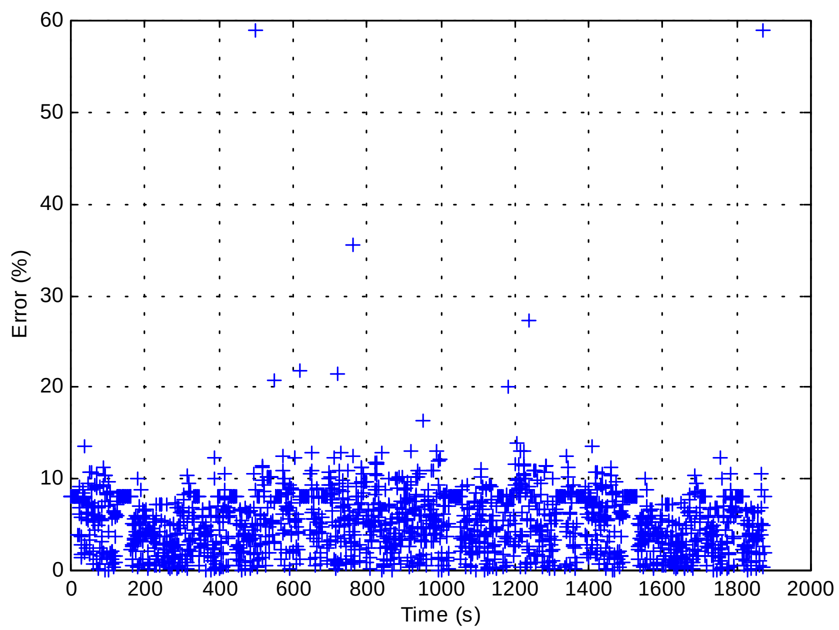

Figure D-3 Fuel Consumption Error for Model N.

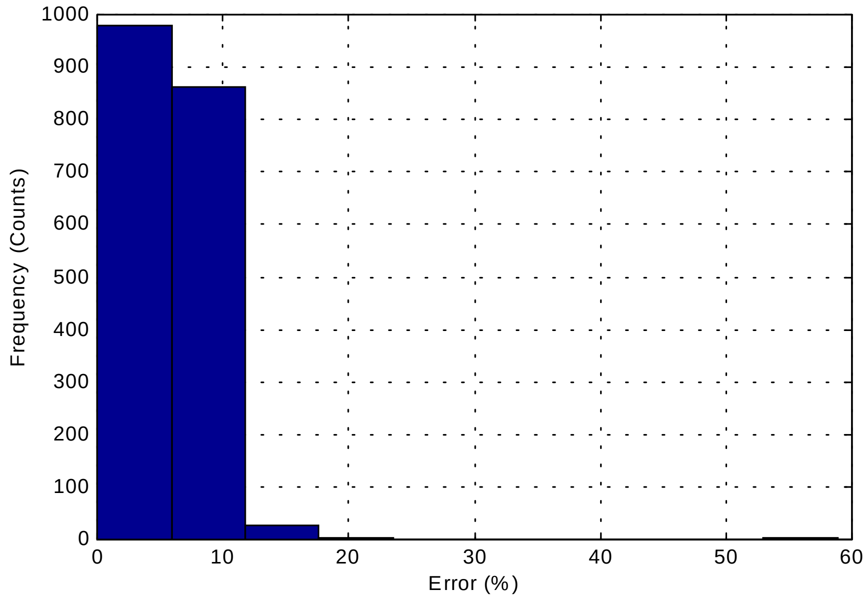

Figure D-4 Error Distribution of Fuel Consumption for Model N.

D-2 Fuel Consumption Modeling Test of Model O (FTP Cycle)

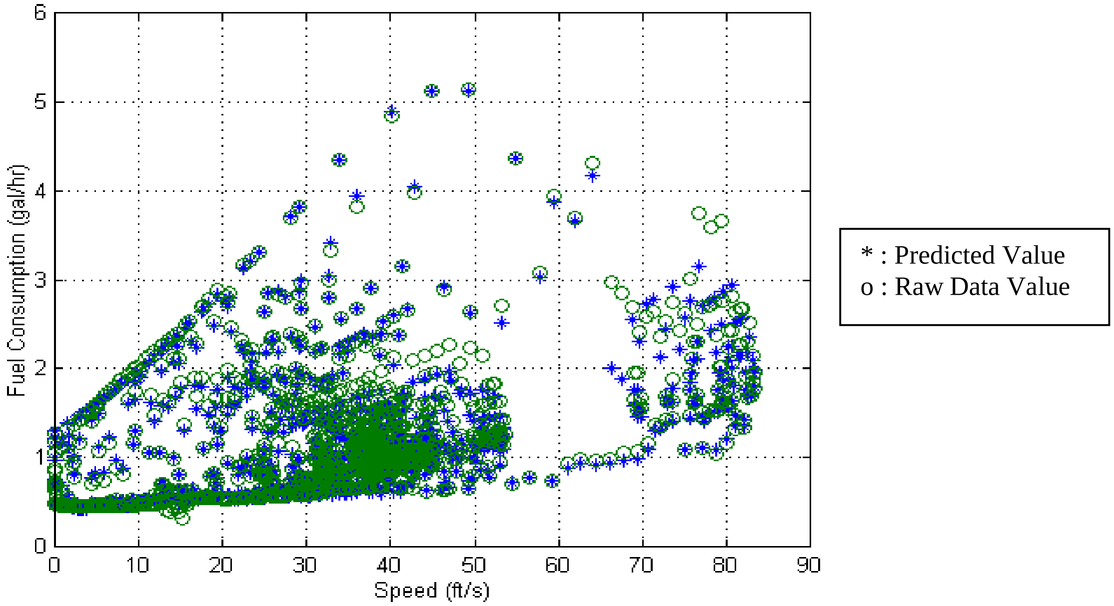

Figure D-5 Fuel Consumption for Model O (Speed Based).

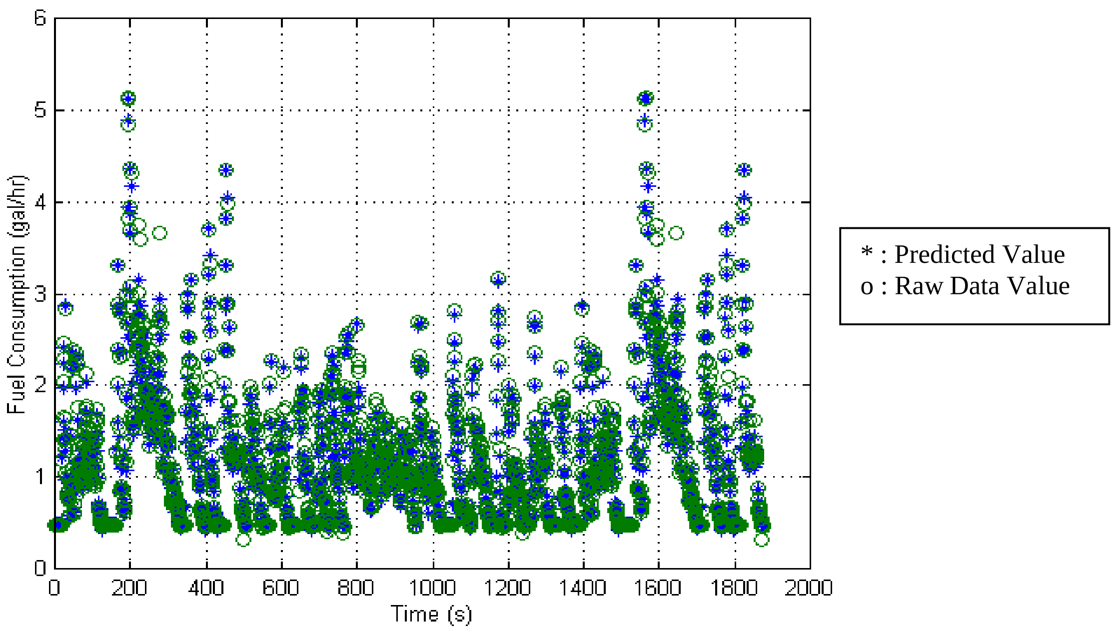

Figure D-6 Fuel Consumption for Model O (Time Based).

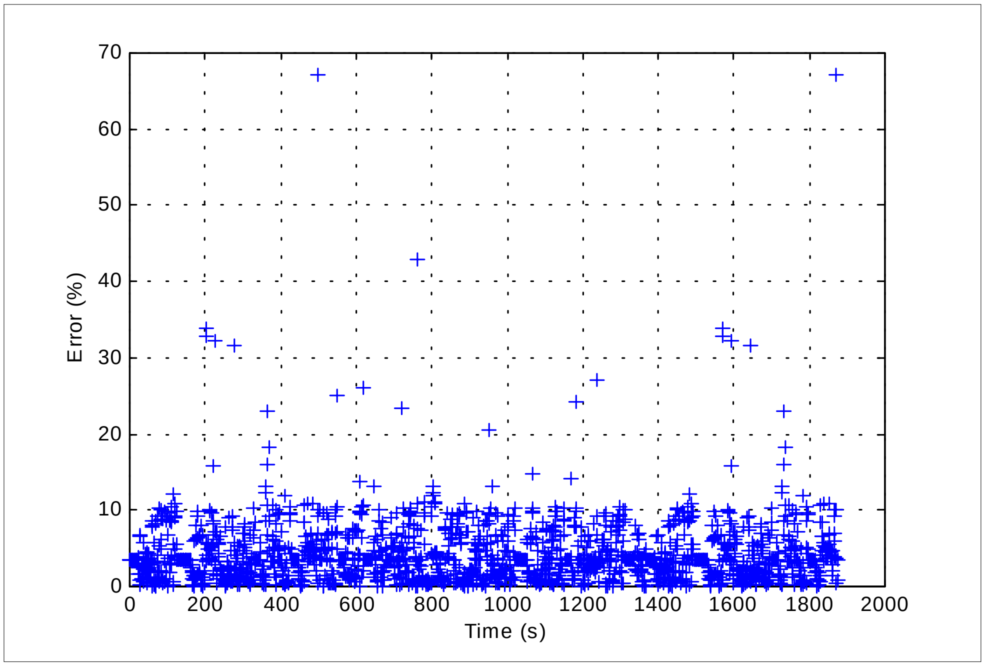

Figure D-7 Fuel Consumption Error for Model O.

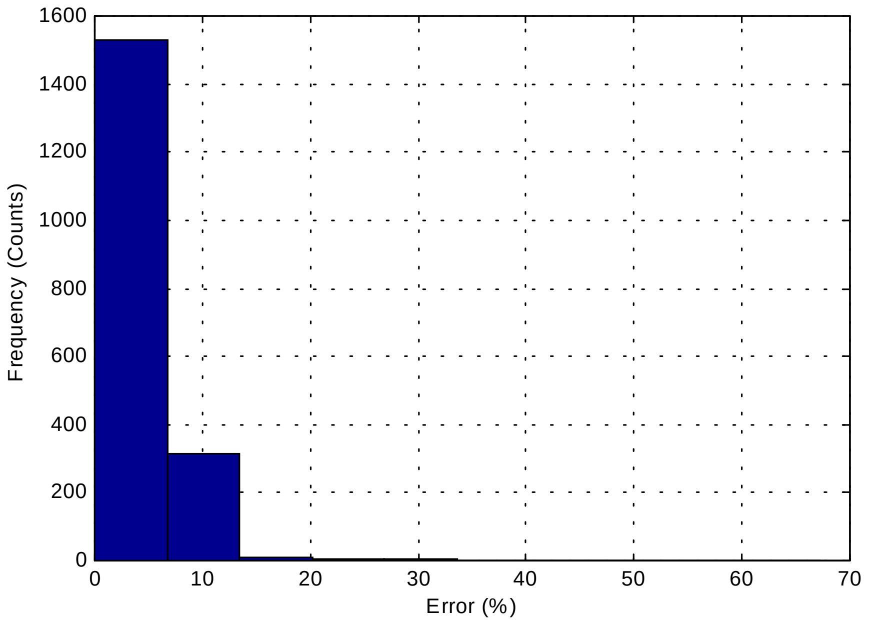

Figure D-8 Error Distribution of Fuel Consumption for Model O.

Appendix E

SAS Output, Fuel emission model of composite vehicle (Model N)

Model: MODEL1
Dependent Variable: FUELLOG

Analysis of Variance

Source	DF	Sum of Squares	Mean Square	F Value	Prob>F
Model	15	1023.43002	68.22867	19688.072	0.0001
Error	1286	4.45661	0.00347		
C Total	1301	1027.88663			

Root MSE	0.05887	R-square	0.9957
Dep Mean	0.50403	Adj R-sq	0.9956
C.V.	11.67954		

Parameter Estimates

Variable	DF	Parameter Estimate	Standard Error	T for H0: Parameter=0	Prob > |T|
INTERCEP	1	-0.679439	0.00953351	-71.268	0.0001
A	1	0.135273	0.00285464	47.387	0.0001
ASQ	1	0.015946	0.00064959	24.547	0.0001
ACU	1	-0.001189	0.00009578	-12.418	0.0001
SPEED	1	0.029665	0.00075765	39.154	0.0001
SSQ	1	-0.000276	0.00001613	-17.097	0.0001
SCU	1	0.000001487	0.00000010	15.361	0.0001
AS	1	0.004808	0.00025394	18.935	0.0001
ASS	1	-0.000020535	0.00000592	-3.471	0.0005
ASSS	1	5.5409285E-8	0.00000004	1.455	0.1458
AAS	1	0.000083329	0.00005388	1.547	0.1222
AASS	1	0.000000937	0.00000121	0.774	0.4390
AASSS	1	-2.479644E-8	0.00000001	-3.160	0.0016
AAAS	1	-0.000061321	0.00000851	-7.203	0.0001
AAASS	1	0.000000304	0.00000020	1.494	0.1355
AAASSS	1	-4.467234E-9	0.00000000	-3.218	0.0013

SAS Output, CO emission model of composite vehicle (Model N)

Model: MODEL1
Dependent Variable: FUELLOG

Analysis of Variance

Source	DF	Sum of Squares	Mean Square	F Value	Prob>F
Model	15	4573.32657	304.88844	2213.309	0.0001
Error	1289	177.56272	0.13775		
C Total	1304	4750.88929			

Root MSE	0.37115	R-square	0.9626
Dep Mean	3.73930	Adj R-sq	0.9622
C.V.	9.92565		

Parameter Estimates

Variable	DF	Parameter Estimate	Standard Error	T for H0: Parameter=0	Prob > |T|
INTERCEP	1	0.887447	0.06007986	14.771	0.0001
A	1	0.148841	0.01798142	8.277	0.0001
ASQ	1	0.030550	0.00409397	7.462	0.0001
ACU	1	-0.001348	0.00060380	-2.233	0.0257
SPEED	1	0.070994	0.00477677	14.862	0.0001
SSQ	1	-0.000786	0.00010167	-7.732	0.0001
SCU	1	0.000004616	0.00000061	7.563	0.0001
AS	1	0.003870	0.00160101	2.417	0.0158
ASS	1	0.000093228	0.00003730	2.500	0.0126
ASSS	1	-0.000000706	0.00000024	-2.943	0.0033
AAS	1	-0.000926	0.00033971	-2.725	0.0065
AASS	1	0.000049181	0.00000763	6.447	0.0001
AASSS	1	-0.000000314	0.00000005	-6.356	0.0001
AAAS	1	0.000046144	0.00005367	0.860	0.3901
AAASS	1	-0.000001410	0.00000128	-1.098	0.2723
AAASSS	1	8.1724008E-9	0.00000001	0.934	0.3506

SAS Output, HC emission model of composite vehicle (Model N)

Model: MODEL1
Dependent Variable: FUELLOG

Analysis of Variance

Source	DF	Sum of Squares	Mean Square	F Value	Prob>F
Model	15	2727.87495	181.85833	2165.459	0.0001
Error	1289	108.25206	0.08398		
C Total	1304	2836.12701			

Root MSE	0.28980	R-square	0.9618
Dep Mean	1.01865	Adj R-sq	0.9614
C.V.	28.44893		

Parameter Estimates

Variable	DF	Parameter Estimate	Standard Error	T for H0: Parameter=0	Prob > |T|
INTERCEP	1	-0.728042	0.04691061	-15.520	0.0001
A	1	0.012211	0.01403997	0.870	0.3846
ASQ	1	0.023371	0.00319659	7.311	0.0001
ACU	1	-0.000093243	0.00047145	-0.198	0.8432
SPEED	1	0.024950	0.00372972	6.689	0.0001
SSQ	1	-0.000205	0.00007939	-2.585	0.0099
SCU	1	0.000001949	0.00000048	4.090	0.0001
AS	1	0.010145	0.00125007	8.115	0.0001
ASS	1	-0.000103	0.00002912	-3.530	0.0004
ASSS	1	0.000000618	0.00000019	3.296	0.0010
AAS	1	-0.000549	0.00026524	-2.069	0.0387
AASS	1	0.000037592	0.00000596	6.312	0.0001
AASSS	1	-0.000000213	0.00000004	-5.524	0.0001
AAAS	1	-0.000113	0.00004191	-2.701	0.0070
AAASS	1	0.000003310	0.00000100	3.302	0.0010
AAASSS	1	-1.739372E-8	0.00000001	-2.545	0.0110

SAS Output, NOx emission model of composite vehicle (Model N)

Model: MODEL1
Dependent Variable: FUELLOG

Analysis of Variance

Source	DF	Sum of Squares	Mean Square	F Value	Prob>F
Model	15	3641.91010	242.79401	2853.458	0.0001
Error	1289	109.67798	0.08509		
C Total	1304	3751.58809			

Root MSE	0.29170	R-square	0.9708
Dep Mean	1.18817	Adj R-sq	0.9704
C.V.	24.55018		

Parameter Estimates

Variable	DF	Parameter Estimate	Standard Error	T for H0: Parameter=0	Prob > |T|
INTERCEP	1	-1.067682	0.04721856	-22.611	0.0001
A	1	0.254363	0.01413214	17.999	0.0001
ASQ	1	0.008866	0.00321758	2.756	0.0059
ACU	1	-0.000951	0.00047455	-2.005	0.0452
SPEED	1	0.046423	0.00375421	12.366	0.0001
SSQ	1	-0.000173	0.00007991	-2.162	0.0308
SCU	1	0.000000569	0.00000048	1.187	0.2353
AS	1	0.015482	0.00125828	12.304	0.0001
ASS	1	-0.000131	0.00002931	-4.483	0.0001
ASSS	1	0.000000328	0.00000019	1.740	0.0820
AAS	1	0.002876	0.00026698	10.771	0.0001
AASS	1	-0.000058660	0.00000600	-9.785	0.0001
AASSS	1	0.000000240	0.00000004	6.162	0.0001
AAAS	1	-0.000321	0.00004218	-7.616	0.0001
AAASS	1	0.000001943	0.00000101	1.925	0.0544
AAASSS	1	-1.257413E-8	0.00000001	-1.828	0.0678

VITA

Kyoungho Ahn was born on February, 1971 in Cheongju, Korea. He received a Bachelor of Engineering degree in the department of Urban Engineering from Chungbuk National University in Korea in 1996. During his undergraduate studies, he served in the Army for about two and a half years. In 1996, he began studies at Virginia Polytechnic Institute and State University to pursue a Master of Science degree in Transportation Engineering. While progressing toward the completion of his master's degree, he worked as a graduate research assistant in the Center for Transportation Research at Virginia Tech.